ENERGY, ENVIRONMENT & STORAGE

AN INTERNATIONAL JOURNAL

Volume-4
Issue-3
September, 2024
ISSN: 2791-6197

Editor in Chief

Dr. Selahaddin Orhan AKANSU

ENERGY, ENVIRONMENT AND STORAGE

EES JOURNAL

Founded and Published by Erciyes Energy Association

Energy, Environment and Storage Journal is indexed in Crossref

Printed in Turkey

ISSN-2791-6197

EES- EDITORIAL BOARD

BOARD MEMBER

AIM AND SCOPE

Energy, Environment and Storage papers consider the prospects of energy technologies, environment, materials, process control and industrial systems. The Energy, Environment and Storage will be published 3 times per year.

Contributions describe novel and significant applications to the fields of:

- Hydrogen Fuels
- Hydrogen and Fuel Cell
- Hydrogen Economic
- Biomass
- Solar PV Technology
- Solar Thermal Applications
- Wind Energy
- Materials for Energy
- Drones and Energy Applications
- Nuclear Energy and Applications
- Hydro Power
- Fuel Technologies (CNG, LNG, LPG, Diesel, Gasoline, Ethanol, etc.)
- Numerical Modelling
- Energy Storage and Systems
- Battery Technologies
- Energy Management
- Heat and Mass Transfer
- Aerodynamics
- Aerospace and Energy Applications
- Combustion
- Electric Vehicle Transportation
- Off-grid Energy Systems
- Environment Management
- Air Pollution
- Water and Wastewater Pollution
- Water and Wastewater Management
- Waste Management
- Global Warming and Climate Change
- Environmental Ecosystem
- Environmental System Modelling and Optimization
- Ecological Applications or Conservation

VOLUME 4, ISSUE 3

SEPTEMBER 2024

CONTENTS

Research Article Energy, Environment and Storage (2024) 04-03:71-78

Energy, Environment and Storage

Journal Homepage: www.enenstrg.com

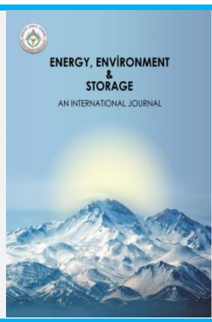

Current Update on Air Pollution or Quality and Meteorological Variables: A Review and Bibliometric Analysis

Merita Gidarjati[1*], Muhammad Ma'arij Harfadli [2], Toru Matsumoto [3]

[1]Graduate Program in Environmental Systems, Graduate School of Environmental Engineering, University of Kitakyushu. ORCID: 0009-0004-0443-0240

[2]Graduate Program in Environmental Systems, Graduate School of Environmental Engineering, University of Kitakyushu. ORCID: 0000-0001-7179-7668

[3]Faculty of Environmental Engineering, University of Kitakyushu. ORCID: 0000-0002-3191-2681

ABSTRACT. The study aims to investigate the existing understanding of air pollution and meteorological variables, with the goal of identifying and assessing research patterns, areas where research is lacking, and variables that are important for air pollution research. The Scopus Database is utilized as a data source, specifically searching for literature published in the last 10 years using keywords "Air pollution" or "Air quality" and "Meteorological variables". The study utilizes VOSviewer software to examine the data, emphasizing noteworthy trends in research on air pollution and climatic factors. The study produced a map and analysis of the expansion in scholarly publication concerning the above themes and it identified four significant clusters. The study also identified statistical models, tools, and sophisticated modeling methodologies utilized for both subjects. The analysis focuses on current patterns, areas of study that need attention, and factors that influence air pollution research. It offers a valuable understanding of the relationship between air pollution, meteorological variables, and their impact on public health. This study enhances our comprehension of the complexity of air pollution and meteorological factors, underscoring the significance of data-driven analysis, modeling methodologies, and interdisciplinary approaches in tackling environmental concerns.

Keywords: Air Pollution, Air Quality, Meteorological Variables

Article History Received: 15.06.2024; Accepted: 27.09.2024; Available online: 30.09.2024
Doi: https://doi.org/10.52924/ENRM8997

1. INTRODUCTION

The World Resources Institute once again ranked Jakarta as the most polluted city in the world in November 2023. At the same time, the poor air quality has put the health of its citizens at risk. The majority of the population in Southeast Asia resides in the areas where air pollution levels surpass the clean air guidelines set by the World Health Organization's (WHO). Most of the source of air pollution come from vehicles, power plants and industrial emissions. According to the 2023 World Air Quality Report, only seven countries managed to meet the WHO $PM_{2.5}$ annual guideline (annual average of 5 μg/m3 or less). The countries listed in the report are Australia, Estonia, Finland, Grenada, Iceland, Mauritius, and New Zealand. The report also indicated that climate conditions and transboundary haze were significant contributors in Southeast Asia, where $PM_{2.5}$ concentrations increased across almost all countries in the region [1].

Air pollution is a crucial environmental concern that has unfortunate effects on human health, ecosystems, and climate change [2] [3]. There are plenty of studies that have investigated the relationship between air pollution or air quality and meteorological variables such as temperature, humidity, wind speed, radiation, etc. [4] [5] [6] [7]. Understanding the complex interactions between air pollution, air quality, and meteorological variables is important for effective air quality management and policy development.

Bibliometric analysis refers to the application of statistical techniques to published literature in order to analyze publication patterns over time and get valuable insights on prominent scientists, nations, and organizations. Bibliometrics is a valuable tool for visualizing the literature and conducting quantitative analysis of developments and growth in scientific publications [8]. Multiple bibliometric studies on air pollution have been published [9] [10] [11] [12] [13] [14] [15]. These studies demonstrate the growing interest in bibliometric analysis of air pollution research, which helps to identify key trends, hotspots, and areas of focus in the field. Several publications have also been published on meteorological variables [16] [17].

Evaluating research output is a crucial process for showcasing the impact and cooperation of a country or region in a specific field. Hence, the objective of this study was to examine internationally published literature on air pollution and meteorological variables. This study will contribute to the field of air pollution research by identifying emerging focus areas and research gaps that may have been largely overlooked. The study will include a variety of relevant research articles, conference papers, and other scientific publications. Additionally, to acquire diverse publication attributes, such as types of publications, subject categories, institutions or affiliations, countries, year trends, and content analysis of keywords, abstracts, and article titles. However, the search limits are for English publications only.

The study will concentrate on examining the current understanding of how air pollution and meteorological variables related. The study also aims to identify and evaluate research trends, research gaps and variables for air pollution research in the Scopus database using VOSviewer software that researches air pollution and meteorological variables influential.

2. MATERIALS AND METHODS

2.1 Data Collection and Screening

Data sources in this study are taken using the Scopus Database. From previous research, Scopus was selected to obtain information from digital libraries and offer various queries through institutional subscriptions [18]. The keywords used in this study are **"**Air pollution**"** or "Air quality" and **"**Meteorological variables**"**. The data used was the literature published over the last 10 years, from 2014 to 2024. The article selection or screening process for this study took several stages that can be seen in the flow chart image (Figure 1). Stage 1 involves the identification of papers with the keywords above, with a total of 1,576 articles analyzed. After applying Stage 2 filtering based on the publication year, we acquired a total of 996 documents as the results. After applying stage 3 filtering, which includes criteria such as document kind (article, conference paper, and book chapter), publishing stage, and English language, a total of 907 items were eligible articles.

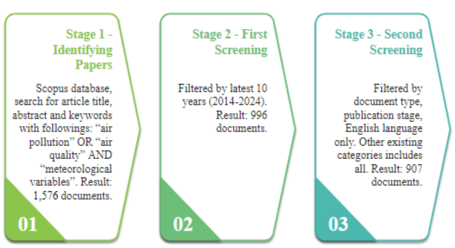

Fig. 1. Flow diagram for article selection process

2.2 Data Analysis

Documents selected in the Scopus database of 907 articles are then downloaded in the csv format and included in the qualitative content analysis using VOSviewer software. The term "keyword" in bibliographic metadata typically serves indexing purposes, containing important information from scientific work [19] [20]. Furthermore, VOSviewer is used to illustrate trends in the form of bibliometrics [21], i.e., publication maps with keywords or terms (term co-occurrence maps) will form a network (co-citation) that is connected based on related research. The more links there are between keywords or terms, the stronger the relationship between them. In this study, for network visualizaiton and overlay analysis, bibliometric data was analyzed using a binary approach for text data and a fractional approach for bibliographic data. The analysis aimed to provide a qualitative understanding of air pollution research trends, gaps, and variables through visual representation and network connections between keywords or terms.

3. RESULTS AND DISCUSSION

In this section, the bibliometric analysis results are discussed based on research trends, research gap, and variables for air pollution research.

3.1 Research Trends

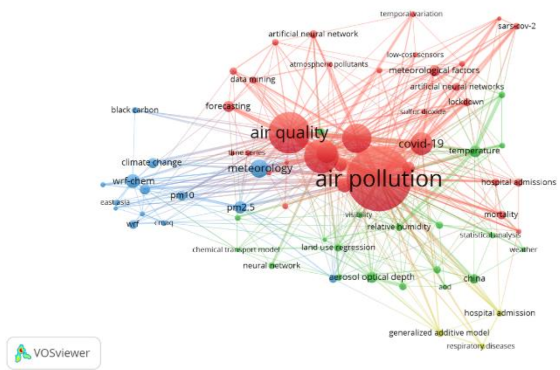

Fig. 2. Map of research cluster

As demonstrated in Figure 2, there are four clusters formed based on the co-occurrence of keywords. The first cluster is entitled Air Pollution and Health Impact: Analyzing Meteorological and Pollutant Data. This cluster focuses on the intersection of air pollution, meteorological variables, and their impacts on public health. It covers a comprehensive range of topics related to air quality and pollutants, including particulate matter ($PM_{2.5}$ and PM_{10}), nitrogen dioxide (NO_2), ozone (O_3), sulfur dioxide (SO_2), and general air pollutants. The emphasis is on understanding how these pollutants, along with various meteorological factors such as temperature and atmospheric boundary layers, affect health outcomes like morbidity, mortality, and hospital admissions [22] [23].

In the context of the COVID-19 pandemic, this cluster examines the correlation between air pollution and the spread and severity of the disease. It discusses how increased levels of atmospheric pollutants can exacerbate respiratory diseases such as asthma, leading to higher mortality and morbidity rates [24]. It highlights the role of advanced prediction and modeling techniques, such as machine learning, artificial neural networks (ANN), and data mining, in forecasting air quality and its health impacts [25]. The influence of lockdowns during the pandemic and their effects on air quality and pollution levels is also explored [26]. Additionally, the cluster includes discussions on temporal variation studies and the use of low-cost sensors for air quality monitoring and management.

The second cluster describes Meteorological Parameters and Public Health: Insights and Implications. This cluster examines the relationship between meteorological parameters and public health outcomes. It includes studies on the health effects on relative humidity, wind speed, and visibility [27] [28]. It also covers the use of land use regression, MODIS (Moderate Resolution Imaging Spectroradiometer) data, and statistical analysis to understand surface ozone, aerosol, and weather patterns [29]. The cluster also stress how important chemical transport models (CTMs) and aerosol optical depth (AOD) are in studying the atmosphere. These models figure out the levels of exposure and health risks that come with different weather situations [30] [31]. The research explores how varying meteorological conditions can modify pollutant concentrations, thus impacting public health epidemiology. This cluster focuses on the role of weather in driving air quality trends and its implications for public health policies.

Further, the third cluster explains Advanced Air Quality Modeling and Atmospheric Studies. This cluster is dedicated to advanced air quality modeling and the study of atmospheric processes. It includes topics such as meteorology, $PM_{2.5}$, PM_{10}, black carbon, and tropospheric ozone. The cluster features the use of models like WRF-Chem (Weather Research and Forecasting model coupled with Chemistry), CMAQ (Community Multiscale Air Quality model), and WRF (Weather Research and Forecasting) to simulate air quality and atmospheric circulation [32] [33]. These models are utilized to predict pollutant behavior, understand the effects of climate change on air quality, and devise effective management strategies, especially in highly polluted regions like East Asia [34] [35]. The cluster highlights the integration of climate models with air quality simulations to provide a comprehensive assessment of air pollution's impact on human health and the environment, particularly focusing on fine particulate matter ($PM_{2.5}$) and its sources.

The fourth cluster portrays Statistical Methods in Assessing Health Outcomes from Air Pollution. This cluster focuses on applying statistical methods to evaluate the health outcomes associated with air pollution. It includes the use of generalized additive models and other statistical tools to analyze hospital admissions and respiratory diseases [36] [37]. The cluster provides insights into how statistical analysis can help in understanding the correlation between air quality and health outcomes, guiding public health interventions and policies [38] [39]. The focus is on understanding the epidemiological aspects of air pollution and its direct effects on public health by using statistical modeling to decipher complex datasets [40]. By identifying key trends and correlations, the research in this cluster aims to inform better regulatory measures and health guidelines to mitigate the adverse effects of air pollution on vulnerable populations.

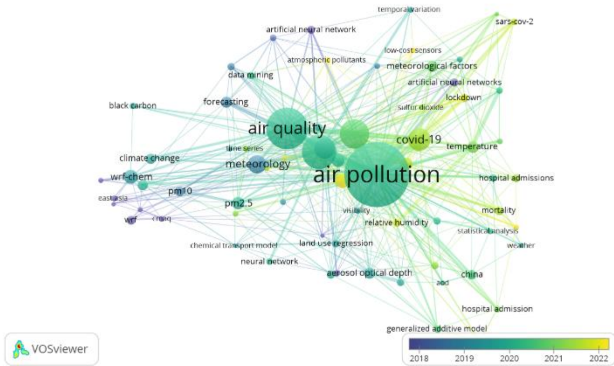

Fig. 3. Overlay Map of Research Year

As demonstrated in Figure 3, there is a relationship among labels (topics), clusters (thematic groupings), the weight of occurrences (frequency or emphasis), and the year of publication. Emerging focus in the first cluster is air pollution (weight 195), air quality (weight 103), and particulate matter (weight 80). They were the most frequently occurring topics, particularly around 2020. This period coincides with increased global awareness of air pollution and its health impacts, likely influenced by the COVID-19 pandemic. Further, COVID-19 Impact labels such as COVID-19 (weight 44), sars-cov-2/severe acute respiratory syndrome coronavirus 2 (weight 8), and related terms like lockdown (weight 11) showed a significant increase in 2020 and 2021, reflecting research into how the pandemic influenced air quality and public health.

The next research trend in the second cluster has shown topics such as temperature (weight 18), humidity (weight 8), and relative humidity (weight 9). These topics have gained attention, especially in 2020 and 2021. This indicates a growing interest in understanding how weather and climate factors impact air quality and health. Terms such as public health (weight 10) and epidemiology (weight 8), which highlight an increasing focus on the intersection of environmental science and public health, also raise the issue of public health integration.

Several terms such as WRF-chem (weight 22), CMAQ (weight 7), and chemical transport model (weight 5) indicate that advanced modeling is a frequently raised issue by researchers in the third cluster. This topic shows a steady increase, with significant research activity around 2019. This indicates advancements in using sophisticated models to study air quality. Climate Change and Pollutants is an interesting topic. Topics like climate change (weight 15), $PM_{2.5}$ (weight 20), and black carbon (weight 8) reflect ongoing concerns and research into how these factors influence atmospheric conditions and public health.

The fourth cluster concentrates on statistical analysis of fundamental topics pertaining to the years 2017-2018. The use of methods like generalized additive model (weight 10) and statistical analysis (weight 7) points to a robust approach in assessing the health impacts of air pollution. Health Implications: In the context of air pollution, labels like hospital admission (weight 8) and respiratory diseases (weight 7) underscore the direct health consequences under investigation.

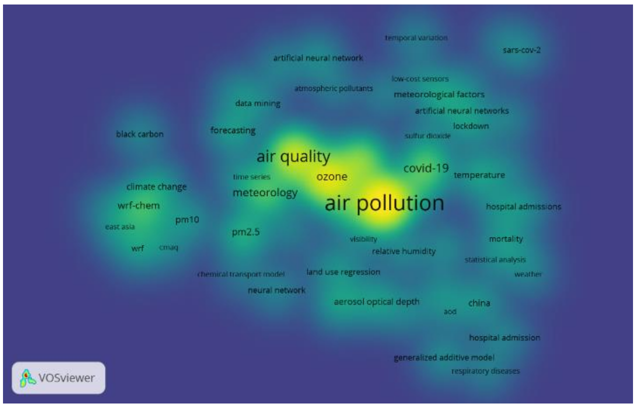

Fig. 4. Research Density Map

The density analysis of the research data revealed concentrated periods of intense study, particularly around 2020 and 2021, which were largely driven by the global impact of the COVID-19 pandemic. The first cluster, which focused on air pollution and health impacts, demonstrated the highest density, with significant emphasis on topics such as air pollution, air quality, and particulate matter. During these years, this cluster also demonstrated increased research on the effects of COVID-19, machine learning, and meteorological variables. The second cluster which covers meteorological parameters and public health, also showed notable density in 2019 and 2020, highlighting the integration of weather factors and public health studies. The third cluster, focused on air quality modeling and atmospheric studies, exhibited dense occurrences in 2019, reflecting advancements in modeling techniques and climate change research. The fourth cluster, dealing with statistical methods and health outcomes, exhibited increased density in 2020 and 2021, emphasizing the application of statistical analysis to health impacts related to air pollution. The overall density trends indicate key periods of research intensity and the evolving focus areas within the field.

3.2 Research Gap

This subchapter will discuss the research gaps based on the VOSviewer analysis results. Table 1 shows the relationship value of each of the lowest labels in each cluster. The total link strength and total occurrences reflect this relationship. The closer a label is to research center, the smaller its relationship value is. This means that these labels can become problems or gaps in research.

Table 1 The value of the weight of total link strength and occurrences

Label	Total link strength	Occurrences
coronavirus	17	5
aerosol	13	5
chemical transport model	12	5
morbidity	15	6
sulfur dioxide	11	6
wind speed	14	7
modeling	13	7
cmaq	13	7
statistical analysis	12	7
temporal variation	11	7
random forest	11	7
sars-cov-2	20	8
humidity	20	8
hospital admission	15	8
prediction	13	8
relative humidity	24	9
land use regression	22	9
data mining	19	9
neural networks	15	9
modis	14	9

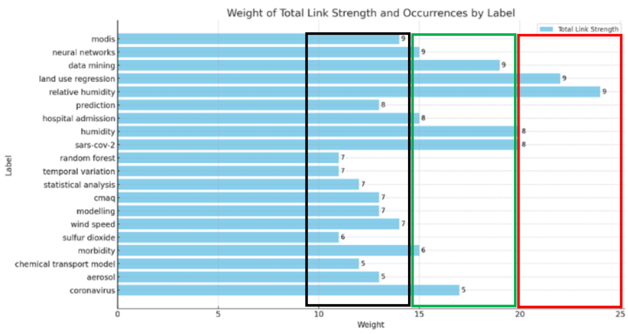

Fig. 5. Research Gap on Air Pollution based on the weight of total link strength and occurrences in each cluster from VOSviewer result. The biggest gap or highest weight is inside red box, the moderate one is inside the green box and the smallest gap or lowest weight is inside the black box.

The bar chart provides a visual representation of lowest weight of total link strength and occurrences for various research labels. This chart can be used to identify potential research gaps and areas that may require more focus. Figure 5 shows that relative humidity, land use regression, sars-cov-2, and humidity have high connectivity but relatively few studies. More frequent and diverse studies in these areas could fill this gap. Researchers have consistently studied neural networks, hospital admission, and coronavirus, and data mining, but additional research could enhance understanding, particularly in the context of air pollution and health. Modes, prediction, temporal variation, statistical analysis, CMAQ, modeling, wind speed, sulfur dioxide, chemical transport models, aerosols, and random forests are terms that have received less emphasis in research, showing potential for new discoveries and wider study.

3.3. Variables for Air Pollution Research

To identify the important variables for air pollution modeling from the data of VOSviewer, the observation can focus on the labels associated with high weights of occurrences and total link strength. These labels often represent key variables and factors frequently studied and considered crucial in the context of air pollution modeling. The following are the variables in Table 2.

Table 2 Variables for air pollution

Category	Variable	Description
Meteorological Variables	Humidity	The amount of water vapor present in the air.
	Wind Speed	The rate at which air is moving horizontally past a given point.
	Relative Humidity	The ratio of the amount of water vapor present in the air to the maximum amount that the air could hold at that temperature.
Pollutants	Sulfur Dioxide	A colourless gas with a pungent odour, primarily emitted from burning fossil fuels.
	Black Carbon	Fine particulate matter consisting of black carbon particles, primarily emitted from incomplete combustion of fossil fuels and biomass.
	Particulate Matter ($PM_{2.5}$ & PM_{10})	Fine particles suspended in the air, with diameters of 2.5 micrometres or smaller ($PM_{2.5}$) and 10 micrometres or smaller (PM_{10}).
	Ozone	A gas molecule composed of three oxygen atoms, often formed through chemical reactions between nitrogen oxides and volatile organic compounds in the presence of sunlight.
Health Impact Indicators	Morbidity	The incidence of disease within a population.
	Hospital Admission	The number of individuals admitted to hospitals due to health issues, often related to air pollution exposure.
	Respiratory Diseases	Disorders affecting the lungs and respiratory system, including conditions such as asthma, bronchitis, and chronic obstructive pulmonary disease (COPD).
Modeling and Analytical Methods	Machine Learning	A field of artificial intelligence that enables computer systems to learn from data and make predictions or decisions without being explicitly programmed.
	Neural Networks	Computational models inspired by the structure and functioning of the human brain, capable of learning complex patterns and relationships from data.
	Random Forest	A machine learning algorithm consisting of multiple decision trees, used for classification and regression tasks.
	Statistical Analysis	Techniques for analysing and interpreting data to uncover patterns, trends, and relationships, often used for hypothesis testing and inference.
	Generalized Additive Model	A statistical model used to explore relationships between predictors and a response variable, allowing for nonlinear and nonparametric relationships.
Data Sources and Tools	MODIS (Moderate Resolution Imaging Spectroradiometer)	in the Earth's environment, including air quality parameters.
	CMAQ (Community Multiscale Air Quality model)	A computational tool used for simulating air quality at regional and local scales, integrating meteorological, emission, and chemical transport processes.
	WRF-Chem (Weather Research and Forecasting model coupled with Chemistry)	A numerical weather prediction model coupled with a chemistry module, used for simulating atmospheric composition and air quality.
Temporal Factors	Temporal Variation	Changes in air pollution levels and other variables over time, influenced by

		factors such as diurnal patterns, seasonal variations, and long-term trends.
	Time Series Analysis	Statistical methods for analysing sequential data collected at regular intervals over time, used to identify patterns, trends, and anomalies.

4. CONCLUSIONS

The results of the bibliometric analysis reveal insightful patterns of air pollution and meteorological variables research. The study explores research trends related to air pollution and meteorological variables. Four clusters were identified based on keyword co-occurrence, covering various aspects such as air pollution, health impacts, meteorological parameters, and advanced air quality modeling. The clusters delve into topics like air quality, particulate matter, nitrogen dioxide, ozone, sulfur dioxide, health outcomes, statistical analysis, and modeling techniques. Significant research activity was noted around 2019-2021, particularly influenced by the COVID-19 pandemic. Emphasis was placed on machine learning, artificial neural networks, statistical methods, and models like WRF-Chem and CMAQ in studying air quality and health impacts. The research gaps identified may include areas where further investigation is needed to enhance understanding, prediction, and management of air pollution and its impacts on public health. Specific gaps in the literature could involve novel methodologies, emerging pollutants, understudied health outcomes, or unexplored interactions between air pollutants and meteorological factors. The study identified emerging focus areas in air pollution research, including the impact of climate change on air quality, statistical methods for assessing health outcomes, and advancements in air quality modeling. Notable topics such as climate change, $PM_{2.5}$, black carbon, statistical analysis, and health implications were emphasized in the clusters.

The findings from this study have several important implications. The identification of key research clusters suggests that future air quality management strategies must account for the increasing role of climate change and its interaction with air pollution. Policymakers and environmental agencies can use this insight to develop more targeted interventions that incorporate both meteorological variables and machine learning models to predict and mitigate air quality issues. This study also highlights the importance of incorporating advanced statistical techniques to improve the understanding of health outcomes related to air pollution, which can guide public health policies and urban planning in high-pollution areas.

Future research in the field of air pollution and meteorological variables could focus on several key areas. Firstly, there is a need for further investigation into the impact of climate change on air quality, particularly considering the evolving environmental conditions and their effects on pollutant levels. Additionally, exploring the application of advanced statistical methods in assessing health outcomes related to air pollution could provide valuable insights into the effectiveness of different analytical approaches. Furthermore, future studies could delve into the integration of machine learning techniques with meteorological data to enhance predictive models for air quality monitoring and forecasting. Lastly, examining the long-term trends and patterns in air pollution, especially in relation to changing meteorological variables, could offer a comprehensive understanding of the dynamics between atmospheric conditions and pollutant concentrations.

In summary, this work provides a foundation for continued advancements in the fields of air quality and meteorological research, with significant potential to inform both science and policy on global level.

Acknowledgments

The authors express their gratitude to the Matsumoto Laboratory, Graduate Programs in Environmental Systems, Graduate School of Environmental Engineering, The University of Kitakyushu, Japan, for their valuable support and assistance in facilitating this research endeavour.

REFERENCES

[1] (2024) 2023 IQAir World Air Quality Report, Region and City $PM_{2.5}$ Ranking.

[2] I. Manisalidis, E. Stavropoulou,A. Stavropoulos, and E. Bezirtzoglou, Environmental and Health Impacts of Air Pollution: A Review, *Front Public Health.*, Vol. 8, pp. 14, 2020.

[3] S.M. Sarkar, B.K. Dhar, M. Fahlevi, S. Ahmed, M.J. Hossain, M. Meshbahur, M.A.I. Gazi, Improving Health in Developing Countrie. Global Challenges, *Global Challenges,* Vol. 7 (8), pp. 2200246, 2023.

[4] H. Huang, X. Liang, J. Huang, Z. Yuan, Z. Hua, H. Ouyang, Y. Wei, X. Bai, Correlations between meteorological indicators, air quality and the COVID-19 pandemic in 12 cities across China, *J. environ. health sci. eng.,* Vol. 188(2), pp. 1491-1498, 2020.

[5] P.K. Sahoo, S. Magla, A. Chauhan, A.K. Pathak, COVID-19 pandemic: An outlook on its impact on air quality and its association with environmental variables in major cities of Punjab and Chandigarh, India, *Environ. Forensics*, Vol. 22(1-2), pp. 143-154, 2021.

[6] Sulaymon, I.D., Zhang, Y., Hopke, P.K., Zhang, Y., Hua, J., Mei, X., COVID-19 pandemic in Wuhan: Ambient air quality and the relationships between criteria air pollutants and meteorological variables before, during, and after lockdown, *Atmos. Res.*, Vol. 250, pp. 105362, 2021.

[7] M. Sarmadi, S. Rahimi, M. Rezae, D. Sanaei, M. Dianatinasab *et al*., Air quality index variation before and after the onset of COVID-19 pandemic: a comprehensive study on 87 capital, industrial and polluted cities of the world, *Environ. Sci. Eur*., Vol. 33 (1), pp. 134, 2021.

[8] Y. Li, Z. Sha, A. Tang, K. Goulding, X. Liu, The application of machine learning to air pollution research: A bibliometric analysis, *Ecotoxicology and Environmental Safety*," Vol. 257, pp. 114911, 2023.

[9] A. Ansari, and A.R. Quafi, Bibliometric Analysis on Global Research Trends in Air Pollution Prediction Research Using Machine Learning from 199102023 Using Scopus Database, *Aerosol Science and Engineering*, Vol. 8(3), pp. 288-306, 2024.

[10] J. Chen, Q. Chen, L. Hu, T. Yang, C. Yi, and Y. Zhou, Unveiling Trends and Hotspots in Air Pollution Control: A Bibliometric Analysis, *Atmosphere*, MDPI, Vol. 15 (6), pp. 630, 2024.

[11] J. Sun, Z. Zhou, J. Huang, and G. Li, A Bibliometric Analysis of the Impacts of Air Pollution on Children, *International Journal of Environmental Research and Public Health*, MDPI, Vol. 17(4), pp. 1277, 2020.

[12] B.G. Olutola, and P. Phoobane, A Bibliometric Analysis of Literature on Prenatal Exposure to Air Pollution: 1994-2022, *Int. J. Environ. Res. Public Health*, Vol. 20(4), pp. 3076, 2023.

[13] W.M. Sweileh, S.W. Al-Jabi, S.H. Zyoud, and A.F. Sawalha, Outdoor air pollution and respiratory health: a bibliometric analysis of publication in peer-reviewed journals (1900-2017), *Multidiscip. Respir. Med*., Vol. 13(1), pp. 15, 2018.

[14] Y. Li, Z. Sha, A. Tang, K. Goulding, X. Liu, The application of machine learning to air pollution research: A bibliometric analysis, *Ecotoxicol. Environ. Saf*., Vol. 257, pp. 114911, 2023.

[15] S. Jain, N. Kaur, S. Verma, Kavita, A.S.M.S. Hosen, and S.S. Sehgal, Use of Machine Learning in Air Pollution Research: A Bibliographic Perspective, *Electronic*, MDPI, Vol. 11(21), pp. 3621, 2022.

[16] O.M. Adisa, M. Masinde, J.O. Botai, and C.M. Botai, Bibliometric Analysis of Methods and Tools for Drought Monitoring and Prediction in Africa, *Sustainability*, MDPI, Vol. 12(16), pp. 6516, 2020.

[17] J. Li, Bibliometric Analysis of Atmospheric Simulation Trends in Meteorology and Atmospheric Science Journals: Update, *Croat.Chemi.Acta*, Vol. 91(1), 2018.

[18] O. Klapka, A. Slaby, Visual analysis of search results in Scopus database focus on sustainable tourism, *Czech Journal of Tourism*, Vol.9(1), pp. 41-53, 2020.

[19] B. S. Ramadan, I. Rachman, N. Ikhlas, S. B. Kurniawan, M.F. Miftahadi, and T. Matsumoto, A comprehensive review of domestic-open waste burning: Recent trends, methodology comparison, and factors assessment, *J. Mater. Cycles Waste Manag*., Vol. 24(5), pp. 1633–1647, 2022.

[20] M. M. Harfadli, B.S. Ramadan, I. Rachman, T. Matsumoto, Challenges and characteristics of the informal waste sector in developing countries: an overview, *J Mater Cycles Waste Manag*, Vol. 26(3), pp. 1294–1309, 2024.

[21] N.A.A. Effah, M. Asiedu, and O.A.S. Otchere, Improvements or deteriorations? A bibliometric analysis of corporate governance and disclosure research (1990–2020), *Journal of Business and Socio-Economic Development*, Vol. 3(2), pp. 118–133, 2023.

[22] C. Magazzino, M. Marco, and S. Nicolas, The relationship between air pollution and COVID-19-related deaths: an application to three French cities, *Applied Energy*, Vol.279, pp. 115835, 2020.

[23] R.K. Singh, M. Drews, M. De la Sen, *et al.*, Highlighting the compound risk of COVID-19 and environmental pollutants using geospatial technology, *Sci Rep*, Vol. 11(1), pp. 8363, 2021.

[24] S. Comunian, D. Dongo, C. Milani, P. Palestini, Air Pollution and COVID-19: The Role of particulate matter in the spread and increase of COVID-19's morbidity and mortality, *Int. J. Environ. Res. Public Health*, Vol. 17(12), pp. 4487, 2020.

[25] M. M. Rahman, K. C. Paul, M. A. Hossain, G. G. M. N. Ali, M. S. Rahman, & J. C. Thill, Machine learning on the COVID-19 pandemic, human mobility and air quality: A review, *IEEE access: practical innovations, open solutions*, Vol. *9*, pp. 72420–72450, 2021.

[26] A.M.F. Mohammed, E.F. Mohamed, I.A. Saleh, M.A. Nasser, Air pollution and COVID-19 lockdown, *Material Sci & Eng*, Vol. 5(4), pp. 111-122, 2021.

[27] I. Jhun, B. A. Coull, J. Schwartz, B. Hubbell, & P. Koutrakis, The impact of weather changes on air quality and health in the United States in 1994–2012, *Environmental research letters*, Vol. 10(8), pp. 084009, 2015.

[28] D. Roberts-Semple, and Y. Gao, Evaluation of air pollution, local meteorology and urban public health, *International journal of environmental technology and management*, Vol. 16(1-2), pp. 160-177, 2013.

[29] R.J. Pope, E.W. Butt, M.P. Chipperfield, R.M. Doherty, S. Fenech, A. Schmidt, S.R. Arnold and N.H. Savage, The impact of synoptic weather on UK surface ozone and implications for premature mortality, *Environmental Research Letters*, Vol. 11(12), pp. 124004, 2016.

[30] Z. Chen, D. Chen, C. Zhao, M.P. Kwan, J. Cai, Y. Zhuang, *et.al.*, Influence of meteorological conditions on $PM_{2.5}$ concentrations across China: A review of

methodology and mechanism, *Environment international*, Vol. 139, pp. 105558, 2020.

[31] E. Austin, A. Zanobetti, B. Coull, J. Schwartz, D.R. Gold, and P. Koutrakis, Ozone trends and their relationship to characteristic weather patterns, *Journal of exposure science & environmental epidemiology*, Vol. 25(5), pp. 532-542, 2015.

[32] M.W. Choi, J.H. Lee, J.W. Woo, C.H. Kim, and S.H. Lee, Comparison of $PM_{2.5}$ chemical components over East Asia simulated by the WRF-Chem and WRF/CMAQ models: On the models' prediction inconsistency, *Atmosphere*, Vol. 10(10), pp. 618, 2019.

[33] J. Hu, J. Chen, Q. Ying, and H. Zhang, One-year simulation of ozone and particulate matter in China using WRF/CMAQ modeling system, *Atmospheric Chemistry and Physics*, Vol. 16(16), pp. 10333-10350, 2016.

[34] C. Gao, A. Xiu, X. Zhang, Q. Tong, H. Zhao, S. Zhang, *et.al*., Two-way coupled meteorology and air quality models in Asia: a systematic review and meta-analysis of impacts of aerosol feedbacks on meteorology and air quality, *Atmospheric Chemistry and Physics*, Vol. 22(8), pp. 5265-5329, 2022.

[35] A. Kumar, R.S. Patil, A.K. Dikshit, and R. Kumar, Application of WRF model for air quality modeling and AERMOD-A survey, *Aerosol and Air Quality Research*, Vol. 17(7), pp. 1925-1937, 2017.

[36] K. Ravindra, P. Rattan, S. Mor, and A.N. Aggarwal, Generalized additive models: Building evidence of air pollution, climate change and human health, *Environment international*, Vol. 132, pp. 104987, 2019.

[37] A. Kladakis, K.M. Fameli, K. Moustris, V.D. Assimakopoulos, and P. Nastos, Investigation into atmospheric pollution impacts on hospital admissions in Attica using regression models, *Environmental Sciences Proceedings*, Vol. 26(1), 25, 2023.

[38] A. Slama, A. Śliwczyński, J. Woźnica, M. Zdrolik, B/ Wiśnicki, J. Kubajek, *et.al.*, Impact of air pollution on hospital admissions with a focus on respiratory diseases: A time-series multi-city analysis, *Environmental Science and Pollution Research*, Vol. 26(17), pp. 16998-17009, 2019.

[39] D. Liu, K. Cheng, K. Huang, H. Ding, T. Xu, Z. Chen, and Y. Sun, Visualization and analysis of air pollution and human health based on cluster analysis: A bibliometric review from 2001 to 2021, *International Journal of Environmental Research and Public Health*, Vol. 19(19), pp. 12723, 2022.

[40] S. Weerasinghe, Statistical modeling of complex health outcomes and air pollution data: Application of air quality health indexing for asthma risk assessment, *Epidemiology Biostatistics and Public Health*, Vol. 14(1), pp. e12092-1-13, 2022.

Review Article

Energy, Environment and Storage (2024) 04-03:79-89

Energy, Environment and Storage

Journal Homepage: www.enenstrg.com

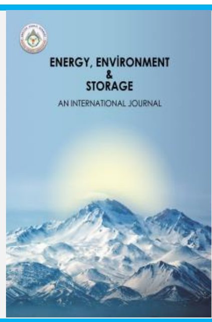

Investigation of Dust Explosion in Food Silos: A Review

Salih AÇIKGÖZ[1*],

[1]*Erciyes University, Faculty of Engineering, Department of Mechanical Engineering, Kayseri, Turkey*

mcsalo@hotmail.com ORCID:0009-0007-8351-3846

ABSTRACT. In this article, dust explosion phenomena and the status of research conducted on silos are reviewed. Dust explosions cause loss of life and property in many industrial facilities. There are many recorded dust explosion cases in our country as well as in the world. For example, in our country, in 2023, a dust explosion occurred in the TMO Kocaeli General Directorate (Derince Port Silo), in which 2 people died and great material damage occurred, as reflected in the national press. When we look at the various dust explosion cases that have occurred in the world, it is understood that they mostly occur in silos used for storage in the agricultural and food sectors. Licensed warehouses have been established in many regions of our country in order to store basic and processed agricultural products that can be standardized with the Agricultural Products Licensed Warehousing Law No. 5300, which came into force after being published in the Official Gazette on 17/02/2005, in safe and healthy conditions in warehouses belonging to licensed warehouse enterprise and continues to be established. It is important to understand the many factors affecting dust explosion, such as dust dispersion, properties, discharge, etc., and to design silos according to these factors. These effects are tried to be determined and understood through experimental or CFD simulations.

Keywords: Dust Explosion, Dust, Sizing, Silo, Computational Fluid Dynamics

Article History: Received: 06.08.2024; Accepted: 20.09.2024; Available online: 30.09.2024

Doi: https://doi.org/10.52924/PCAF5076

1. INTRODUCTION

1.1. Definition of Dust

There are various standards for dust definitions:

- In the TS EN 60079-10-2: 2015 standard, it is stated that dust includes flammable dust and flammable volatiles. Combustible dust is defined in the standard as finely divided solid particles with a nominal size of 500 µm or less, which can form explosive mixtures with air at atmospheric pressure and normal temperature. Flammable volatile is defined as a solid particle with a nominal size greater than 500 µm that can form an explosive mixture with air at atmospheric pressure and normal temperature [1].

- According to BS 2955: 1958 [2,3], substances with a grain size of less than 1000 µm are defined as 'powders', while when the particles are smaller than 76 µm in diameter they are called 'dust'.

- According to NFPA [4], "dust" is any finely divided solid with a diameter of 420 µm or less that, when suspended in air, presents a risk of fire or explosion on contact with an ignition source.

1.2. Dust Explosion

An explosion begins with the rapid burning of flammable dust particles suspended in the air. The intensity and speed of the explosion depend on the grain fragmentation of any solid that can burn in air [4]. Depending on the small particle size, combustion can be more rapid and explosive up to a certain stage. If the burning dust particles are not in a closed area, a sudden fire will occur. However, if the burning dust particles are in a partially closed environment, the heat generated by the combustion, the spread of flame along the dust particles, and the formation of large amounts of heat and reaction products, can cause rapid pressure build-up. This can also cause an explosion. The intensity of the explosion depends on the degree of confinement in the enclosed space, depending on the particle size, as well as the amount of energy released due to heat losses. In some

[*]Corresponding author: mcsalo@hotmail.com

exceptional cases, even if the dust particles are not in the enclosed space, if the reactions due to combustion occur faster than the pressure can disperse at the edge of the cloud, a devastating explosion can occur [5].

1.3.Dust Explosion Pentagon

Like all fires, dust fires also occur as a result of the combination of a flammable material (dust) with an ignition source in the presence of oxygen. According to this explanation, if one of the three components in the fire triangle in Fig. 1 is not present, a fire will not occur [6].

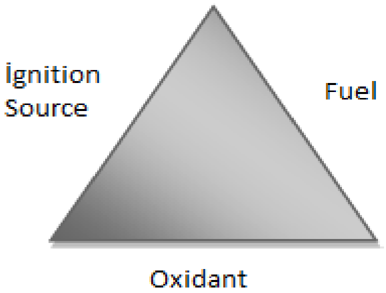

Fig. 1. Fire triangle.

Dust explosion requires two more components besides the three components in the fire triangle. These two components are; keeping the dust suspended and confining the dust cloud in a certain volume. By adding these two components to the fire triangle, the dust explosion pentagon in Fig. 2 is formed [6].

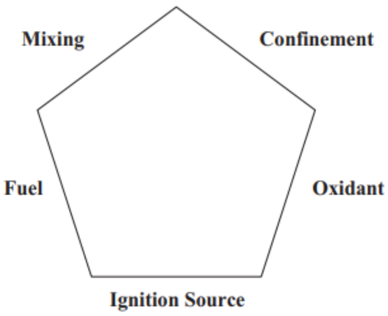

Fig. 2. Dust explosion pentagon.

Dust explosions have very high energy and can create pressure waves strong enough to destroy structures or harm people in the surrounding area. People exposed to dust explosions are usually harmed by burning due to the burning dust cloud or by flying pieces of equipment and collapsing walls caused by the explosion [7].

1.4. Domino Effect

Dust explosions occurring in a facility are divided into two classes as primary or secondary explosions. Primary dust explosions are explosions that occur as a result of the dust cloud coming into contact with any ignition source inside a piece of equipment such as a mixer, dryer, filter, elevator, pneumatic carrier, silo, etc., since the necessary dust concentrations for an explosion seldom gather outside the processing vessels [6,7]. This may cause the vessel to rupture if there is no adequate pressure relief device/ventilation or if the material resistance pressure is too low [6].

Secondary dust explosions are explosions that occur when dust accumulated nearby is lifted and ignited by the impact of a primary explosion (Fig. 3) [4]. Although it is crucial to attempt to remove the chance of primary dust explosions happening, additionally it is crucial to stop the initial explosion from triggering a chain reaction that results in secondary explosions, as secondary dust explosions are invariably more damaging than primary dust explosions.) [3,8,9].

Due to a dust explosion happening in one section of the conveying system, the pressure and/or flames might travel to other sections through the connecting pipes. For instance, experiments performed on an explosion in a vented bag filter with a reduced explosion pressure below 500 mbar have indicated that the explosion is likely to propagate to the inlet pipe. This potential for spreading could result in the explosion growing with increasing severity throughout the system [10]. Due to the turbulence effect, the flame traveling through the channel tends to speed up. This leads to a jet flame entering the second vessel. As a consequence, even the ventilation of the second vessel where the flame disperses cannot prevent high combustion rates under high pressures, and the amount of dust contained alone does not pose much of a danger [11].

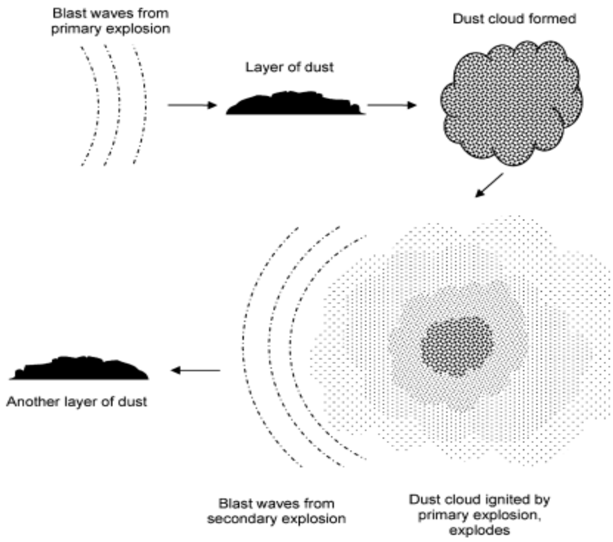

Fig. 3. Chain reaction in dust explosion.

1.5. In-depth Case Reports On Several Major Dust Explosions

Indeed, a representative table is provided, listing dust explosions that are likely to occur daily in all industrialized countries [12].

According to dust explosion statistics, a large percentage of dust explosions occur in silos designed for storage in the agricultural and food industries [5].

In addition, not included in Table 1 the dust explosion that last occurred in our country in 2023 at the TMO Kocaeli General Directorate (Derince Port Silo) caused the death of 2 people and great material damage [27].

Table 1.Illustrative case examples of dust explosion occurrences (1911–2004)

Date	Location	Material	Plant/building	Dead/injured	Reference
	Turin, Italy	Wheat flour	Bakery	2i	[5]
1807	Leiden, The Netherlands	Black powder	Ship	151d/2000i	[14]
1911	Glascow, UK	▪	▪	5d/8i	[13]
1911	Liverpool, UK	▪	▪	37d/100i	[13]
1911	Manchester, UK	▪	▪	3d/5i	[13]
1913	Manchester, UK	▪	▪	3d/5i	[13]
1916	Duluth, MN	Grain	Steel bin	-	[15]
1919	Cedar Rapids, IA	Corn starch	Starch plant	43d	[13]
1924	Peking, IL	Corn starch	Starch plant	42d	[13]
1924	USA	Sulphide dust	▪	1d/6i	[13]
1924	USA	Sulphide dust	▪	1d/1i	[13]
1924	USA	Sulphide dust	▪	2d/1i	[13]
1926	USA	Sulphide dust	▪	3d/1i	[13]
1930	Liverpool, UK	▪	▪	11d/32i	[13]
1944	Kansas City, KS	Grain dust	▪	▪	[13]
1949	Port Colbourne, CA	Grain	Steel bin	-	[15]
1952	Bound Brook, NJ	Phenolic resin dust	Hammer mill	5d/21i	[13]
1952	Saskatchewan	Grain dust	Shipping bin	6d/14i	[15]
1955	Waynesboro, GA	Grain dust	Feed plant	3d/13i	[15]
1956	South Chicago	Grain dust	Elevator	-	[15]
1958	Kansas City	Grain dust	Elevator	-	[15]
1960	Canada	Sulphide dust	▪	2d/–	[13]
1960	Albern, Vienna	Grain dust	▪	-	[15]
1962	St. Louis, MO	Grain dust	Feed plant	3d/13i	[13]
1964	Paisley, UK	▪	▪	2d/34i	[13]
1965	London, UK	Flour	Flour mill	4d/37i	[15]
1969	Sweden	Sulphide dust	▪	2d/1i	[13]
1970	Kiel, FRG	Grain dust	Grain silo	6d/18i	[13]
1970	Germany	Grain dust	Silos on shipping canal	6d/17i, loss $10 million	[15]
1970	Norway	Wheat grain dust	Silo	▪	[5]
1971	New Orleans	Bushel	Elevator	▪	[15]
1972	Norway	Silicon	Milling section	5d/4i	[5,16]
1973	Norway	Aluminum	Mixing vessel	5d/2i	[5]
1974	Canada	Sulphide dust	Fox mines	▪	[13]
1974	Preska, South Africa	Sulphide dust	Mines	▪	[13]
1975	Norway	Fish meal	Fish meal grinding plant	1d/1i	[5]
1976	Norway	Barley/oats dust	Silo	-	[5]
1976	Oslo, Norway	Malted barley dust	Silo	-	[5]
1977	Galvesto, TX	Grain dust	Grain silo	15d	[13]
1977	Westwego, Louisiana	Grain dust	Grain silo	36d/10i	[16]
1979	Lerida, Spain	Grain dust	Grain silo	7d	[13]
1979	Canada	Sulphide dust	Ruttan mines	▪	[13]
1980	Germany	Coal	Cement factory	-	[5]
1980	Iowa,USA	Corn dust	Bucket elevator	-	[17]
1980	Minnesota,USA	Corn dust	Cross tunnel, bucket elevators	13i	[17]
1980	Naples, Italy	Corn dust	Grain silo	8i	[13]
1980	Ohama,NE,USA	Corn dust	Head house	Loss $3,300,000	[13]
1980	St. Joseph,MO,USA	Corn dust	Shipping bin	1d/4i, loss $2,000,000	[17]

Table 1(Countined)

Date	Location	Material	Plant/building	Dead/injured	Reference
1981	Canada	Sulphide dust	Mattabi mines	*	[13,16]
1981	Corpus Christi, TX	Grain dust	Bucket elevator/Elevator	9d/30i	[17]
1981	Bellwood, NE, USA	Grain dust	Bucket elevator	Loss $6,400,000	[13]
1981	Germany	Coal	il dust burner plant, cement wc	-	[5]
1982	British Columbia, Canada	Coal	Silo	-	[5]
1983	Anglesey, UK	Aluminum	Aluminum powder production	2i	[5]
1984	USA	Coal	Silo	-	[5]
1985	Australia	Sulphide dust	Elura mines	*	[16]
1985	Canada	Sulphide dust	Lynn lake	*	[13]
1985	Germany	Coal	Silo	1i	[5]
1985	Norway	Rape seed flour pellets	Silo	-	[5]
1986	Canada	Sulphide dust	Brunswick mines	*	[13]
1986	Sweden	Sulphide dust	Langsele mines	*	[13]
1986	Canada	Sulphide dust	Dumugami mines	*	[13]
1986	Australia	Sulphide dust	Woodlawn	*	[13]
1987	Canada	Sulphide dust	GECO mines	*	[13]
1987	China	Textile dust	Dust collection system	58d/177i	[18,19]
1987	Oslo, Norway	Malted barley dust	Silo	-	[5]
1988	Norway	Wheat grain dust	Silo	-	[5]
1988	Sweden	Coal	Silo	-	[5]
1989	Sweden	Palletized wheat bran	Silo	-	[5]
1990	Japan	Benzoylperoxide	Storage	9d/17i	[20]
1992	Moriya, Japan	Potassium chlorate and aluminum dust	Mixing operation	3d/58i	[20]
1994	Okaharu, Japan	Cotton waste	Textile mill	*	[13]
1994	Tokyo, Japan	Rubber waste	Shoe factory	5d/22i	[13]
1997	Japan	Tantalum dust	*	1d/1i	[22]
1997	Blaye, France	Grain	Storage	11d	[21]
1999	Michigan	Coal dust (cause for secondary explosion)	Powerhouse	6d/14i	[23]
1999	Massachusetts	Resin	Oven	3d/12i	[24]
2000	Japan	Mg–Al alloy		d/1i	[13]
2000	Modesto California	Aluminum dust	*	*	[16]
2002	Mississippi	Rubber	Recycling plant	5d/*	[25]
2003	Kentucky	Resin	Production line	7d	[26]
2003	Kinston, NC	Polyethylene	Pharmaceutical plant	6d/38i	[26]
2004	Avon, OH	Lacquer dust	*	*	[16]

* Details not available.

2. TYPES OF SİLOS

Today, there are various bulk materials, the total number of which reaches several thousand. Concrete or metal welded silos are used to store these materials [28 – 37].

2.1.Metal Silos

Metal silos are closed cylindrical structures made of airtight galvanized iron sheet. Metal silo technology is effective against insect and rodent damage and effectively protects the harvested grains (SDC, 2008a; FAO, 2008; CIMMYT, 2009a, b). Since the metal silo is not airtight thanks to its insulation, it eliminates the oxygen inside. As a result, it causes the possible harmful insects to die. It also entirely removes any pests or pathogens that might infest the grains inside. It allows the grains to be stored for a long time. Metal silos usually have a carrying capacity between 100 and 3000 kg (SDC, 2008a; FAO, 2008; CIMMYT, 2009a, b) [38].

Crop storage effectiveness is influenced by the duration of storage, the volume of storage, and losses (including quality deterioration) that occur during storage.) [39]. Metal silos can be used in different sizes depending on the need.

Metal silo, a technology used in many countries, provides the following key benefits:

i. It ensures that products are stored in high quality for a long time,
ii. It does not leave any residue in the fumigation that is effective in combating pests and it is airtight,
iii. It significantly reduces the use of pesticides,
iv. They take up little space depending on their location,
v. It significantly reduces post-harvest losses,
vi. It allows small-volume producers to benefit from fluctuating market prices,
vii. It keeps away rodents and other pests that could jeopardize consumer health if consumed,
viii. It can be constructed with local workmanship and materials (FAO, 2008) [38].

2.2.Metal Silo Types

Metal silo types are shown in Fig. 4. Today, silos are stored by filling them with bulk materials carried by horizontal transport systems (chain, belt or helical conveyors) and elevators, which are vertical transport systems, under the control of SCADA and PLC (Programmable Logic Controller).

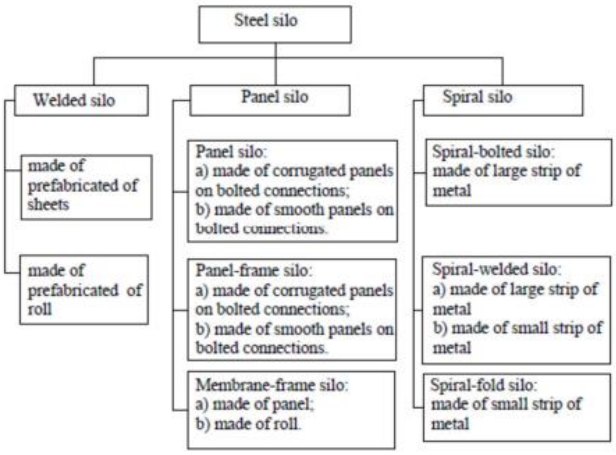

Fig. 4. Classification of metal silos.

If we talk about it in this section the PLC (Programmable Logic Controller) and SCADA (Supervisory Control and Data Acquisition) system used as an automatic system for control and monitoring of grain storage [40, 41].

The main variable that is essential for proper storage of grains is the input variables that will be controlled using PLC. After the SCADA system obtains the necessary information and monitors the general situation, all operational functions (various grain processing equipment such as transportation, cleaning, weighing, ventilation, etc.) are performed by the SCADA user's operating and monitoring interface [42, 43].

PLC is a digital computer that performs control logic, sequencing, timing, arithmetic data processing and counting functions. PLC is designed to withstand multiple environments and temperature etc. Processor (CPU) is the brain of PLC. It has microprocessors to provide logic and control communication between modules. The memories record the results of the logical operations performed by the processor. The IO section consists of input and output modules. This system forms the interface through which the plant devices are connected to the controller [44, 45]. The programming device enters the desired program into the processor's memory. The power supply provides 24 V DC power to the modules. Ladder logic is a programming language primarily used to develop software for PLCs. It conveys a program using a graphical diagram that reflects the circuit diagrams of relay logic hardware [46, 47].

The term SCADA (Supervisory Control and Data Acquisition) generally denotes centralized systems that oversee and manage entire facilities or networks of systems distributed across extensive areas. A Human-Machine Interface (HMI) is a system that shows duration data to an operator, allowing the operator to manage and control the duration. The HMI is frequently linked to the databases and software applications of the SCADA system to access data required for current maintenance, logistical details, and management information, including comprehensive schematics for specific sensors or machines and troubleshooting guides from expert systems (Fig. 5) [48].

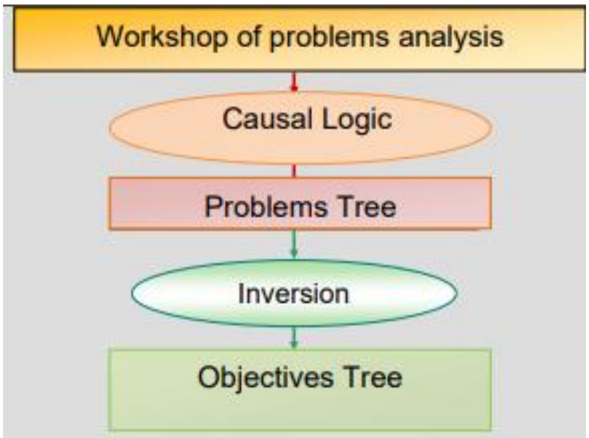

Fig. 5. OOPP method.

Silos are usually either on the ground with a flat base or elevated with a conical base with a steel construction (Fig.6) [49,50]. The opportunity to extract the stored product by gravity feeding makes the conical base very attractive (Fig. 6b), but it has disadvantages such as the height of the structure, the reduced storage capacity, the high energy required to transport the stored product to the storage, the damage to the particles due to the fall of the stored product from a height and the complexity of the structural design. Flat-based silos are lightweight structures, but they are more affected by the wind when empty and are more sensitive to asymmetry during storage [50]. The primary structural components of the silo are the roof, the enclosure and the base. The general appearance of flat and conical-based silos is shown in Fig. 6 [49].

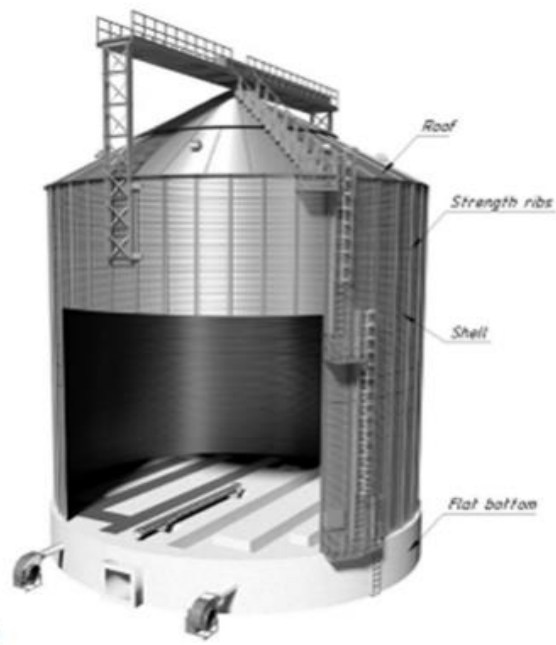

a)

b)

Fig. 6. Elevated (conical bottom) and above ground (flat bottom) silos: a) above ground (flat bottom silo), b) elevated (conical bottom silo) [49].

2.2.a. Welded Silos

Welded silos are made of cylindrical metal sheets welded together as seen in Figs. 6a and 6b. They are divided into two types according to the manufacturing method: prefabricated and roll sheet. Sheet metal silos are made of separate metal sheets welded to a single enclosure. Roll silos made of a single roll with a height that matches the height of the cylinder. In the course of installation, the roll is opened vertically around the foundation to create a complete silo wall. The most well-known benefits of these silos are their tightness and durability [49].

2.2.b. Panel Silos

As seen in Fig. 7c, panel silos are cylindrical structures composed of corrugated or flat sheets that are joined together with bolts. The corrugated panel profile, which provides more resistance against the lateral load of the silo, contributes to metal savings. In industrial silos, supports are created with strength bars to offset the reduction in the panel's load-bearing capacity due to the corrugated profile. The advantages of prefabricated silos are resistance to large radial loads, lack of welding, and high strength. The disadvantage of these silos is the extensive number of bolted flange joints [49]. This form of silo is widely used in both the private and public sectors in our country.

Panel frame silos (Fig. 7d), a type of panel silo, have bent profile panels connected by bolts. Gasketed washers are mounted under the bolt heads to seal the silo. The silo has a conical roof and consists of ring-shaped and radial slats on which the flooring is placed. In addition to its advantages such as the absence of welded joints and its durability, it has disadvantages such as the many bolted joints, leakage, excessive metal usage and elevated labor expenses) [49].

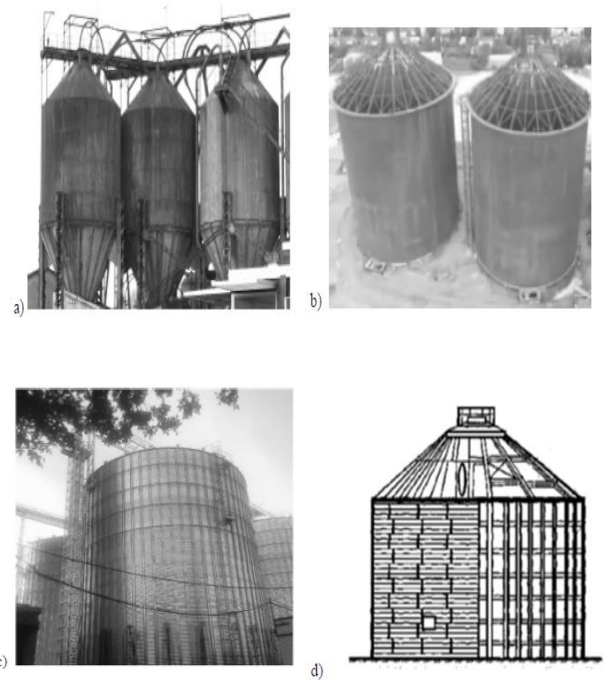

Fig. 7. Different types of metal silos: a, b) welded silos; c) panel type; d) panel frame type [49].

Membrane frame silos were engineered at a research facility in Moscow [51]. The major structural part of these silos), the membrane, is in the shape of a cylinder, made of tape with a thickness of 0.6-1 mm and a width of 1250 mm. This silo option has disadvantages such as excessive material consumption and complicated installation, but it allows full use of the calculated resistance due to the fact that only the membrane, which takes the tensile force, is covered [49].

2.2.c. Spiral Silos

Spiral bolted silos (Fig. 8a) are cylindrical structures made of spirally curved metal strips, the edges of which are connected by bolts at certain intervals with a corner or channel lath. In addition to their advantages such as high strength, their connections are not welded, the roll gap edge does not require additional processing and there are no molded edges for height. Despite their advantages, the need for special and additional equipment for the formation of the enclosure and assembly, the numerous drilling operations for the bolt assembly slots and the assembly of additional vertical beams for wall strength are disadvantages [49].

Spiral welded silo (Fig. 8b) is a cylindrical silo made of a spiral curved metallic strip with welded edges. The rolled geometric billet thickness is 1 – 4 mm, while the width is 300 – 1250 mm. The disadvantage is that a lot of welding is done in the silo field and the edges need to be processed additionally. In addition to the advantage of impermeability, another advantage is its durability [49].

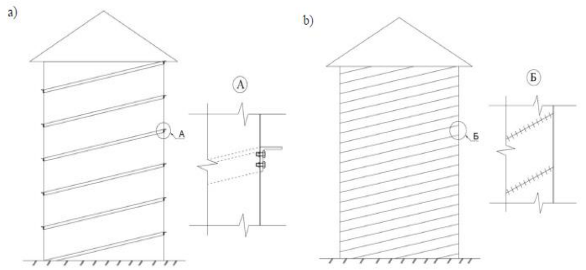

Fig. 8. Spiral silo variations: a) spiral bolted; b) spiral welded [49].

Spiral folded silos (Fig. 9) are cylindrical structures consisting of a spiral connection by double folding of steel strip. This silo, which was first built in Germany in 1969, was conceived in 1968 by German researcher Xavier Lipp, who processed metal sheets using special equipment (Fig. 9) [52]. Some of its advantages are short installation time, low number of assemblers required, low maintenance, earthquake resistance, low cost, long life, and leak-proofness. Its disadvantages include the fact that the silo volume does not exceed 10 thousand m³ and additional costs such as transportation of assembly equipment to the silo installation site [49].

Fig. 9. Spiral -fold silos: Xaver Lipp's first spiral-fold silo, 1969 [49].

3.CATEGORIZATION OF DUSTS

A coating of dust is considered ‘flammable’ if it can be set off by a source of ignition and the resulting fire in the area can continue to spread significantly once the ignition source is gone) [10].

According to the composition of the dust, information on whether it is explosive can be obtained by referring to the list of dusts tested experimentally and published by HM Factory Inspectorate, UK Department of Employment. This classification applies to dusts at or around 25 °C (ambient temperature) at the time of ignition [53].

The combustion class is an additional indicator of a dust layer's ignitability and burning intensity [54,55]. This categorization is based on the way a defined pile behaves when subjected to a gas flame or a hot platinum wire as the ignition source):

a. CC1: no ignition; no spontaneous combustion.

b. CC2: short-term ignition and quick extinguishing; short-term local combustion.

c. CC3: localized burning or flash without propagation; local continuous combustion without spreading.

d. CC4: spread of a glowing fire; burning to spread.

e. CC5: propagation of an open flame; expanding open flame.

f. CC6: explosive combustion; violent burning.

A third type of dust classification is determined by the “K_{St} value”. The "K_{St} value" expresses the highest pressure rate increase when a dust in a 1 m³ container ignites. In other words, it is the intensity of the dust explosion [56]. The K_{St} concept was defined by Bartknecht [57,58], who based it on the so-called cube root law, as follows:

$$\left(\frac{dP}{dt}\right)_{max} V^{1/3} = constant \equiv K_{St} \qquad (1)$$

In the International Standards Organization (ISO), the K_{St} (bar m/s) value, numerically defined by $(\mathrm{dP/dt})_{max}$ (bar/s) in 1 m³ standard test [59], is expressed as a 'specific dust constant'.

The abbreviation 'St' is derived from the German word staub, meaning dust.

Explosivity is ranked according to K_{St} as follows:

K_{st}	= Group St0: Non-explosible		Increasing Explosibility ↓
$0 < K_{st} < 200$	= Group St1	weak	
$200 < K_{st} < 300$	= Group St2	strong	
$300 < K_{st}$	= Group St3	very strong	

Finally, an explosibility index was developed by The Bureau of Mines that ranks dusts against Pittsburgh coal. The explosibility index (IE) developed is equal to the outcome of the explosion intensity (ES) and the ignition susceptibility:

$$\mathrm{IE} = \mathrm{ISxES} \qquad (2)$$

$$IS = \frac{(MITxMIExMEC)_{P_c}}{MITxMIExMEC)_{sample}} \qquad (3)$$

$$ES = \frac{(MEPxMRPR)_{P_c}}{(MEPxMRPR)_{sample}} \qquad (4)$$

In the equations, MEC represents the lowest explosive concentration, MEP denotes the highest explosion pressure, MIE refers to the minimum energy required for ignition, MIT stands for the minimum temperature needed to ignite and MRPR stands for the maximum rate of pressure rise. The subnotations P_c and sample refer to the Pittsburgh coal and sample. This explosibility index is a comparative measure. Therefore, less influenced by the equipment used, although determining it necessitates performing a complete series of tests) [3,8].

4. SOME STUDIES ON DUST EXPLOSION

Alberto Tascón et al. simulated dust explosions in a 16.3 m³ vented silo utilizing a business CFD (computational fluid dynamics) software (Fig. 10). The model used is a cylindrical steel silo with a steel silo with a cylindrical shape and a conical base and concentric chambers, built and equipped in the external experimental zones of the ETSIA School of Agricultural Engineering (Escuela Técnica Superior de Ingenieros Agrónomos) at the Polytechnic University of Madrid. The silos built for these experiments are made of steel and there are three of them, each possessing a distinct chamber non-concentricity. These silos were formerly employed to gauge the pressure applied by the materials contained within [60]. Corn starch values were taken as reference in the simulations.

In their simulations, a silo roof acting as a non-inertial ventilation panel and an inertial ventilation device were modeled. Various parameters that have an effect on the pressures generated by the explosion were investigated, including the properties of the beginning dust cloud, the dimension and place of the dust cloud, and the ignition position. Additionally, various sizes of ventilation areas and activation pressures were considered. The obtained data were reported to be in agreement with explosion venting standards. The findings reveal that the negative pressures created can be of equal magnitude to the overpressures. For the inertial ventilation roof, the pressures and the associated ventilation areas were shown to be in accordance with NFPA 68 [61].

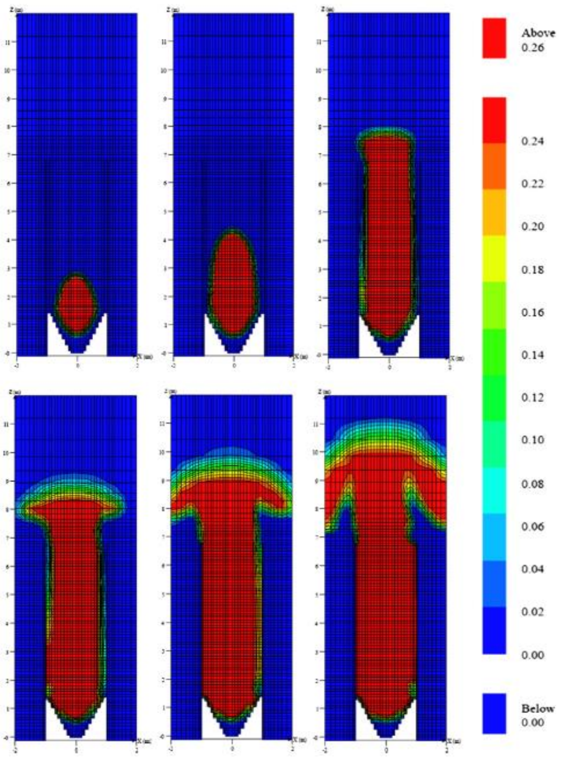

Fig. 10. Simulated flame progression. Contours show the mass fraction of the combustion product (kg/kg). Six time intervals are depicted: 0.384 s, 0.428 s, 0.505 s, 0.520 s, 0.531 s, and 0.550 s. Condition set 1. A=2.84 m². $\mathbf{P_{stat}}$= 0.03 bar (3 kPa) [61].

C.Murillo et al. studied to characterize the behavior of transient gas-solid flow in a revised Hartmann tube (Fig. 11) or related devices. They performed experimental research to assess the parameters affecting the typical properties of flammable solids. For the analysis, the evolution of dust clouds composed of various solid materials within the tube was assessed using fast-motion videos and particle dimension evaluations. They observed that two-phase flow caused changes in the particle dimension spread and separation levels determined during the dispersion process [62].

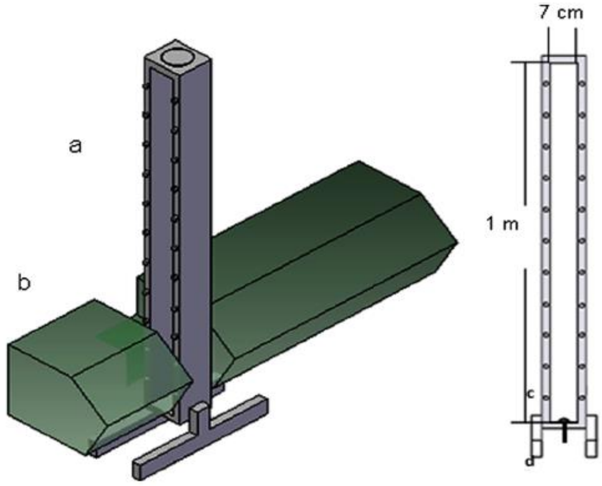

Fig. 11. Experimental apparatus designed for analyzing solid material dispersion. a) Dispersion Tube, b) Particle dimension spread analyzer, c) Dispersion Nozzle, d) Gas Inlet [62].

By modeling the conditions within the aforementioned special test equipment with the CFD (computational fluid dynamics) program ANSYS FLUENT® (Fig. 12), an improved analysis was carried out at micrometric and submicrometric scales in order to evaluate the phase behavior of micrometric aluminum particles, which are dispersed flammable solids in air. Then they compared the data obtained with the CFD model. A computational fluid dynamics (CFD) simulation utilizing the Euler-Lagrangian approach was created using the ANSYS FLUENT program. They aimed to evaluate the flow characteristics related to the clustering and breaking of dispersed particles. Experimental data were used to accurately determine the changes in particle size distributions and to adapt a shattering model using CFD simulation. According to the results achieved from the simulation and experimental trials, the flow behavior of the aluminum powder dispersion in the first stages in the revised Hartmann tube was determined to be in the form of a flat profile. They found that the dispersion of the solid form and the progression of the internal gas flux are significantly affected by the change in the shape of the flow field and the air injection. They recommended the positioning of ignition sources 10 cm above the nozzle according to the mixture homogeneity due to the separation between the aluminum powders. They recommended a minimum ignition delay of 50 to 60 ms(minimum ignition lag of 50 to 60 ms) depending on the phase separation levels and the average diameter of the analyzed sample) [62].

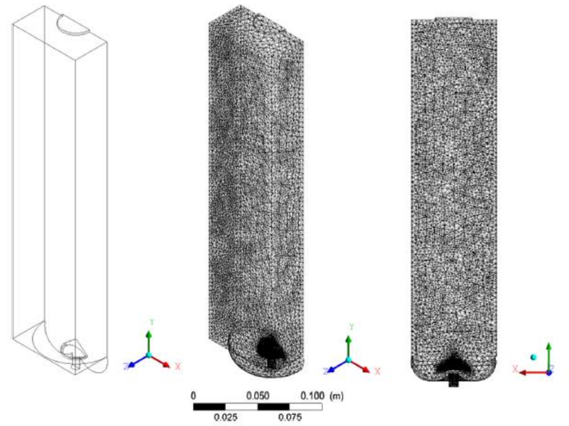

Fig. 12. Overview of the flow field. a) Gas Injection, b) Dispersion Nozzle, c) Outlet [62].

5. CONCLUSIONS

As it is known, different types of products are stored in silos. During storage, explosions can occur as a result of dust spreading and coming into contact with the ignition source. The pressure created by the explosions can cause material damage and even death [6]. In order to overcome the engineering challenges encountered in silo design and dust explosion protection, it is important to understand the characteristics and spreading movement of the dust and to determine the maximum pressure that can occur with an explosion. In addition to experimental studies, studies are also carried out on the aforementioned issues with the computational fluid dynamics method. It is important to examine the effects of diverse variables on the explosion ventilation in silos, encompassing the properties of the beginning dust cloud, the size of the dust cloud, its location, ignition point, the shape of the enclosed area, and the size of the ventilation.

In addition to preventing factors that may cause explosions in grain silos, studies will have a significant role in preventing the spread of flame and pressure when an explosion occurs, ensuring that the building material is manufactured from materials or designed to be resistant to the pressure and flame that will occur, and also determining the locations of silos, which are complex structures, that are prone to explosion in all precautions.

By determining the location where dust formation occurs and in which area of the transport units the explosion density is reached while the product is being transported during the filling or emptying of silos, the dust can be efficiently evacuated from the transport units through dust collection units. In addition, measures can be taken to avoid the dispersion of pressure and flame in order to prevent secondary explosions.

In a grain silo, there are various transport units as well as dust collection units, silo scales, volumetric scales, silos, filling bunkers, etc. All units operate as a whole under PLC and SCADA control. The transport techniques and design forms of the units can be redesigned to reduce the severity of the explosion.

In grain silos, products such as wheat, barley, triticale, corn, rye, oats, etc. are stored. Storage and unloading operations are carried out using common transport lines. For this reason, there are dusts of these products in silos and other units. The studies to be carried out will be a source of generating ideas in silo design according to the pressure or flame situations that could happen by considering the characteristics of the attributes of the dusts of the products to be stored.

In our world with a population of approximately 8 billion people, where food safety has also gained importance due to the significant impact of global climate change, scientific studies are aimed to minimize the material damage, negative effects on human health and loss of life, and possible accidents that may occur as a result of explosions in silos built with great effort and cost, even if they cannot be prevented.

It is important to be able to predict how explosive dusts spread in facilities, what the density, location and sources that can cause explosions are, and the pressures that can occur as a result of explosions through future studies. As a result of the studies to be carried out on the aforementioned issues, it will contribute to the development of issues such as the design of systems that will safely discharge the pressure that will occur due to explosions and the development of new units based on material strength, thus preventing explosions, preventing material accidents, and providing longer-term healthier product storage in grain warehouses.

REFERENCES

[1] Turkish Standards Institute, TS EN 60079-10-2:2015 Explosive Atmospheres - Part 10-2: *Classification of Hazardous Areas - Combustible Dust Atmospheres Standard*.

[2] BS2955: 1958, *Glossary of Terms Relating to Powders*, No. 505, British Standard Institute, London, 1958.

[3] F.P. Lees, *Lees' Loss Prevention in the Process Industries* (Partially updated by S. Mannan), vols. 1–3, Elsevier/Butterworth-Heinemann, Oxford, 2005.

[4] NFPA 68, *Guide for Venting of Deflagrations*, National Fire Protection Association, 2002.

[5] R.K. Eckhoff, *Dust Explosions in the Process Industries*, 3rd ed. Gulf Professional Publishing, USA,2003.

[6] Tasneem A., Abbasi S.A., *Dust explosions–Cases, causes, consequences, and control*, Elsevier, Sayfa: 7-44, 2006.

[7] U.S. Chemical Safety Board (CSB), *Investigation Report Combustible Dust Hazard Study*, Sayfa:0-0, 2006

[8] F.P. Lees, *Loss Prevention in the Process Industries—Hazard Identification, Assessment and Control*, vol. 2, Butterworth Heinemann, London, 1996.

[9] R.D. Pickup, D*ust explosion case study: 'Bad things can still happen to good companies'*, Process Safety Prog. 20 (2001) 169–172.
[10] R. Siwek, *Determination of technical safety indices and factors influencing hazard evaluation of dusts*, J. Loss Prevent. Process Ind. 9 (1996) 21–31.
[11] P. Kosinski, A.C. Hoffmann, *Dust explosions in connected vessels: mathematical modelling*, Powder Technol. 155 (2005) 108–116.
[12] C. Proust, A few fundamental aspects about ignition and flame propagation in dust clouds, J. Loss Prevent. Process Ind. 19 (2005) 104–120.
[13] G. Vijayaraghavan, Impact assessment, modelling, and control of dust explosions in chemical process industries, MTech Thesis, Department of Chemical Engineering, Coimbatore Institute of Technology, 2004.
[14] H.J. Reitsma, The explosion of a ship, loaded with black powder, in Leiden in 1807, Int. J. Impact Eng. 25 (2001) 507–514.
[15] O.F. Theimer, Cause and prevention of dust explosions in grain elevators and flour mills, Powder Technol. 8 (1973) 137–147.
[16] S.K. Kuriechan, Causes and impacts of accidents in chemical process industries and a study of the consequence analysis software, MPhil Thesis, Pondicherry University, 2005.
[17] C.W. Kauffman, R.F. Hubbard, An Investigation of Fourteen Grain Elevator Explosions Occurring between January 1979 and April 1981, Occupational Safety and Health Administration, Washington, DC, 1984.
[18] X. Bowen, The explosion accident in the Harbin Linen textile plant, EuropEx Newslett. (6) (1988).
[19] Z. Hailin, Investigation of the dust explosion in Harbin linen factory, Unpublished English manuscript, 1988 (cited in [5]).
[20] Failure Knowledge Database, Japan Science and TechnologyAgency, http://shippai.jst.go.jp/en/Detail?Ffn=0&id=CC1200059&.
[21] J. Barton (Ed.), Dust Explosion Prevention and Protection: A Practical Guide, Institution of Chemical Engineers (IChemE), Warwickshire, 2002.
[22] National Institute of Occupational Safety and Health, Japan, www.anken.go.jp/english/kenkyu/houkoku/rr 99 03.html.
[23] MIOSHA News, vol. 3, no. 3, OSHA, Michigan, 1999.
[24] R. Zalosh, A tale of two explosion, in: Proceedings of the 34th Annual Loss Prevention Symposium, American Institute of Chemical Engineers, New York, 2000.
[25] OSHA press release on Rouse Polymerics investigation,2000, http://www.osha.gov/pls/oshaweb/owadisp.show document?p table= NEW RELEASES&p id=9830 (cited in [26])
[26] W.L. Frank, Dust explosion prevention and the critical importance of housekeeping, Process Safety Prog. 23 (2004) 175–184.
[27] https://www.ntv.com.tr/turkiye/silolarda-yasanan-patlamada-tmo-ile-taseron-firma-yetkilileri-asli-kusurlu bulundu,ZKaxIr4520CLQM90MStfGA.
[28] Brown, C.J. & Nielsen, J. (Ed.). 2011). *Silos: Fundamentals of Theory, Behaviour*. London and New York: E &FN Spon.
[29] Rotter, J.M. (2001). *Guide for the Economic Design of Circular Metal Silos*. CRC Press.
[30] Elliott, M.D, Teh, L.H.Ahmed, A. (2019). *Behaviour and strength of bolted connections failing in shear*. Journal of Constructional Steel Research, 153, 320-329. https://doi.org/10.1016/j.jcsr.2018.10.029
[31] McCalmont, J.R. (1939). *Silo types and construction*. Washington: U.S. Dept. of Agriculture.
[32] Thomson, F.M. (1997). Storage and Flow of Particulate Solids.
[33] Sielamowicz, I., Balevicius, R. (2013). *Exrerimental and computation analysis of granular material flow in model silos*. Institute of Fundamental Technological Research Polish Academy of Sciences Exrerimental, Warsaw.
[34] Schulze, D. (2009). P*owders and Bulk Solids*. Behavior, Characterization, Storage and Flow. Springer.
[35] Demidov, S.V., Fisenko, A.S., Myslin, V.A. et al. (1984). *Architectural design of industrial enterprises*. Moscow, Stroyizdat.
[36] Rosenblit, G.L. (1953). *Steel structures of buildings and structures of the coal industry*. Moscow: Ugletekhizdat.
[37] Razumov, K.A., Petrov, V.A. (1982). *Design of processing plants*. Moscow, Nedra.
[38] T. Tefera, F. Kanampiu, H. D.Groote, J. Hellin, S. Mugo, S. Kimenju, Y. Beyene, P. M. Boddupalli, B. Shiferaw, M. Banziger (2010).*Review The metal silo: An effective grain storage technology for reducing post-harvest insect and pathogen losses in maize while improving smallholder farmers' food security in developing countries*.Nairobi,Kenya. doi:10.1016/j.cropro.2010.11.015.
[39] Thamaga-Chitja, J.M., Hendriks, S.L., Ortmann, G.F., Green, M., 2004. *Impact of maize storage on rural household food security in Northern Kwazulu-Natal*. Tydskrif vir Gesinsekologie en Verbruikerswetenskappe 32, 8-15.
[40] Glaa, R., Lakhoua, M.N., El Amraoui, L., Using SA-RT method and SCADA for the analysis and the supervision of a hydrogen circuit, Journal of Electrical Engineering, vol. 16, no. 3, 2016.
[41] Lakhoua, M.N., SCADA application of a water steam cycle of a thermal power plant, ICMSAO 2013,IEEE, Hammamet, April 28-30, 2013.

[42] Zhang, C., Zhou, X., Shi, Z., A novel method for measuring the moisture distribution of grain in the silo based on microwave image technology, International Conference on Advanced Mechatronic Systems (ICAMechS), 2017, p. 157-162.

[43] Vogt, M., Gerding, M., Silo and tank vision: applications, challenges, and technical solutions for radar measurement of liquids and bulk solids in silos, vol. 18, IEEE Microwave Magazine, 2017.

[44] Gergely, E.I., Coroiu L, Silaghi H., Dependability analysis of PLC I/O systems used in critical industrial applications, Studies in Computational Intelligence, vol. 417, 2013, p. 201 - 217.

[45] Sheng, Z., Cuicui, J., Hua, S., Application of Siemens PLC and WinCC in the monitoring-control system of bulk grain silo, Chinese Control and Decision Conference (CCDC), 2018, p. 4689 - 4693.

[46] Yigit, E., İsiker, H., Toktas, A., Tjuatja, S., CS-based radar measurement of silos level, IEEE International Geoscience and Remote Sensing Symposium (IGARSS), 2015, p. 3746 - 3749.

[47] Karoui, M.F., Alla, H., Chatti, A., Monitoring of dynamic processes by rectangular hybrid automata, Nonlinear Analysis: Hybrid Systems, 2010.

[48] Lakhoua, M.N., Review on SCADA Cyber security for critical infrastructures, Journal of Computer Science and Control Systems, vol. 10, no. 1, 2017.

[49] S. Pichugin, K. Oksenenko. *Comparatıve Analysıs Of Desıgn Solutıons Of Metal Sılos*. Academic Journal. Series: Industrial Machine Building, Civil Engineering. − 2 (53)2019. https://doi.org/10.26906/znp.2019.53.1890.

[50] J. M. Rotter. *Metal silos*. University of Edinburgh,UK. Progress in Structural Engineering and Materials 1998 Vol I(4): 428-435.

[51] Kiselev, B.E. (1988). *Cylindrical spiral-wound capacity of the membrane-frame type. Design and construction of agricultural facilities*. Ser.: Building materials and structures, buildings and structures, 1, 29-30.

[52] Xaver Lipp. Retrieved from https://xaver-lipp.com/

[53] P.R. Amyotte, A. Basu, F.I. Khan, *Dust explosion hazard of pulverized fuel carry-over*, J. Hazard. Mater. 122 (2005) 23–30.

[54] ISSA, *Determination of the Combustion and Explosion Characteristics of Dusts*, International Social Security Agency, Mannheim, 1998.

[55] J. Gummer, G.A. Lunn, *Ignitions of explosive dust clouds by smouldering and flaming agglomerates*, J. Loss Prevent. Process Ind. 16 (2003) 27–32.

[56] R.K. Eckhoff, *Partial inerting—an additional degree of freedom in dust explosion protection*, J. Loss Prevent. Process Ind. 17 (2004) 187–193.

[57] W.Bartknecht,*Brenngas-undStaubexplosionen, ForschungsberichtF45*.Koblenz Bundesinstitut fur Arbeitsschutz, Federal Republic of Germany,1978 (cited in [2]).

[58] W. Bartknecht, Explosionen, *Ablauf und Schutzmassnahmen*, *Springer-Verlag*, Berlin, 1981 (cited in [2]).

[59] *International Standards Organization*, *Explosion Protection Systems*. Part 1. Determination of Explosion Indices of Combustible Dusts in Air, ISO 6184/1, ISO, Geneva, 1985.

[60] A. Ramírez, J. Nielsen, F. Ayuga, *Pressure measurements in steel silos with eccentric hoppers*, Powder Technol. 201 (2010) 7–20.

[61] A. Tascón, P, J. Aguadob, *CFD simulations to study parameters affecting dust explosion venting in silos*, Powder Technology 272 (2015) 132–141. http://dx.doi.org/10.1016/j.powtec.2014.11.031

[62] C. Murillo,O.Dufaud, N. Bardin-Monnier, O. López, F. Munoz, L. Perrin, *Dust explosions: CFD modeling as a tool to characterize the relevant parameters of the dust dispersion*, Chemical Engineering Science 104 (2013)103–116. http://dx.doi.org/10.1016/j.ces.2013.07.029

Energy, Environment and Storage

Journal Homepage: www.enenstrg.com

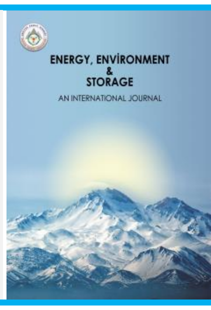

Air Cleaning Plants

Sibel Avunduk[1]

[1]*Vocational School of Health Care, Mugla Sıtkı Kocman University, Marmaris, Mugla, 48187, Turkey*

Tel:0905355565901; E-mail: sibelavunduk@mu.edu.tr

ABSTRACT. Air quality, both outdoor and indoor, is the most critical element that we must protect for the entire environment. While the deterioration of air quality primarily causes respiratory diseases in living things, it also causes corrosive effects on non-living things, such as corrosion caused by acid rain, which results from air pollution. Therefore, it is necessary to monitor and prevent air pollution by various methods. WHO plays an active role in protecting air quality through its mission. Plants are indispensable beings for the environment and life. They balance the CO_2 concentration, temperature, and humidity in the air. Plants use CO_2, light, and water during photosynthesis, which is necessary for their growth and development. They reduce the CO_2 concentration in the environment. In addition, plants, depending on their leaf characteristics, can trap particulate matter in the atmosphere. Many studies have proven that plants positively affect indoor and outdoor air quality. In this review, we aim to summarize the results of some selected studies, provide information about the air purification capacities of the researched plants, and emphasize the topic's importance.

Keywords: diesel, 1,4-dioxane, UV irradiation, chemical stability

Article History: Received: 12.09.2024; Accepted: 29.09.2024; Available Online: 30.09.2024

Doi : https://doi.org/10.52924/JTNJ4189

1. INTRODUCTION

According to WHO, "Air pollution is the contamination of the indoor or outdoor environment by any chemical, physical or biological agent that modifies the natural characteristics of the atmosphere." [1]

In the 1970s, when it was determined that atmospheric pollution was at severe levels. In contrast, the World Health Organization (WHO) determined that pollution was at urban and industrial levels, and the World Meteorological Organization (WMO) started keeping weather records on continental and global scales.[2] WHO's primary goal is to protect people's health in cities. To determine the causes of air pollution, WMO measures air pollution concentrations, investigates their effects on climate, covering continents and the world, and tries to estimate their temporal characteristics. [2] United Nations Environment Program (UNEP) and World Environment Monitoring System (GEMS) further support WHO and WMO enforcement guidelines. [2] GEMS; disseminating early warning systems, determining atmospheric pollution worldwide, and assessing its impact on climate, revealing critical problems related to land use and agriculture.

WHO projects make micro-level (urban) measurements. On the other hand, the WMO network makes measurements at the macro level (continental and world scale) and compares them. GEMS is tightly dependent on WHO projects and WMO records. [2]

Two leading causes of air pollution are the increasing population and, depending on it, industry development.

WHO has classified substances that impair air quality as outdoor and indoor air pollutants. Outdoor air pollutants determined by WHO are PM_{10}, $PM_{2.5}$, O_3, NO_2, SO_2 and CO. In addition, the WHO scanned the scientific studies on indoor air pollution and identified eight substances with definitive evidence that they are polluting and harmful as indoor air pollutants. These pollutants are benzene, CO, formaldehyde, naphthalene, NO_2, polycyclic aromatic hydrocarbons, radon, trichloroethylene, and tetrachlorethylene.

Clean air is the most necessary condition for human life. Both indoor and outdoor air pollution causes respiratory and other illnesses in living beings.

The effects of outdoor pollutants on humans, plants, and materials are summarized in Table 1.

Table 1. The effects of outdoor pollutants

Outdoor Pollutant	Effects on Human	Effects on Plant	Effects on Material
PM_{10}, $PM_{2.5}$	Cerebrovascular, ischemic hearth disease, acute lower respiratory infections, chronic obstructive pulmunary disease(COPD), **Lung cancer mortality** [3]	PMs accumulating on the leaves of green plants resulting in failure of assimilation and photosynthesis and weakening of plant development. [2,4]	They corrode materials, especially if the relative humidity is above 75%, erode building surfaces, and damage and destroy the paint of painted surfaces. [2,4]
O_3	**Respiratory Mortality.** Children, older people, and people with asthma especially are susceptible. [3]	Reduces the agricultural harvest rate and prevents the growth of forests. It disrupts plants' photosynthesis mechanism, causing less carbon dioxide absorption. [5]	causes premature deterioration of buildings [5]
NO_2	**Respiratory Mortality.** Children, older people, and people with asthma especially are susceptible. [3]	causes the brown and dark brown colored burns and spots the leaf edges, the leaves fade, chlorophyll and starch were destroyed. Physiologically, assimilation decreases. [2,4]	shows slight corrosive effect [6]
CO	**Cardiovascular Mortality:** Ischemic hearth disease (IHD) [3]	Plants are more resistant to the effect of CO than animal organisms. That's why they show damage in very high concentrations. [2,4]	Carbon monoxide is a relatively unreactive gas under ambient air conditions and is not absorbed by building materials or ventilation system filters. [7]
SO_2	**Respiratory Mortality.** Children, older people, and people with asthma especially are susceptible. [3]	High concentrations of SO_2 cause acute damage :chlorophyll is rapidly lost, cells disintegrate, and necrosis occurs. In chronic damage: gradual chlorophyll breakdown and chlorosis formation occur without any cellular collapse. This causes a reduction in metabolic activity and a decrease in photosynthesis, and development is generally suppressed. [2,4]	Historical buildings, national buildings, cathedrals, and statues are all destroyed by contact with byproducts of sulfur oxides. Sulfuric acid haze likewise destroys cotton, linen, and nylon. SO_2 increases the corrosion rate of metals such as iron, steel, zinc, copper, and nickel if the relative humidity is above 70%. [2,4]

The effects of indoor pollutants on humans and animals are summarized in Table 2.

Table 2. The effects of indoor pollutants

Indoor Pollutant	Effects on Human & animal
Benzene	Acute myeloid leukaemia, Genotoxicity [7-9]
Formaldehyde	Sensory irritation [7,10]
CO	When acute exposure-occured, exercise intolerance and increase in symptoms of ischaemic heart disease [7,11]
Naphthalene	Respiratory tract lesions causing to inflammation and malignancy in animal studies [7,12]
NO_2	Bronchoconstriction, airway inflammation, and reduced immune defense cause a raised ability for respiratory infection. [7,13]
Polycyclic aromatic hydrocarbons	Lung cancer [7,14]
Radon	Lung cancer Implicative evidence of an related with other cancers, in particular leukaemia and cancers of the extrathoracic airways [7,15]
Trichloroethylene	Carcinogenicity (liver, kidney, bile duct and non-Hodgkin's lymphoma), with the presumption of genotoxicity [7,16]
Tetrachloroethylene	Effects in the kidney suggestive of early renal disease and impaired performance [7,17]

As people spend more time indoors, there is growing unease about indoor air quality. Constructing highly sealed buildings boosts thermal capability but decreases fresh air ventilation. Aggregating and continued exposure to indoor air pollution may result in harmful health outcomes. [18]

Continuous exposure to air pollutants, the concentration of indoors can even be higher than outdoors, may bring about respiratory and cardiovascular diseases, eventually contributing to the so-called 'sick building syndrome' (SBS) and 'building-related illnesses' (BRI). [19]

Sick building syndrome (SBS) is defined by symptoms such as headaches, nausea, lightheadedness, eye irritation, mucous membranes, and respiratory systems [20]. The SBS affects people's well-being, health, and, most importantly, productivity in indoor environments. High CO_2 levels and low humidity contribute to sicknesses, such as eye dryness, migraines, and reduced academic performance. [21] SBS has proven to be challenging to understand. At the same time, symptom frequencies tend to be higher in women due to historical reasons, social position, lack of knowledge of female physiology, and chemical hypersensitivity [22]. Furthermore, poor indoor air quality (IAQ) increases absenteeism and negative emotions [23]. This underlines the significant impact of SBS on productivity, a key concern for all stakeholders.

Plants balance CO_2 concentration, temperature, and humidity [21, 24]. They use CO_2, water, and light via photosynthesis, which is fundamental for their growth and survival [25]. During photosynthesis, plants can minimize the CO_2 levels in the environment [26]. In addition, photosynthesis in plants produces negative air ions that benefit human health [27]. However, the current research on the correlation between CO_2 levels and plants' capacity to remove CO_2 is limited, highlighting the need for further exploration in this area. Plants' ability to alleviate PM and CO_2 alters among plant species and environmental conditions [28].

Air phytoremediation (AP) is an ecological remediation technology that utilizes green plants to eliminate pollutants from polluted air [29, 30]. Some plants can assimilate, degrade, or modify toxic contaminants in the air into less toxic ones, making it possible to remove airborne pollutants via AP technology [29,31].

For an extensive review of published articles on air-cleaning plants, we collected the articles using databases such as Google Scholar, Science Direct, Web of Science, Scopus, and Science finder since 1980. We initially collected the references using the keyword "Air-cleaning plants," and then keywords such as "Phytoremediation" and "Bioremediation" were utilized to conduct a more comprehensive survey of references. After thoroughly reviewing the initially selected references, we finally chose 75 papers.

2. THE PLANTS REMOVING THE INDOOR AIR POLLUTANTS

Our literature survey revealed four reviews that overlapped the topic of "plants removing indoor pollutants." Since we read seven plants mentioned in all four reviews, this section mentioned the articles on their seven plants clearing indoor pollutants.

2.1 Chlorophytum comosum (Spider Plant)

The removal of benzene, toluene, cigarette smoke, xylene, formaldehyde, ethylbenzene, and the mixture of benzene, toluene, octane, and trichloroethylene, α-Pinene, i.e volatile organic compounds-VOCs, Particulate matter (PM), and CO_2 were investigated on *Chlorophytum comosum*.

Figure 1. The photo of *Chlorophytum comosum* [32]

Sriprapat et al. [33] tested the removal capacity of toluene and ethylbenzene on the plants *Aloe vera, Sansevieria masoniana, Sansevieria trifasciata, Sansevieria hyacinthoides, Sansevieria ehrenbergii, Kalanchoe blossfeldiana, Dracaenaderemensis, Codiaeum variegatum, Chlorophytum comosum, Dracaena sanderiana, Cordyline fruticosa, Aglaonema commutatum*. The highest removal values are for toluene, *S. trifasciata,* ethylbenzene, *C. comosum*. Also *S. trifasciata* and *S. hyacinthoides* had a high value in the absorption of toluene and ethylbenzene.

Another Sriprapat et al. study [34] showed the experimental data for eight species of plant, involving *Sansevieria trifasciata*, *Euphorbia milii*, *Epipremnum aureum*, *Syngonium podophyllum*, *Hedera helix*, *Chlorophytum comosum*, *Dracaena sanderiana*, and *Clitoria ternatea*, for eliminating benzene in air and water pollutants. These indoor plants are eminent for their high tolerance to toxic pollutants. During 96 hours, it presented that *C. comosum* had the most potential among other plants for eliminating benzene from air and water pollutants.

Torpy et al. [35] researched CO_2 removal of *Chlorophytum comosum* and *Epipremnum aureum* using green wall technology.

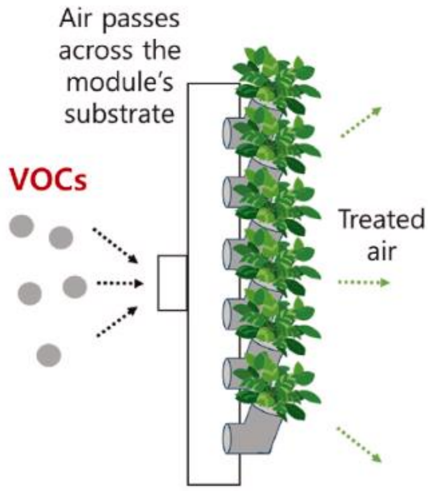

Figure 2. Active green wall system [36]

Both of the plants were active in CO_2 elimination at densities higher than 50 μmol/m^{2}s. When the intensity of the light elevated, the green wall achieved meaningful reductions in high CO_2 concentrations within a sealed room environment.

Xu et al. [37] studied the formaldehyde removal performance of *Chlorophytum comosum*. They found its volatile organic compound (VOC) removal performance to be 90%, 92%, and 95% at the light intensities of 80, 160, and 240 μmol/m^{2}s, respectively.

In the third research study by Sriprapat et al. [38], they screen fifteen plant species to determine their capability to remove xylene volatile aromatic compounds. The results exhibited that the most active plants for xylene removal after 24 hours were *C. comosum, A. commutatum, P. martianum, A. rotundum, and F. albivenis*. These plants could take up xylene at a rate of around 0.66±0.00, 0.65±0.03, 0.68±0.00, 0.66±0.00, and 0.64 ±0.54 mmol/m^2-leaf area, respectively. But, after 24 hours of xylene exposure, their activity was not the best. At 48 hours, the results exhibited that *Z. zamiifolia* reduced xylene levels significantly better than other plants ($P \leq 0.05$). This plant showed the highest xylene removal efficiency, with uptake of 0.81 ±0.01 mmol/m^2 leaf area, around four times higher than that of *G. lingulata*, the least effective of the 15 species tested. At 72 hours, *Z. zamiifolia* showed consistently high xylene removal ability. This plant could take up approximately 88 % of xylene within 72 hours of fumigation.

In 2020, Siswanto et al. [39] investigated the *comosum*, *Sansevieria trifasciata*, with a 120 m^3 /h airflow rate in a 24 m^3 testing room. This chamber experiment used the simulated cigarette smoke containing 120–150 ppm of formaldehyde, 127–145 ppm of acetone, 13–35 ppb of benzene, and 30–70 ppb of xylene. After 24 hours, VOC (Volatile Organic Compound) removal performance was 80–90%.

The removal capacity of the mixture of benzene, toluene, octane, trichloroethylene, and α-Pinene of *Chlorophytum comosum* together with 27 plant species were tested. [40] *Hemigraphis alternata, Hedera helix, Hoya carnosa*, and

Asparagus densiflorus had the best elimination efficiencies for all contaminants; *Hemigraphis alternata* showed superior removal activity for all five VOCs (i.e., benzene; 5.54 ± 0.29, toluene; 9.63 ± 0.94, Octane; 5.58 ± 0.68, TCE; 11.08 ± 0.99, and a-pinene; 12.21 ± 1.61). VOCs removal performance of *Chlorophytum comosum for* benzene; 0.75 ± 0.11, Toluene; 3.18 ± 0.14, Octane; 1.70 ± 0.08, Trichloroethylene; 2.86 ± 0.13, α-Pinene; 4.17 ± 0.21 μg/ m^3 h cm^2-leaf area.

Gawronska et al. [41] displayed that the accumulation percentage of large PM (PM_{10}) of *Chlorophytum comosum* was 68, and of fine PM ($PM_{2.5}$) was 7 in indoor environments. Irga et al. [42] used spider plant green wall to test PM removal. They found it has excellent potential for PM removal. They also displayed that the rate of air affects PM removal. The 11 L/s of airflow rate has the highest filtration among the tested rates of 4 to 15 L/s, and the removal efficiency reached up to 53 ± 10%.

2.2 Chrysanthemum morifolium (Garden Mum, Autum Mum)

Figure 3. The photo of *Chrysanthemum morifolium* [43]

Chrysanthemum morifolium, a decorative perennial shrub, could remove formaldehyde in liquid nutrient solution and soil conditions [44-45].

2.3 *Dracaena deremensis* (Corn plant)

Figure 4. The photo of Dracaena deremensis [46] & Dracaena fragrans Lemon Lime [47]

In 2004, Orwell et al. [48] searched the 25 ppm benzene removal capacity of *Dracaena deremensis.* They found its' removal performance of 188±48 ppm/d m^2-leaf area. In their other study, Orwell and his colleagues [49] investigated 100 ppm toluene and its xylene removal capacity. They obtained these removal data: Toluene in single: 549 ± 31.8, Xylene in single: 336 ± 21.8, Toluene in mixture: 284 ± 27.3, Xylene in mixture: 229 ± 11.4 mg/m^3 d.

Mosaddegh and co-workers [50] researched the application of a mixture of benzene, toluene, ethylbenzene, and xylene (each two ppm) to the plant. The results were 0.52 for benzene, 0.24 for toluene, and 0.76 mg/ d m^2-leaf area for ethylbenzene and xylene.

Sriprapat et al. [33] studied the *Dracaena fragrans* Lemon Lime. They measured its removal performance against toluene and ethylbenzene (each 20 ppm). After 72 hours, the plant eliminated 2.12 ± 0.17 μmol toluene and 2.36 ± 0.11 μmol ethylbenzene.

2.4 *Epipremnum aureum* (Golden pothos)

Figure 5. The photo of *Epipremnum aureum* [51]

Epipremnum aureum is one of the most typical plants for phytoremediation of indoor VOCs, including benzene and formaldehyde [34,43, 45,52-55]. This plant has different names, such as golden pothos, Ceylon creeper, hunter's robe, ivy arum, and silver vine [36]. It can remove formaldehyde (61.7% removal in 12 hours) and total volatile organic compounds (TVOCs) (30.0% removal in 12 hours) from tobacco smoke [56].

Epipremnum aureum has also been tested using some biofilter systems.

One is developed by Ibrahim et al. [57] as a botanical indoor air biofilter prototype utilizing *Epipremnum aureum* horizontally cultivated into Kenaf fiber. The act of the biofilter in eliminating VOCs after entering aromatic compounds was evaluated in a lab-scale chamber (0.24 m^3), displaying a single-pass removal efficiency of TVOCs of 46 ± 4.02%. Another tested system, an activated carbon-based phytofiltration system planted with *Epipremnum aureum*, was set up to control indoor VOCs in an office area (265 m^3) in New York, USA, over four days [58]. The system demonstrated tremendous single-pass removal efficiencies of formaldehyde (100–91.3%) and TVOCs (51.5–38.4%).

Wang and Zhang [58] checked the short and long-term strength of an activated carbon-based phytofiltration system in a full-scale chamber. This system used a mixture of granular activated carbon and shale pebbles (1:1, v/v) as the plant growth medium, with *Epipremnum aureum* horizontally planted (Fig. 6). The single-pass removal activity of toluene (2.16 ppm) by the system were 91.7%

and 77.2% at airflow rates of 250 and 930 m^3/h, respectively. Similarly, the single-pass removal activity of formaldehyde (1.64 ppm) was 98.7% and 69.0% at 250 and 930 m^3/h, respectively. The phytofiltration system reduced outdoor ventilation rates, resulting in 10–15% energy savings.

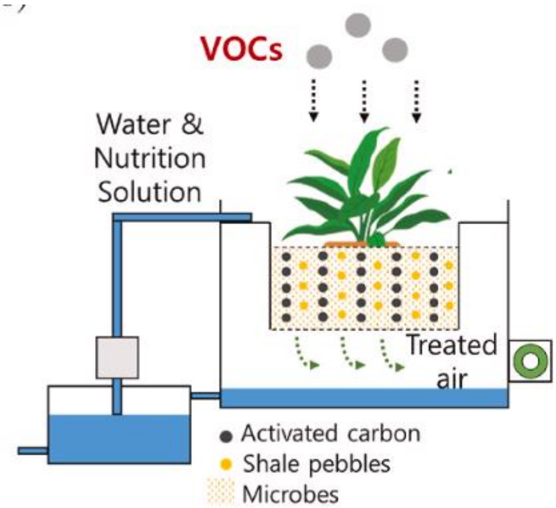

Figure 6. Phytofiltration System [36]

2.5 *Hedera helix* (English Ivy)

Figure 7. The photo of Hedera helix [59]

English ivy, *Hedera helix*, has green leaves for the year and is a climbing plant growing on surfaces like cliffs, walls, and trees. It also grows as horizontal surfaces. This plant is accepted to remove indoor VOCs, containing benzene, formaldehyde, and a mixture of benzene, toluene, octane, TCE, and α-pinene [44, 60, 34, 40, 61]. The removal rates of *Hedera helix* were 3.63, 8.25, 5.10, 8.07, and 13.28 μg/m^3 h m^2-leaf area for benzene, toluene, octane, TCE, and α-pinene, respectively, under mixed gases (each ten ppm) [40].

2.6 *Sansevieria trifasciata* (Snake plant, Mother-in-law's tongue)

Sansevieria trifasciata (sin. *Dracaena trifasciata* [63]) is a perennial plant that forms dense strands and spreads through its creeping rhizomes [64].

Figure 8. The photo of *Sansevieria trifasciata* [62]

This plant's removal performance of benzene [34] and toluene-ethylbenzene [33], a mixture of benzene, toluene, octane, trichloroethylene, and α-Pinene (each 10 ppm) [40] has been studied. The removal of benzene is 25.40 ± 0.14 μmol/h m^2-leaf area [34], 2.68 ± 0.19 μmol for toluene, and 2.74 ± 0.13 μmol for ethylbenzene in 72 hours [42]. For the mixture of VOCs study, the removal of benzene is 1.76 ± 0.48; toluene is 4.97 ± 0.70; octane is 2.73 ± 0.50; trichloroethylene is 4.61 ± 0.81; α-Pinene is 5.49 ± 1.31 μg/ m^3h cm^2-leaf area. Additionally, Permana et al. [65] did experiments utilizing a 24 m^3 chamber to measure VOCs removal by a botanical biofilter from cigarette smoke at various distances (100–315 cm). The biofilter consisted of Sansevieria trifasciata planted in soil and coconut fiber. Within 24 h, the biofilter achieved removal rates of TVOCs, formaldehyde, and acetone ranging from 40 to 65%, 46 to 69%, and 31 to 61%, respectively. Interestingly, VOCs removal was exceptionally high at a distance of 100 cm, suggesting that the biofilter likely created airflow vortices at that height.

2.7 *Syngonium podophyllum* (Arrowhead plant)

Figure 9. The photo of Syngonium podophyllum [66]

Syngonium podophyllum is a favorite houseplant known for eliminating benzene (103.4 ng/m^3 h cm^2-leaf area), toluene

(161.6 ng/m^3 h cm^2-leaf area), and formaldehyde (0.5 µg/cm^2-leaf area in 6 h) [67, 34, 68, 61].

3. THE PLANTS REMOVING THE OUTDOOR AIR POLLUTANTS

Following the similar logic in the previous section, this section includes articles about the four most mentioned and studied plants that clean pollutants in the outdoor environment.

3.1 *Sophora japonica*

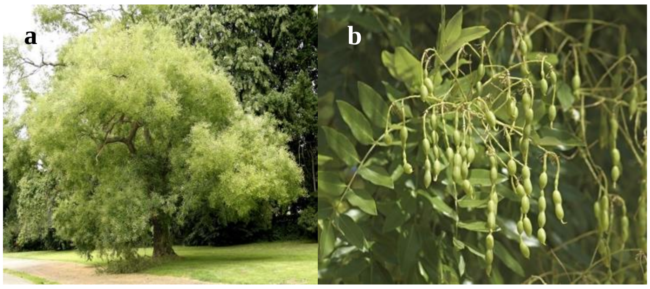

Figure 10. The photos of *Sophora japonica*[a69-b70]

Sophora japonica, the **Japanese pagoda tree [71]** (also called the **Chinese scholar tree** and **pagoda tree;** syn. *Styphnolobium japonicum)* is a species of lovely tree.

Zhang et al. [72] selected nine plant species for their research from among the dominant roadside plant species: two shrubs (*Euonymus japonicus, Rosa chinensis*), one climber species (*Parthenocissus quinquefolia*), and six tree species, including two conifers (*Pinus tabuliformis, Sabina chinensis*) and four broadleaved trees (*Sophora japonica*, *Ulmus pumila*, *Populus sp., and Ginkgo biloba*).

Sophora japonica, with its unique morphological characteristics, including significant trichomes, a dense network of grooves, and a complex cuticular wax layer, displayed the topmost PM capture capacity [73]. Needles of some species of conifers have thicker wax layers that contribute to PM deposition, suggesting that these species may have a high capacity for accumulating PM [74-76]. PM capture efficiency (362.98 µg/cm^2) and its wax layers could trap large amounts of $PM_{2.5}$; this high potential is essential for successful phytoremediation. *Sophora japonica* also showed the largest APTI (air pollution tolerance index) at both sites (traffic pollution and water reservoir). Combining the effect size of air pollution on membrane lipid peroxidation with APTI might better reflect plants' tolerance to air pollution. Shi et al. [77-78] reached the same result about *Sophora japonica* in their research.

Yue et al. [79] investigated the retention characteristics of five tree species' water-soluble and water-insoluble particulate matter in Beijing, China. They found that *Sophora japonica* has high PM (water-soluble PM and water-insoluble PM) capacities.

The team made a significant comparison in a unique study about the NOx absorption ability of *Sophora japonica* [80]. They explored the nitrogen contribution of traffic-related NOx at the road-adjacent sites (23.0%), which was higher than that of traffic-related NOx at sites far from the road (16.4%). This comparison highlighted the influence of traffic-related NOx emissions on the *S. japonica* in near-road green spaces, characterized by lower δ15N values.

3.2 *Salix babylonica*

Figure 11. The photos of *Salix babylonica* [a81-b82]

*Salix babylonica***,** known as **Babylon willow** or **weeping willow in public,** is a species of willow growing wildly in northern China but cultivated for millennia elsewhere in Asia, being traded along the Silk Road to southwest Asia and Europe. [83-84]

In a research of Wang et al. [85], measured the retention capacity of *Ulmus pumila, Salix babylonica, Ginkgo biloba*. The accumulation of $PM_{2.5}$ of *Salix babylonica* was detected as high after *Ulmus pumila* because it has a thin wax film and wax tubes.

Luo et al. [86] conducted a dynamic analysis of the retention ratio of six tree species, including *Salix babylonica*, in rainfall conditions. This research compared the broad-leaved trees (*Salix babylonica, Acer elegantulum*) with needle-leaved trees (*Pinus tabuliformis* and *Pinus bungeana*). The findings, which revealed the stronger ability of needle-leaved trees to retain $PM_{2.5}$ than broadleaved trees and the unique prismatic structure of their leaves, have significant practical implications for environmentalists and researchers alike.

Liu et al. [87] meticulously studied different PM types' retention capacity and efficiency. Their thorough research involved measuring the PM retention efficiencies of easily removable (ERP), difficult-to-remove (DRP), and total removable (TRP) particles on the leaf retention efficiency (AE_{leaf}). They found that *Pinus tabuliformis* absorbs particles with the largest average diameter (34.2 µm), followed by *Ginkgo biloba* (20.5 µm), *Sabina chinensis* (16.4 µm), *Salix babylonica* (16.0 µm), and *S. japonica* (13.1 µm). The high retention efficiencies of *S. babylonica* and *P. tabuliformis* for different particulate matter sizes (TRP and ERP of $PM_{2.5–5}$ and $PM_{5–10}$, and $PM_{>10}$ and TSP with the highest AE_{leaf}) further validate the meticulousness of their research.

In the research of Yue et al. [79], *Salix babylonica* has a high retention capacity of water-soluble PM (WSPM) after *Sophora japonica*. The water-insoluble PM (WIPM) comes after *Sophora japonica* and *P. tabuliformis*.

3.3 *Ginkgo biloba*

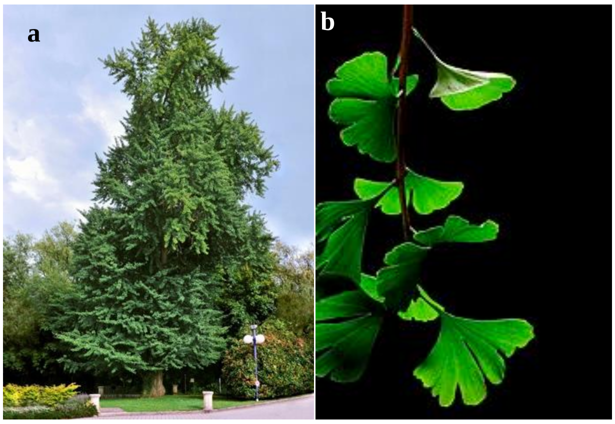

Figure 12. The photos of *Ginkgo biloba* [ab 88]

Ginkgos are enormous trees, typically coming to a height of 20–35 m [89], with some China specimens reaching over 50 m (165 ft). Their branches have an angular crown shape and are long and somewhat erratic. The tree is usually deep-rooted and invulnerable to wind and snow damage.

According to Zhang et al. [72], *Ginkgo biloba* trapped the lowest amount of PM, and the grooves on its leaf surfaces were the sparsest. In the study of Yue et al. [79], *Ginkgo biloba* has the third highest retention capacity of water-soluble PM (WSPM) after *Sophora japonica* and *Salix babylonica*. *Ginkgo biloba* has the second lowest retention capacity of water-insoluble PM (WIPM) after *S. chinensis*. Liu et al. [87] have found moderate retention efficiency in *Ginkgo biloba*. Wang et al. [85] also studied on this plant. After their experiments, they determined that the thick wax tubes of *Ginkgo biloba* reduced the interface area for locating particles and had the least capacity for PM capture.

3.4 *Sabina chinensis*

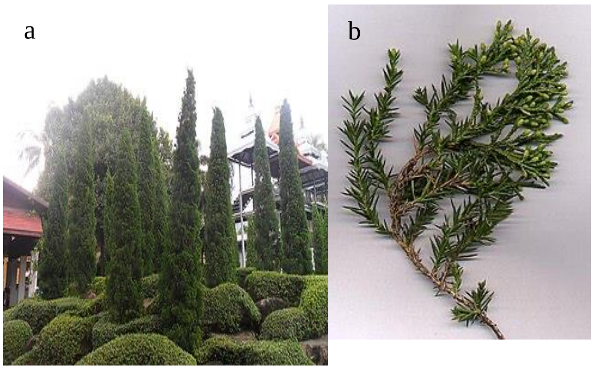

Figure 13. The photos of *Sabina chinensis* [ab90]

Sabina chinensis (syn. Juniperus chinensis [91]) is a famous ornamental tree or shrub suitable for gardens and parks. It lives in harsh coastal conditions of hot sun and sandy, fast-draining soils.

Xie et al. [92] studied the PM retention of different trees (*Cedrus deodara, Acer palmatum, Sabina chinensis, Metasequoia glyptostroboides, Buxus sinica, Magnolia grandiflora*) under various wind conditions. The ranking of PM retention is *Cedrus deodara* > *Acer palmatum* > *Sabina chinensis* > *Metasequoia glyptostroboides* > *Buxus sinica* > *Magnolia grandiflora*, i.e., *Sabina chinensis* has the third-most PM retention capacity. In Liu et al.'s [87] investigation, *Sabina chinensis* was third in the particular absorption ranking after *Pinus tabuliformis* and *Ginkgo biloba*. However, Yue et al.'s research revealed that *Sabina chinensis*'s water-soluble and water-insoluble retention efficiency had the lowest values compared with the other studied plants. In another different concept of PM retention research [72], *Sabina chinensis* and *P. tabuliformis* had high PM as the in-wax PM (PMWT) at both sites (traffic pollution and water reservoir), showing that conifers can potentially catch a significant amount of PM in their thicker wax layers.

4. CONCLUSIONS

Air-phytoremediation is a research field with a vast literature collection. The studies accelerate after the 2000s. As a result of our literature survey, we encountered the removal capacity of indoor pollutants on 140 plants. Some plants' removal efficiency has been studied against all indoor pollutants. Only one or two indoor pollutants for some. Different techniques and, depending on that, various units have been used to measure removal capacity, like µmol in 72 hours, mmol/ d cm^2-leaf area, and $\mu g/m^3h$ cm^2-leaf area. Since then, we have made a column graphic using only the removal data [36], which have the same units to summarize the removal efficiency of plants for some indoor pollutants (Figure 14-16).

According to the review by Bandehali et al. [97], recommended Peace Lily (*Spathiphyllum*), Ficus species (*Ficus Decora* Burgundy), Calathia (Calathia Species), Dieffenbachia (Dieffenbachia Species), Golden Pothos (*Epipremnum aureum*) against **ozone** indoor pollutant; *Schefflera actinophylla* and *Ficus benghalensis* against **toluene and xylene**; *Hedera helix* against **only toluene**; *Syngonium podophyllum, Sansevieria trifasciata, Euphorbia milii, Chlorophytum comosum, Epipremnum aureum, Dracaena sanderiana, Hedera helix, Clitoria ternatea* against **benzene**; ficus; golden pothos; spider fern; Christmas cactus (*Schlumbergera x buckleyi*) against **trichloroethylene, tetrachloroethylene 1,2-dichloroethane benzene, toluene m, p-xylene**, Spider plants (*Chlorophytum comosum L.*) against **PM**; *Aloe vera, Sansevieria masoniana, Sansevieria trifasciata, Sansevieria hyacinthoides, Sansevieria ehrenbergii, Kalanchoe blossfeldiana, Dracaena deremensis, Codiaeum variegatum, Chlorophytum comosum, Dracaena sanderiana, Cordyline fruticosa, Aglaonema commutatum* against **toluene, ethylbenzene**; *Chamaedorea seifritzii, Aglaonema modestum, Hedera helix, Ficus benjamina, Gerbera jamesonii, Dracaena deremensis, Dracaena marginata, Dracaena massangeana, Sansevieria laurentii, Spathiphyllum, Chrysanthemum morifolium, Dracaena deremensis* against **benzene, trichloroethylene, formaldehyde;** Golden Pothos against **formaldehyde**.

Although it has been inferred that plants give us clean indoor air from the considerable research collection, the research is still limited. The experiments were conducted in sealed and controlled chambers [98]. The conditions within sealed chambers do not scale up to those of natural indoor environments, which have high AER (air exchange rate), large volumes, and persistent VOC emissions. The conclusion of Cummings & Waring [38] that plants have an unimportant effect on indoor VOC loads is coherent with the results of field works that did not notice actual VOC decreasing when plants were planted in buildings. Regardless of potted plants not considerably changing indoor VOC concentrations, conducting chamber experiments on plants can remain a significant effort. There is still much to be acquired information about the mechanisms of botanical uptake of VOCs. Extended laboratory and field investigations must evolve a more outright and nuanced understanding of the coaction between plants and indoor environmental outcomes.

Considering the removal capacity of outdoor pollutants by plants, the research is concentrated on PM removal. Outdoor plants, trees, shrubs, meadows, and other plants have been studied. According to our literature survey, the PM retention capacity of 136 plants has been researched. Leaf roughness, cuticle characteristics, and ability to absorb moisture are essential for PM retention and caught by plants. However, not only the morphological conditions but also the physiological and developmental properties of leaves, in addition to the plant flowering form, the meteorological conditions, the traffic flows, the distance to the source, and the PM characteristics, make the processes of accumulation, wash-off, and resuspension of PM more difficult than expected, and its effect on air quality, demanding and complex [78]. It is found that, like Beckett et al. [99] and the other outdoor research, all trees examined captured large quantities of airborne particulates from the health-damaging size fractions (particle diameters of 10-2.5 µm, 2.5-1 µm, and <1 µm). For example, coniferous species were found to trap more particles than broad leaves, with pines (Pinus spp.) capturing significantly more material than cypresses (Cupresses spp.). Trees near a busy road caught substantially more material from the huge particle size fraction than those at a rural background site.

Beckett et al. [99] drew the main conclusions from their study as follows:

- Trees can trap an important amount of health-damaging particles from the atmosphere, potentially improving local air quality.

- Their study reveals significant species differences in trees' ability to capture pollutant particles, suggesting that conifers may be the most effective choice for pollution-control plantings.

- Among the broad-leaved species they studied, those with rough leaf surfaces demonstrate the highest effectiveness in capturing particles, a crucial finding for future planting decisions.

While significant research has been done on the air-cleaning ability of various plants, there is an urgent need for more experimental studies using diverse methods. As researchers, we aim to identify the most effective air-cleaning plants, such as Chlorophytum comosum, Chrysanthemum morifolium, Dieffenbachia compacta, and Epipremnum aureum, enhance their cultivation conditions, and potentially create fast-growing plants that can thrive in extreme conditions and have a high capacity for removing air pollutants.

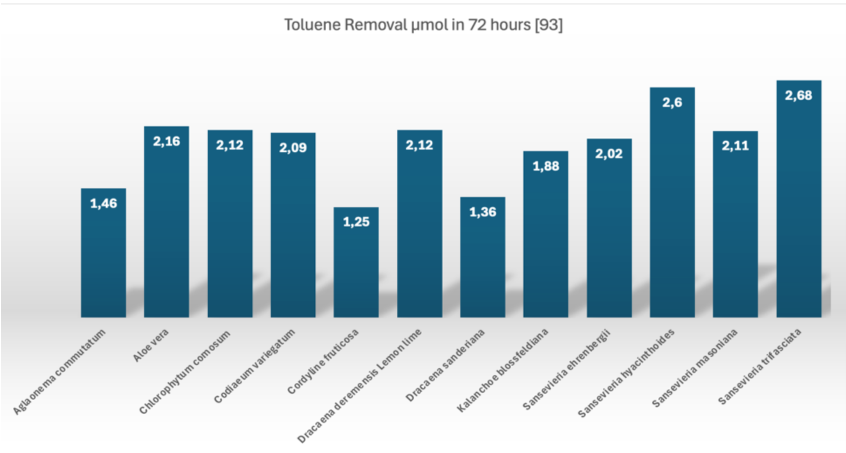

Figure 14 Toluene Removal of some plants (µmol in 72 hours)

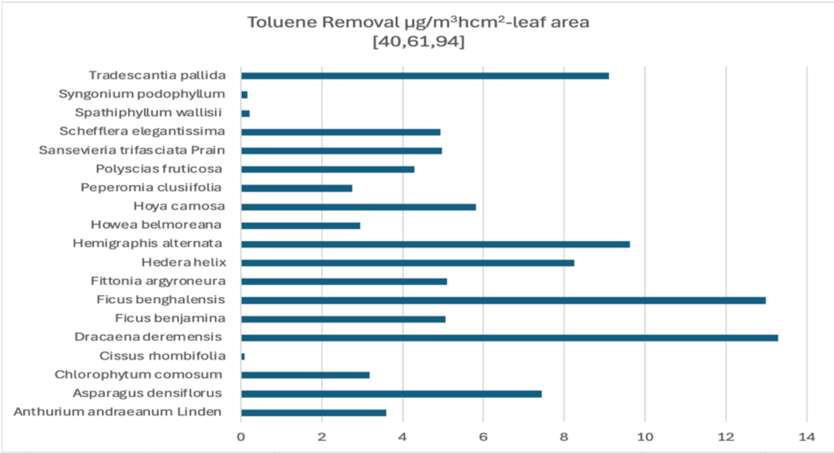

Figure 15 Toluene Removal of some plants (µg/m^3hcm^2-leaf area)

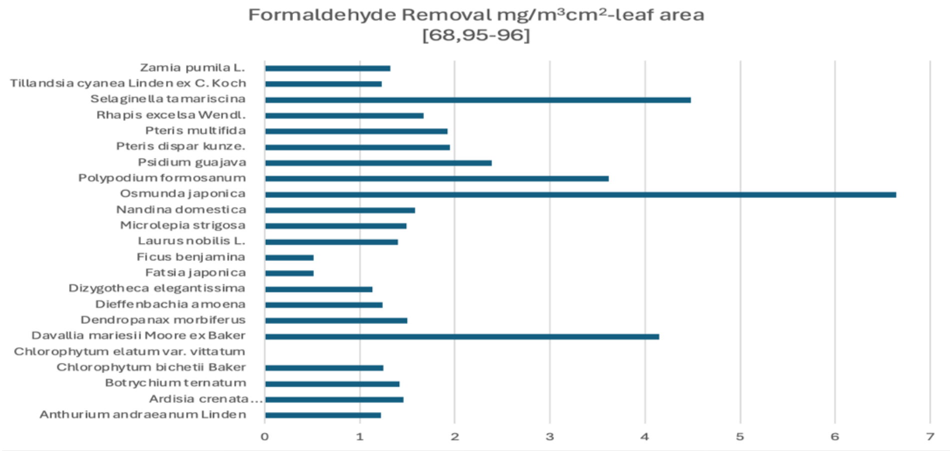

Figure 16 Formaldehyde Removal of some plants (mg/m^3cm^2-leaf area)

REFERENCES

[1]https://www.who.int/health-topics/air-pollution#tab=tab_1

[2] B. Cuma Air pollution and Controlling Lecture Notes Istanbul University, Faculty of Engineering, Department of Environment Engineering

[3] WHO global air quality guidelines. Particulate matter ($PM_{2.5}$ and PM_{10}), ozone, nitrogen dioxide, sulfur dioxide and carbon monoxide. Geneva: World Health Organization. Licence: CCBY-NC-SA3.0IGO, 2021.

[4] T. Oğuz Can, Chap. 3: "Air Pollution and Atmosphere" Ankara University Environmental Pollution Lecture Notes.

[5]The fact sheet on ground-level ozone pollution, Ministry of Environment and Urbanization, General Directorate of Environmental Management, 2014.

[6]S. Oesch, M. Faller, Environmental effects on materials: The effect of the air pollutants SO_2, NO_2, NO and O_3 on the corrosion of copper, zinc and aluminium. A short literature survey and results of laboratory exposures, Corrosion Science, 39(9), 1505-1530, 1997.

[7] WHO guidelines for indoor air quality: Selected Pollutants. Geneva: The World Health Organization European Center for Environment and Health, Bonn Office, 2010.

[8] Kirkeleit J Riise T, Bråtveit M E Moen B Increased risk of acute myelogenous leukemia and multiple myeloma in a historical cohort of upstream petroleum workers exposed to crude oil. Cancer Cause Control, 2008, 19:13–23.

[9] Pandey AK Bajpayee M , Parmar D , Kumar R, Rastogi S K , Mathur N , Thorning, P, de Matas M, Shao Q, Anderson D, Dhawan A, Multipronged evaluation of genotoxicity in Indian petrol- pump workers. Environmental and Molecular Mutagenesis, 2008, 49:696–707.

[10] Noisel N, Bouchard M, Carrier G. Evaluation of the health impact of lowering the formaldehyde occupational exposure limit for Quebec workers. Regulatory Toxicology and Pharmacology, 2007, 48:118–127.

[11] Bell ML Peng R D, Dominici F, and Samet J M Emergency hospital admissions for cardiovascular diseases and ambient levels of carbon monoxide: results for 126 United States urban counties, 1999–2005. Circulation, 2009, 120:949–955.

[12] North DW, Abdo K M, Benson J M , Dahl A R , Morris J B , Renne R , Witschi H, A review of whole animal bioassays of the carcinogenic potential of naphthalene. Regulatory Toxicology and Pharmacology, 2008, 51:S6–14.

[13] Barck C, Lundahl J , Halldén G , Bylin G , Brief exposures to NO2 augment the allergic inflammation in asthmatics. Environmental Research, 2005, 97:58–66.
[14] Peluso M, Munnia A, Hoek G, Krzyzanowski M, Veglia F, Airoldi L, Autrup H, Dunning A, Garte S, Hainaut P, Malaveille C, Gormally E, Matullo G, Overvad K, Raaschou-Nielsen O, Clavel-Chapelon F, Linseisen J, Boeing H, Trichopoulou A, Trichopoulos D, Kaladidi A, Palli D, Krogh V, Tumino R, Panico S, Bueno-De-Mesquita H B, Peeters P H, Kumle M, Gonzalez C A, Martinez C, Dorronsoro M, Barricarte A, Navarro C, Quiros J R, Berglund G, Janzon L, Jarvholm B, Day N E, Key T J, Saracci R, Kaaks R, Riboli E, Vineis P, DNA adducts and lung cancer risk: a prospective study. Cancer Research, 2005, 65:8042–8048.
[15] Darby S, Hill D , Auvinen A, Barros-Dios J M , Baysson H, Bochicchio F, Deo H , Falk R, Forastiere F, Hakama M, Heid I, Kreienbrock L, Kreuzer M, Lagarde F, Mäkeläinen I, Muirhead C, Oberaigner W, Pershagen G,Ruano-Ravina A , Ruosteenoja E, Rosario A S, Tirmarche M, Tomáscaron L, Whitley E, Wichmann H-E, Doll R, Radon in homes and risk of lung cancer: collaborative analysis of individual data from 13 European case-control studies. British Medical Journal, 2005, 330:223–227.
[16] Dry cleaning, some chlorinated solvents and other industrial chemicals. Summary of data reported and evaluation. Lyon, International Agency for Research on Cancer, 1995 (IARC Monographs on the Evaluation of Carcinogenic Risks to Humans, Vol. 63).
[17] Lauwerys R, Herbrand J , Buchet J P, Bernard A, Gaussin J, Health surveillance of workers exposed to tetrachloroethylene in dry-cleaning shops. International Archives of Occupational and Environmental Health, 1983, 52:69–77.
[18] P. J. Irga, T. J. Pettit, F. R. Torpy, The phytoremediation of indoor air pollution: a review on the technology development from the potted plant through to functional green wall biofilters Rev Environ Sci Biotechnol 17:395–415,2018.
[19] Federico Brilli, Silvano Fares, Andrea Ghirardo, Pieter de Visser, Vicent Calatayud,Amalia Muñoz,Isabella Annesi-Maesano, Federico Sebastiani, Alessandro Alivernini, Vincenzo Varriale, and Flavio Menghini, Plants for Sustainable Improvement of Indoor Air Quality Trends in Plant Science, 23(6), 2018.
[20]Sowa,J.Hendiger,J.Maziejuk,M.Sikora,T.Osuchowski, Ł.Kamin´ska, H. Potted plants as active and passive biofilters improving indoor air quality. IOP Conf. Ser. Earth Environ. Sci., 290, 012150,2019.
[21] Bui, H.-T. Park, J. Lee, E. Cho, W. Kwon, H. Park, B.-J. Assessment of the Air Cleaning Performance and Humidity and Temperature Control by Five Evergreen Woody Plants. Atmosphere,14,1819, 2023.
[22] Niza, I.L. de Souza, M.P. da Luz, I.M. Broday, E.E. Sick building syndrome and its impacts on health, well-being and productivity: A systematic literature review. Indoor Built Environ. 2023.
[23] Deng, L. Deng, Q. The basic roles of indoor plants in human health and comfort. Environ. Sci. Pollut. Res. Int., 25, 36087–36101, 2018.
[24] Gubb, C. Blanusa, T. Griffiths, A. Pfrang, C. Interaction between plant species and substrate type in the removal of CO_2 indoors. Air Qual. Atmos. Health, 12, 1197–1206, 2019.
[25] Wu, Y. Zhong, H. Li, J. Xing, J. Xu, N. Zou, H. Water use efficiency and photosynthesis of Calamagrostis angustifolia leaves under drought stress through CO_2 concentration increase. J. Plant Interact., 17, 60–74,2022.
[26] Dominici, L. Fleck, R. Gill, R.L. Pettit, T.J. Irga, P.J. Comino, E. Torpy, F.R. Analysis of lighting conditions of indoor living walls: Effects on CO_2 removal. J. Build. Eng., 44, 102961, 2021.
[27] Zhang, Z. Tao, S. Zhou, B. Zhang, X. Zhao, Z. Plant stomatal conductance determined transpiration and photosynthesis both contribute to the enhanced negative air ion (NAI). Ecol. Indic., 130, 108114,2021.
[28] Cummings, B.E. Waring, M.S. Potted plants do not improve indoor air quality: A review and analysis of reported VOC removal efficiencies. J. Expo. Sci. Environ. Epidemiol., 30, 253–261, 2020.
[29] B. Zhang, D. Cao, S. Zhu, Use of Plants to Clean Polluted Air: A Potentially Effective and Low-Cost Phytoremediation Technology "Editorial: Air phytoremediation," BioResources 15(3), 4650-4654, 2020.
[30] Gawronski, S. W., Gawronska, H., Lomnicki, S., Saebo, A., and Vangronsveld, J., "Plants in air phytoremediation," in: Advances in Botanical Research, Academic Press, Vol. 83, pp. 319-346, 2017.
[31] Omasa, K., Saji, H., Youssefian, S., and Kondo, N. (eds.), Air Pollution and Plant Biotechnology: Prospects for Phytomonitoring and Phytoremediation, Springer Science & Business Media, 2012.
[32]https://en.wikipedia.org/wiki/Chlorophytum_comosum
[33] Sriprapat, W. Suksabye, P. Areephak, S. Klantup, P. Waraha, A. Sawattan, A. Thiravetyan, P., Uptake of toluene and ethylbenzene by plants: Removal of volatile indoor air contaminants. Ecotoxicol. Environ. Saf., 102, 147–151, 2014.
[34] Sriprapat, W. Thiravetyan, P. Efficacy of ornamental plants for benzene removal from contaminated air and water: Effect of plant associated bacteria. Int. Biodeterior. Biodegrad., 113, 262–268, 2016.
[35] Torpy, F. Zavattaro, M., Irga,P. Green wall technology for the phytoremediation of indoor air: A system for the reduction of high CO_2 concentrations. Air Qual. Atmos. Health, 10, 575–585, 2016.
[36] M-H. Yuan, S. Kang, K-S. Cho, A review of phyto- and microbial-remediation of indoor volatile organic compounds, Chemosphere 359, 1421202024.
[37] Xu, Z.J., Wang, L., Hou, H.P., Formaldehyde removal by potted plant-soil systems. J. Hazard Mater. 192, 314–318, 2011.
[38] Sriprapat, W., Boraphech, P., Thiravetyan, P., Factors affecting xylene-contaminated air removal by the ornamental plant Zamioculcas zamiifolia, Environ. Sci. Pollut. Res. 21, 2603–2610, 2014.
[39] Siswanto, D., Permana, B.H., Treesubsuntorn, C., Thiravetyan, P., Sansevieria trifasciata and Chlorophytum comosum botanical biofilter for cigarette smoke phytoremediation in a pilot-scale experiment- evaluation of multipollutant removal efficiency and CO_2 emission. Air Qual. Atmos. Health 13, 109–117, 2020.

[40] Yang, D.S., Pennisi, S.V., Son, K.C., Kays, S.J., Screening indoor plants for volatile organic pollutant removal efficiency. Hortscience 44, 1377–1381, 2009.
[41] Gawronska, H. Bakera, B. Phytoremediation of particulate matter from indoor air by *Chlorophytum comosum* L. plants. Air Qual. Atmos. Health, 8, 265–272, 2014.
[42] Irga, P. Paull, N. Abdo, P. Torpy, F. An assessment of the atmospheric particle removal efficiency of an in-room botanical biofilter system. Build. Environ., 115, 281–290, 2017.
[43]https://tr.m.wikipedia.org/wiki/Dosya:Chrysanthemum_morifolium_08NOV.jpg
[44] Aydogan, A., Montoya, L.D.,. Formaldehyde removal by common indoor plant species and various growing media, Atmos. Environ. 45, 1352–2310, 2011.
[45] Wolverton, B., Wolverton, J., Plants and soil microorganisms: removal of formaldehyde, xylene, and ammonia from the indoor environment. J. Miss. Acad. Sci. 38, 11–15, 1993.
[46]https://commons.wikimedia.org/wiki/File:Dracaena_deremensis1.jpg
[47]https://commons.wikimedia.org/wiki/File:Dracaena_deremensis_lemon_lime.jpg
[48] Orwell, R.L., Wood, R.A., Tarran, J., Torpy, F., Burchett, M.D., Removal of benzene by the indoor plant/substrate microcosm and implications for air quality. Water Air Soil Pollut. 157, 193–207, 2004.
[49] Orwell, R.L., Wood, R.A., Burchett, M.D., Tarran, J., Torpy, F., The potted-plant microcosm substantially reduces indoor air VOC pollution: II. Laboratory study. Water Air Soil Pollut. 177, 59–80, 2006.
[50] Mosaddegh, M.H., Jafarian, A., Ghasemi, A., Mosaddegh, A., Phytoremediation of benzene, toluene, ethylbenzene and xylene contaminated air by D. deremensis and O. microdasys plants. J. Environ, Health Sci. 12, 39, 2014.
[51] https://tr.wikipedia.org/wiki/Epipremnum
[52] Cai, N., Wang, X.M., Qiao, Z.Q., Li, Y.X., Zeng, H.J., Liu, S.S., Li, W.D., Absorptive capacity of formaldehyde of three kinds of shade-tolerant plants indoors. Hunan Forestry Sci. Technol. 44, 75–78, 2017.
[53] Kim, K.J., Kil, M.J., Jeong, M.I., Kim, H.D., Yoo, E.H., Jeong, S.J., Pak, C.H., Son, K., Determination of the efficiency of formaldehyde removal according to the percentage volume of pot plants occupying a room. Korean J. Hortic. Sci. Technol. 27, 305–311, 2009. (Korean with English abstract).
[54] Liu, G., Xiao, M., Zhang, X., Gal, C., Chen, X., Liu, L., A review of air filtration technologies for sustainable and healthy building ventilation. Sustain. Cities Soc. 32, 375–396, 2017.
[55] Rodgers, K., Handy, R., Hutzel, W., Indoor air quality (IAQ) improvements using biofiltration in a highly efficient residential home. J. Green Build. 8, 22–27, 2013.
[56] Liu, C., Zhang, N., Sun, L., Gao, W., Zang, Q., Wang, X., Potted plants and ventilation effectively remove pollutants from tobacco smoke. Int. J. Low Carbon Technol. 17, 1052–1060, 2022.
[57] Ibrahim, I.Z., Chong, W.T., Yusof, S., Wang, C.T., Xiang, X., Muzammil, W.K., Evaluation of common indoor air pollutant reduction by a botanical indoor air biofilter system. Indoor Built. Environ. Times 30, 7–21, 2021.
[58] Wang, Z., Zhang, J.S., Characterization and performance evaluation of a full-scale activated carbon-based dynamic botanical air filtration system for improving indoor air quality. Build. Environ. 46, 758–768, 2011.
[59]https://tr.m.wikipedia.org/wiki/Dosya:Hedera_helix_Leaves_3008px.jpg
[60] Chen, L.Y., Lin, M.W., Chuah, Y.K., Investigation of a potted plant (Hedera helix) with photo-regulation to remove volatile formaldehyde for improving indoor air quality. Aerosol Air Qual. Res. 17, 2543–2554, 2017.
[61] Yoo, M.H., Kwon, Y.J., Son, K., Kays, S.J., Efficacy of indoor plants for the removal of single and mixed volatile organic pollutants and physiological effects of the volatiles on the plants. J. Am. Soc. Hortic. Sci. 131, 452–458, 2006.
[62]https://it.wikipedia.org/wiki/File:Starr_070906-9018_Sansevieria_trifasciata.jpg
[63] "Sansevieria trifasciata". World Checklist of Selected Plant Families. Royal Botanic Gardens, Kew. Retrieved 2020-02-18.
[64] "Snake Plant". Better Homes & Gardens. Retrieved 2021-06-15.
[65] Permana, B.H., Thiravetyan, P., Treesubsuntorn, C., Effect of airflow pattern and distance on removal of particulate matters and volatile organic compounds from cigarette smoke using Sansevieria trifasciata botanical biofilter. Chemosphere 295, 133919, 2022.
[66]https://en.wikipedia.org/wiki/Syngonium_podophyllum
[67] Irga, P.J., Torpy, F.R., Burchett, M.D., Can hydroculture be used to enhance the performance of indoor plants for the removal of air pollutants? Atmos. Environ. 77, 267–271, 2013.
[68] Wolverton, B.C., Mcdonald, R.C., Watkins, E.A., Foliage plants for removing indoor air pollutants from energy-efficient homes. Econ. Bot. 38, 224–228, 1984.
[69]https://tr.wikipedia.org/wiki/Dosya:Sophora_japonica_JPG2Aa.jpg
[70] https://tr.wikipedia.org/wiki/Japon_soforası
[71] USDA, NRCS (n.d.). "Styphnolobium japonicum". The PLANTS Database (plants.usda.gov). Greensboro, North Carolina: National Plant Data Team. Retrieved 4 December 2015.
[72] Weiyuan Zhang, Yuzhen Zhang, Jirui Gong, Bo Yang, Zihe Zhang, Biao Wang, Chenchen Zhu, Jiayu Shi, Kexin Yue, Comparison of the suitability of plant species for greenbelt construction based on particulate matter capture capacity, air pollution tolerance index, and antioxidant system, Environmental Pollution 263 114615, 2020.
[73] Leonard, R.L., McArthur, C., Hochuli, D.F., Particulate matter deposition on roadside plants and the importance of leaf trait combinations. Urban For. Urban Green. 20, 249-253, 2016.
[74] Beckett, K.P., Freer-Smith, P.H., Taylor, G., Urban woodlands: their role in reducing the effects of particulate pollution. Environ. Pollut. 99, 347-360, 1998.
[75] Sæbø, A., Popek, R., Nawrot, B., Hanslin, H.M., Gawronska, H., Gawronski, S.W., Plant species differences in particulate matter accumulation on leaf surfaces. Sci. Total Environ. 427-428, 2012.

[76] Sisodia, A., Dutta, S., Air pollution tolerance index of certain plant species: a study of National Highway no-8, India. J. Environ. Res. Devel. 10 (4), 723-728, 2016.
[77] Shi J, Zhang G, An H, Yin W, Xia, X, Quantifying the particulate matter accumulation on leaf surfaces of urban plants in Beijing, China. Atmos Pollut Res 8:836–842, 2017.
[78] E. Chávez-García, B. González-Méndez, Particulate matter and foliar retention: current knowledge and implications for urban greening, Air Quality, Atmosphere & Health 14:1433–1454, 2021.
[79] C. Yue, K. Cui, J. Duan, X. Wu, P. Yan, C. Rodriguez, H. Fu, T. Deng, S. Zhang, J. Liu, Z. Guo, B. Xi, Z. Cao, The retention characteristics for water-soluble and water-insoluble particulate matter of five tree species along an air pollution gradient in Beijing, China, Science of the Total Environment 767, 145497. 2021.
[80] C. Gong, C. Xian, Y. Su, Z. Ouyang, Estimating the nitrogen source apportionment of Sophora japonica in roadside green spaces using stable isotope, Science of the Total Environment 689, 1348–1357.2019.
[81]https://tr.wikipedia.org/wiki/Salix_babylonica
[82]https://identify.plantnet.org/tr/useful/observations/1016702979
[83] Flora of China: *Salix babylonica*
[84]*"Salix babylonica". Germplasm Resources Information Network. Agricultural Research Service, United States Department of Agriculture.* Retrieved 15 December 2017.
[85] Wang H, Shi H, Wang Y . Effects of weather, time, and pollution level on the amount of particulate matter deposited on leaves of Ligustrum lucidum. Sci World J 2015:1–8, 2015.
[86] Luo J, Niu Y, Zhang Y Y Tian, X Zhou, Dynamic analysis of retention PM2.5 by plant leaves in rainfall weather conditions of six tree species. Energy Sources, Part A Recover Util Environ Eff 42:1014–1025, 2020.
[87] J. Liu, Z. Cao, S. Zou, H. Liu, X. Hai, S. Wang, J. Duan, B. Xi, G. Yan, S. Zhang, Z.Jia, An investigation of the leaf retention capacity, efficiency and mechanism for atmospheric particulate matter of five greening tree species in Beijing, China, Science of the Total Environment 616–617417–426, 2018.
[88] https://en.wikipedia.org/wiki/Ginkgo_biloba
[89] *Ansari, Abid A. Gill, Sarvajeet Singh, Abbas, Zahid Khorshid, Naeem, M. Plant Biodiversity: Monitoring, Assessment and Conservation. 2016. CABI.* ISBN 978-1-78064-694-7.
*[90]*https://en.wikipedia.org/wiki/Juniperus_chinensis
[91]https://www.worldfloraonline.org/taxon/wfo-0000437907.
[92] Xie C, Kan L, Guo J, Jin S, Li Z, Chen D, Li X, Che S A dynamic processes study of PM retention by trees under different wind conditions. Environ Pollut 233:315–322,2018.
[93] Sriprapat, W., Boraphech, P., Thiravetyan, P., Factors affecting xylene- contaminated air removal by the ornamental plant Zamioculcas zamiifolia. Environ. Sci. Pollut. Res. 21, 2603–2610, 2014.
[94] Kim, K., Kim, H., Khalekuzzaman, M., Yoo, E., Jung, H., Jang, H., Removal ratio of gaseous toluene and xylene transported from air to root zone via the stem by indoor plants. Environ. Sci. Pollut. Res. 23, 6149–6158, 2016.
[95] Kim, K.J., Jeong, M.I., Lee, D.W., Song, J.S., Kim, H.D., Yoo, E.H., Jeong, S.J., Han, S.W., Kays, S.J., Lim, Y.W., Kim, H.H., Variation in formaldehyde removal efficiency among indoor plant species. Hortscience 45, 1489–1495, 2010.
[96] Kim, K.J., Kil, M.J., Song, J.S., Yoo, E.H., Son, K.l., Kays, S.J., Efficiency of volatile formaldehyde removal by indoor plants: contribution of Aerial plant parts versus the root zone. J. Am. Soc. Hortic. Sci. 133, 521–526, 2008.
[97] Bandehali,S.Miri,T. Onyeaka, H. Kumar, P. Current State of Indoor Air Phytoremediation Using Potted Plants and Green Walls. Atmosphere, ,12,473, 2021.
[98] A. Aydogan, R. Cerone, Review of the effects of plants on indoor environments, indoor and Built Environment, 30(4) 442–460, 2021.
[99] K. Paul Beckett, Peter Freer-Smith, and Gail Taylor, Effective tree species for local air- quality management Journal of Arboriculture 26(1) 12-19, 2000.

Research Article

Energy, Environment and Storage (2024) 04-03:102-108

Energy, Environment and Storage

Journal Homepage: www.enenstrg.com

Effects of Magnetic Fields and Nanoparticle Additives on Diesel Engine Emissions and Performance: A Comprehensive Experimental Analysis

Mehmet Sarıtaş[1*], Volkan Sabri Kül[2]

[1*] *Erciyes University, Faculty of Engineering, Department of Mechanical Engineering, Kayseri, Türkiye, email: mehmetsaritas@erciyes.edu.tr ORCID: 0000-0001-6576-689X*

[2] *Erciyes University, Faculty of Engineering, Department of Mechanical Engineering, Kayseri, Türkiye, email: volkanskul@gmail.com ORCID: 0000-0002-6412-6062*

ABSTRACT. In the present study, performance and emission changes in a compression ignition engine were investigated by combining two methods. The first method involves adding nanoparticle additives to diesel fuel. Titanium dioxide (TiO2) with a particle size of 21 nm was used as nanoparticle. TiO_2 was added to diesel fuel at doses of 50 mg and 100 mg per 1 kg (50 and 100 ppm). After adding the nanoparticle to the diesel fuel, each mixture was stirred with a mechanical stirrer for one hour. In the second method, a magnetic field of 1 tesla was created around the fuel. Neodymium magnets were placed circularly around the diesel fuel line to create the magnetic field. The experiments were carried out at 660 RPM engine speed and 100% torque. During the experiments, data on engine performance, in-cylinder pressure and emissions were recorded. This study aims to contribute to the development of alternative fuel applications to improve performance and emissions in compression ignition engines.

Keywords: Nanoparticle, Magnetic Field, Diesel, Emissions, Performance

Article History: Received: 24.09.2024; Accepted: 29.09.2024; Available Online: 30.09.2024

Doi: https://doi.org/10.52924/ZYRI4684

1. INTRODUCTION

The energy consumption of modern societies is vital for economic growth and social development. However, increasing energy demand poses a threat to environmental sustainability and presents significant challenges in combating climate change [1]. In this context, accelerating the transition to renewable energy sources and enhancing energy efficiency has become a critical necessity [2]. Sustainable energy management has emerged as an important issue, not only for reducing environmental impacts but also for ensuring a secure energy supply for future generations. Research focusing on alternative fuel sources, such as biodiesel, demonstrates the potential to replace fossil fuels [3].

In recent years, the effects of nanoparticles on biodiesel performance have attracted considerable research interest. In applications using nanoparticle-enhanced biodiesel, a notable reduction in motor emissions and a significant improvement in fuel efficiency have been observed [3]. Kumar et al. (2019) comprehensively investigated the effects of various nanoparticle types on biodiesel performance, revealing the positive impacts of titanium dioxide and aluminum nanoparticles on engine power and emissions [4]. These nanoparticles were found to enhance atomization during the combustion process, allowing for more homogeneous combustion and thereby facilitating more efficient energy conversion [3][4].

The effects of magnetic field applications on engine emissions and performance have also become an important area of research in recent years. Experimental studies conducted by Niaki et al. (2020) demonstrated that magnetic field applications positively influence performance, combustion dynamics, and emission characteristics in internal combustion engines [5]. It has been shown that magnetic fields improve fuel atomization, thereby increasing combustion efficiency and reducing emissions [6]. For example, experiments indicated that magnetic fuel conditioning resulted in a 19% reduction in NOx emissions and a 13% decrease in CO2 emissions, while mechanical efficiency increased by 7%. These results suggest that magnetic fields affect molecular structure, facilitating better atomization of the fuel and creating a more homogeneous fuel-air mixture. Additionally, the use of CuO nanofuel contributes to emission reductions and enhances engine performance, making a significant contribution to sustainable energy solutions. The integration of nanoparticle additives and magnetic field applications plays a critical role in enhancing environmental sustainability and improving the performance of internal combustion engines. This integration aims to increase the operational efficiency of engines while minimizing environmental impacts, thereby targeting reductions in emissions and improvements in engine efficiency [7].

In this study, six experiments were conducted to evaluate the performance and emission characteristics of diesel fuel. In the first phase, pure diesel fuel was used as a reference to investigate combustion performance. In the second phase, four neodymium magnets were employed to create a magnetic field of 1 Tesla around the fuel line. Pure diesel was subjected to this magnetic field during combustion, and the combustion characteristics were recorded. In the third phase, pure diesel fuel with 50 ppm TiO2 was burned in the same magnetic field, and the effects of TiO2 on the combustion process were examined in detail. The obtained data were compared with those of pure diesel. Finally, a similar procedure was performed with 100 ppm TiO2, and the combustion efficiency and emission characteristics of this mixture were compared with previous experiments. This process represents an important step in understanding the effects of TiO2 concentration on combustion, providing significant findings regarding the roles of magnetic fields and TiO2 additives in the combustion process of diesel fuel. The obtained data aim to contribute to the development of alternative fuel mixtures and applications to enhance the performance of diesel engines and reduce emissions.

2. MATERIALS AND METHODS

2.1 Experimental Setup

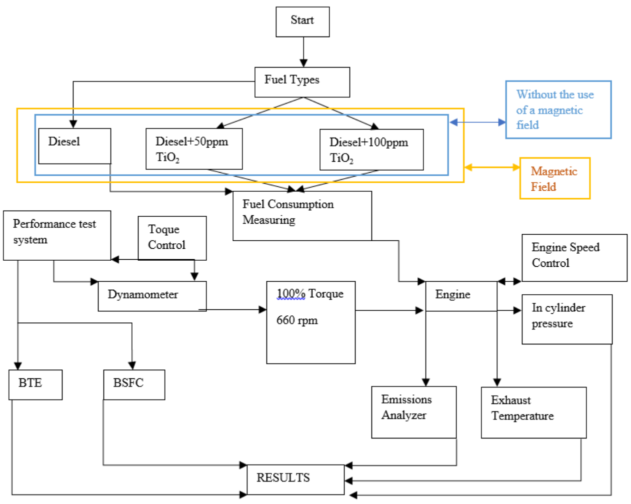

Fig.A The Experimental Workflow

In the present study, the workflow schematically shown in Figure A was followed. A six-cylinder compression ignition engine was used in the experiments. 50 mg and 100 mg TiO2 were added for every 1000 g of diesel fuel. Titanium dioxide (TiO2) with a particle size of 21 nm was used as nanoparticle. The mixtures were mixed with a mechanical stirrer at 1000 RPM for one hour. The fuels were coded as D for diesel, D_50ppm + 50 ppm TiO2 for diesel, and D_100ppm + 100 ppm TiO2 for diesel. Neodymium magnets were placed around the diesel fuel line to create a magnetic field of 1 tesla. In the experiments conducted with a magnetic field, the label "Magnetic" was added to the fuel codes to indicate the type of experiment. These three fuel types were tested in a compression ignition engine with and without a magnetic field. The experimental results are discussed in Section 3. A balance with a sensitivity of 0.5 g was used for fuel consumption measurement. Exhaust emissions were measured using a Bosch BEA 60 analyzer. Recording of engine performance data was facilitated by the PCS engine performance measurement system.

2.2 Fuel and nanoparticles properties

Table 1 represents the properties of fuel and nanoparticles used in the study.

Tablo 1. Diesel and TiO_2 specifications

Properties	TiO_2	Diesel
Boiling point	1600 °C (1013 hPa)	-
Particle size	21 nanometer	-
Density	4,500 kg/cm3 (25 °C)	820-845 kg/m3
Stoichiometric ratio	-	14,92 (app.)
Molar mass	233.38 g/mol	-
Flash point	-	55 °C
ignition Temperature	-	Auto-186–230 °C
Higher Heating Value	-	45.6 MJ/kg
Low heat Value	-	42.7 MJ/kg
Melting Point	1560 °C	-
Cetane Number	-	51
Viscosity	-	2.0- 4.5 mm^2 /s

2.3 Uncertainty analysis

Uncertainty analysis is presented in Table 2. To calculate uncertainty analysis use Eq.1 and to calculate total uncertainty use Eq. 2 [17, 18].

$$W_R = \left[\left(\frac{\partial R}{\partial x_1} * w_1 \right)^2 + \left(\frac{\partial R}{\partial x_2} * w_2 \right)^2 + \left(\frac{\partial R}{\partial x_3} * w_3 \right)^2 + \cdots + \left(\frac{\partial R}{\partial x_n} * w_n \right)^2 \right]^{1/2}$$

[1]

$$TU = \sqrt{UNO^2 + UCO^2 + UHC^2 + UCO_2{}^2 + UBte^2 + UBsfc^2}$$
[2]

Tablo 2. Uncertainty analysis [16]

Item	Uncertainty ratio
NO_x	0.71%
CO	1.73%
HC	1.26%
CO_2	0.54%
Bte	1.68%
Bsfc	1.47%
Total Uncertainty	**%3.22**

3. RESULTS, FIGURES AND TABLES

3.1 Engine Performance

In this section, three key parameters related to engine performance will be discussed. The first is Brake Thermal Efficiency (BTE), which is calculated as shown in Equation 3 and serves as a crucial factor in evaluating engine performance. The second is Brake Specific Fuel Consumption (BSFC), as presented in Equation 4. It is expected that the BTE and BSFC values will exhibit an inverse relationship. The graphs obtained from this experiment align with this expectation. [8]

$$\eta_{th} = \frac{P_b}{\dot{m}_f \times LHV} \quad (3)$$

P_b: *braking power*,
$\dot{m}_f$: *fuel mass flow rate*,
LHV: *the lower heating value of the fuel*

$$bsfc = \frac{\dot{m}_f}{P_b} \quad (4)$$

P_b: *braking power*,
$\dot{m}_f$: *fuel mass flow rate*,

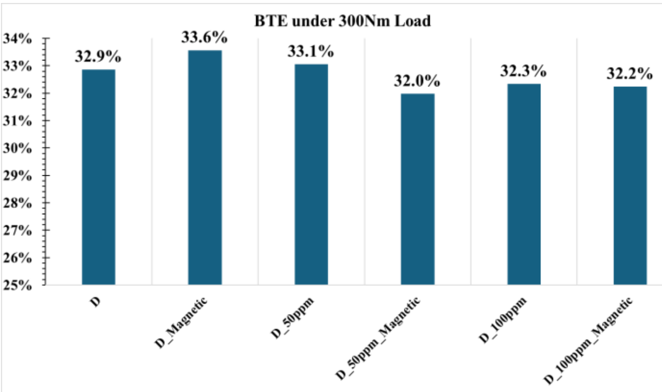

Fig.B BTE under 300Nm Load

The effects of different fuel mixtures and magnetic field applications on the brake thermal efficiency (BTE) under a constant load of 300 Nm were analyzed. The BTE values for each configuration, including pure diesel (D), magnetic field applied diesel (D_Magnetic), diesel with 50 ppm and 100 ppm TiO2 additives (D_50ppm and D_100ppm), and these fuel mixtures subjected to magnetic field conditions, are summarized in **Fig.B.**

The baseline BTE value for pure diesel (D) under 300 Nm load was recorded at 0.3287, serving as the reference point for further comparisons. When a magnetic field was applied to the pure diesel (D_Magnetic), the BTE increased significantly to 0.3357. This result demonstrates the positive influence of the magnetic field on the combustion efficiency of pure diesel. The increase in BTE suggests that the magnetic field may enhance fuel atomization and promote better combustion, leading to a more efficient energy conversion process.[5]

The addition of 50 ppm of an additive to the diesel fuel (D_50ppm) resulted in a slight increase in BTE, with a value of 0.3305. This suggests that the additive improves the combustion characteristics of diesel, leading to better thermal efficiency than pure diesel without additives. The improved efficiency could be attributed to the catalytic effects of the additive, which likely enhances the combustion process, reducing unburnt hydrocarbons and improving fuel-air mixing.[9]

In contrast, when 100 ppm of the additive was introduced into the diesel fuel (D_100ppm), the BTE dropped to 0.3234. This result indicates that while the additive has a positive impact at lower concentrations (50 ppm), increasing its concentration to 100 ppm does not yield further improvements and, in fact, slightly reduces the combustion efficiency compared to both pure diesel and the 50-ppm mixture. This could be due to potential over-saturation of the fuel with the additive, leading to incomplete combustion or unfavorable reactions in the combustion chamber.[10]

When 50 ppm and 100 ppm boron additions were compared in a prior study, the 50 ppm additive showed the maximum efficiency. Additionally, 50 ppm is more efficient than 100 ppm, according to this study. It was shown once more that lower ppm concentrations have a more favorable effect on efficiency, notwithstanding the element's difference. In order to ensure the comparability of the results, the 50 and 100 ppm additive levels were also chosen to enable comparison with the boron additive ratios used in the study by Kül and Akansu (2022).[10]

The application of a magnetic field with 50 ppm of the additive (D_50ppm_Magnetic) resulted in a BTE of 0.3198, lower than both pure diesel and the 50 ppm additive without the magnetic field. This indicates that the combination may interfere with optimal combustion conditions. For the 100 ppm mixture (D_100ppm_Magnetic), the BTE slightly increased to 0.3224, but remained below that of pure diesel and the 50 ppm additive, suggesting limited enhancement at higher concentrations.

The magnetic field showed the most notable positive impact when applied to pure diesel, significantly improving BTE. While lower concentrations of additives

(50 ppm) can enhance efficiency, their combination with a magnetic field may lead to performance reduction. At higher concentrations (100 ppm), the benefits diminish, with the magnetic field providing only marginal improvements. These findings highlight the importance of carefully optimizing both additive concentrations and magnetic field applications for optimal combustion efficiency.

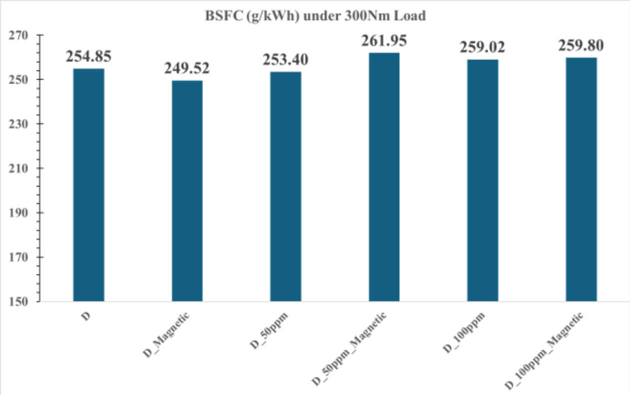

Fig.C BSFC under 300Nm Load

Magnetic field applied to pure diesel (D_Magnetic) reduced BSFC to 249.5192, indicating that the fuel molecules were organized for more efficient combustion. The literature also supports that magnetic fields enhance atomization of hydrocarbon fuels, leading to increased combustion speed [11].

The BSFC of diesel fuel with 50 ppm additive (D_50ppm) was recorded as 253.3981. Additives, especially nanoparticle-based ones, are known to enhance combustion efficiency. For example, TiO2 nanoparticles can catalyze the combustion process, leading to better energy conversion, thereby reducing BSFC.[12]

The BSFC of diesel fuel with a 50 ppm additive under a magnetic field was recorded at 261.9512, representing the highest value observed. This indicates that the simultaneous use of the additive and magnetic field may interfere with optimal combustion conditions, potentially leading to increased fuel consumption.

The BSFC of diesel with a 100 ppm additive was measured at 259.0244, indicating higher fuel consumption compared to pure diesel and 50 ppm additive. This suggests that the 100 ppm additive may disrupt combustion conditions and reduce fuel efficiency.

The BSFC of diesel with a 100 ppm additive under a magnetic field is 259.8039, which is higher than pure magnetic diesel and similar to 100 ppm without magnetic treatment. This indicates no significant improvement in fuel consumption.

In Terms of in Cylinder Pressure

Fig. D shows the change in In-Cylinder Pressure (ICP) representing the combustion processes of diesel fuels. The graph reveals the relationship between crank angle and in-cylinder pressure for an engine under a load of 300 Nm. The combustion processes of different fuels are divided into six main phases:

Phase 1: Ignition Delay

In the fuels D_50ppm_Magnetic, D_100ppm_Magnetic, the ignition delay occurs approximately 1 degree earlier compared to other fuels. This early ignition can be attributed to the nanoparticle additive TiO_2 , which accelerates the combustion reaction. TiO_2 can reduce ignition delay by promoting a more homogeneous and efficient combustion process, leading to earlier fuel ignition and positively impacting engine performance. [13]

Phase 2: Combustion Initiation and Fuel Vaporization

During this phase, TiO_2 nanoparticles enhance the fuel's surface area, thereby improving evaporation and combustion efficiency. The magnetic effect polarizes the fuel molecules, improving the air-fuel mixture. Both additives contribute to a more homogeneous combustion, optimizing the pressure curve. [13,14]

Phase 3: Complete Combustion of the Fuel

This phase represents the stage where the fuel is fully combusted, resulting in a complete explosion. Efficient fuels have been observed to exhibit a steeper slope during this phase. The higher combustion curves of the D_Magnetic and D_50ppm fuels enable these fuels to accelerate complete combustion, generating higher pressure. This phase, characterized by high efficiency, reflects the fuel's maximum energy output.

Phase 4: Work Production and Peak Point

In this stage, where work is produced and the graph reaches its peak, it is preferable for this section of the graph to be as flat as possible for diesel engines. The flatter peak points of the D_Magnetic and D_50ppm fuels help optimize engine performance. A flat peak indicates a smooth explosion and prevents sudden pressure changes, which allows for more efficient engine operation. [15]

Phases 5 and 6: Pressure Decline

Following the completion of combustion, these phases begin with a rapid and then gradual decrease in pressure. The rate of pressure decline is similar across different fuels during this phase. The process continues as the cylinder pressure returns to atmospheric pressure. [15]

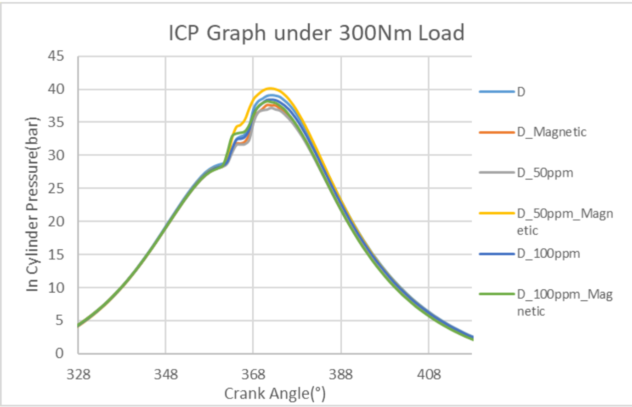

Fig.D ICP Graph under 300Nm Load

3.2 Exhaust Emissions

HC Emission

Hydrocarbon (HC) emissions are harmful gases released into the atmosphere because of incomplete combustion.

Pure diesel (D) fuel produced the highest HC emissions. This result is closely related to the high carbon content and combustion characteristics of diesel fuel, which contribute to incomplete combustion and, subsequently, the release of a higher quantity of hydrocarbons into the atmosphere.

The magnetic field application (D_Magnetic) significantly reduced HC emissions. The application of a magnetic field improved fuel combustion efficiency, reducing incomplete combustion. The magnetic field aids in better atomization of the fuel and promotes a more homogeneous combustion process, thus effectively lowering HC emissions.

TiO2 additive (D_50ppm and D_100ppm) demonstrated a considerable reduction in HC emissions, primarily due to its catalytic properties. The 100 ppm level of TiO2 was more effective than the 50 ppm, further reducing incomplete combustion. TiO2 enhances oxidative reactions during combustion, promoting a cleaner and more complete burn of the fuel.

Combination of TiO2 and Magnetic Field (D_50ppm_Magnetic and D_100ppm_Magnetic) achieved the lowest HC emissions. The combined catalytic effect of TiO2 and the efficiency boost from the magnetic field resulted in an optimized combustion process, both chemically and physically. This combination effectively minimized hydrocarbon emissions to their lowest levels.

The application of 100 ppm TiO2 combined with a magnetic field emerged as the most effective solution for reducing hydrocarbon emissions. This combination has the potential to significantly mitigate the environmental impact of diesel fuel, offering a viable strategy for minimizing HC emissions in diesel engines.

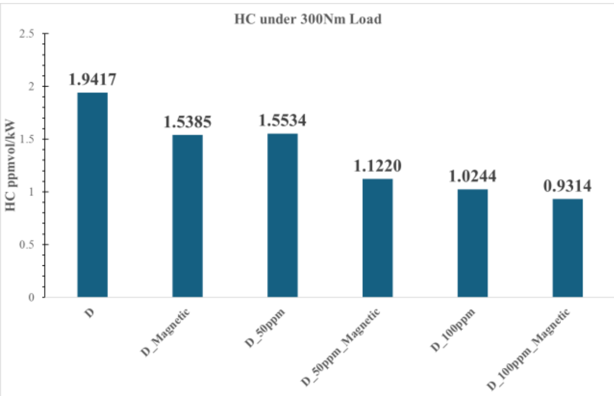

Fig.E HC Emission under 300Nm Load

CO Emission

Carbon monoxide (CO) emissions result from incomplete combustion, where carbon in the fuel does not fully convert to CO2[19]. Pure diesel (D) produced the highest CO emissions, while the application of a magnetic field (D_Magnetic) significantly reduced emissions by enhancing combustion efficiency. TiO2 additives (D_50ppm and D_100ppm) further lowered CO emissions, with 50 ppm being slightly more effective. The combination of TiO2 and a magnetic field (D_50ppm_Magnetic and D_100ppm_Magnetic) achieved the lowest emissions, optimizing combustion through both catalytic and physical improvements. 100 ppm TiO2 with a magnetic field proved the most effective in reducing CO emissions and improving diesel efficiency.

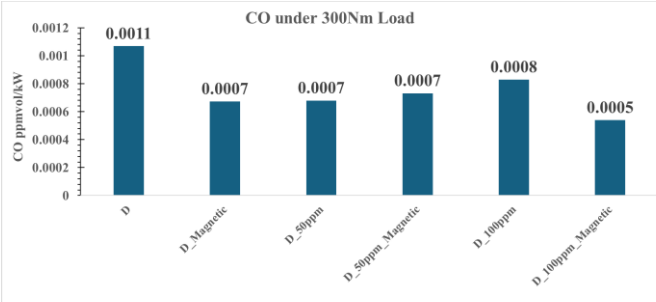

Fig.F CO Emission under 300Nm Load

NO Emission

Nitrogen oxide (NOx) emissions arise from high-temperature combustion in diesel engines. This situation increases with in-cylinder conditions as well as fuel and air homogeneity[20]. This analysis shows that pure diesel (D) generates moderate NO emissions, while the application of a magnetic field (D_Magnetic) slightly increases them due to enhanced combustion efficiency and higher temperatures. TiO2 additives (D_50ppm and D_100ppm) also modestly raise NO emissions by improving combustion and increasing temperatures, with little difference between the two concentrations. The highest NO emissions occur with the combination of TiO2 and magnetic fields (D_50ppm_Magnetic and D_100ppm_Magnetic), which boosts combustion efficiency but leads to significant temperature increases. Overall, while these enhancements improve combustion performance, they also result in higher NO emissions, underscoring the need for balanced emission control strategies.

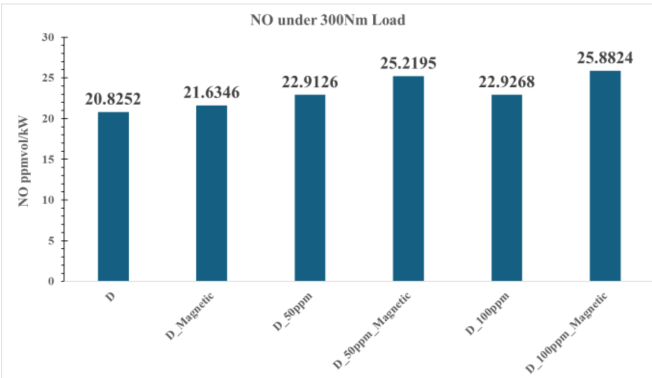

Fig.G NO Emission under 300Nm Load

4.CONCLUSION

This study examined the performance and emission characteristics of a compression ignition engine supplied with titanium dioxide (TiO_2) nanoparticle additives and subjected to magnetic field application. The experiments were conducted under a constant load of 300 Nm, analyzing key performance metrics such as brake thermal efficiency (BTE), brake specific fuel consumption (BSFC), in-cylinder pressure (ICP), and exhaust emissions.

The findings indicated that the application of a magnetic field slightly increased the BTE of pure diesel fuel, rising from 0.3287 to 0.3357. The addition of 50 ppm of TiO_2 resulted in a slight increase in BTE to 0.3305, while increasing the concentration to 100 ppm decreased the BTE to 0.3234; this suggests that excessive TiO_2 may hinder combustion efficiency. It was observed that the interaction between TiO_2 and the magnetic field negatively affected performance, especially at lower additive concentrations; this combination resulted in lower BTE values compared to pure diesel. However, due to the lack of significant differences between the percentage values, the magnetic field application and nanoparticle addition did not provide a meaningful change in overall engine efficiency.

The results of the study demonstrate that smaller concentrations (ppm) of additives have a more favorable effect on efficiency, notwithstanding variations in the type of element utilized. Furthermore, enhanced efficiency was not a result of raising the dosage amount. In order to compare the findings with those of the study by Kül and Akansu (2022), 50 and 100 ppm additive concentrations were chosen. These kinds of comparisons show that further research is required in the future to determine whether low-dose applications have an efficiency-enhancing effect.

The in-cylinder pressure analysis revealed six combustion phases and demonstrated that TiO_2 nanoparticles reduced ignition delay and improved combustion initiation. Notably, the addition of 50 ppm TiO_2 achieved the best performance in the combustion processes, while combining TiO_2 with the magnetic field disrupted combustion dynamics and resulted in less favorable conditions; in this context, the observed differences were insufficient for significant interpretation.

In terms of exhaust emissions, pure diesel exhibited the highest HC and CO emissions, which were significantly reduced by the magnetic field and TiO_2 additives, particularly at 100 ppm. The combination of 100 ppm TiO_2 and a magnetic field provided the lowest HC and CO emissions, proving to be an effective strategy for mitigating environmental impact. However, it was also observed that the improvements in combustion efficiency due to TiO_2 and magnetic fields led to higher NO emissions due to increased combustion temperatures.

Overall, this study highlights the complexity of optimizing fuel formulations and combustion conditions in compression ignition engines. The findings suggest that TiO_2 nanoparticles and magnetic field applications can enhance combustion efficiency and reduce certain emissions, but careful evaluation of additive concentrations and interactions is necessary to balance performance and emission outcomes. Future research should focus on further improving these parameters to enhance the environmental sustainability of diesel engines.

REFERENCES

[1] Waheed, R., Sarwar, S., & Wei, C. (2019). The survey of economic growth, energy consumption and carbon emission. Energy Reports, 5, 1103-1115. https://doi.org/10.1016/j.egyr.2019.07.006

[2] Demirbas, A. (2009). Biofuels securing the planet's future energy needs. Energy conversion and management, 50(9), 2239-2249. https://doi.org/10.1016/j.enconman.2009.05.010

[3] Soudagar, M. E. M., Nik-Ghazali, N. N., Kalam, M. A., Badruddin, I. A., Banapurmath, N. R., & Akram, N. (2018). The effect of nano-additives in diesel-biodiesel fuel blends: A comprehensive review on stability, engine performance and emission characteristics. Energy conversion and management, 178, 146-177.Alamu, O. J., et al. (2020). "Effects of different nanoparticles on biodiesel performance: A review." Energy Reports, 6, 526-540. https://doi.org/10.1016/j.enconman.2018.10.019

[4] Kumar, S., Dinesha, P., & Bran, I. (2019). Experimental investigation of the effects of nanoparticles as an additive in diesel and biodiesel fuelled engines: a review. Biofuels, 10(5), 615-622. https://doi.org/10.1080/17597269.2017.1332294

[5] Niaki, S. R. A., Zadeh, F. G., Niaki, S. B. A., Mouallem, J., & Mahdavi, S. (2020). Experimental investigation of effects of magnetic field on performance, combustion, and emission characteristics of a spark ignition engine. Environmental Progress & Sustainable Energy, 39(2), e13317. https://doi.org/10.1002/ep.13317

[6] Öztürk, O., & Taştan, M. (2024). A review of magnetic field assisted combustion. International Journal of Energy Studies, 9(1), 175-198. https://doi.org/10.58559/ijes.1412125

[7] Sahoo, R. R., & Jain, A. (2019). Experimental analysis of nanofuel additives with magnetic fuel conditioning for diesel engine performance and emissions. Fuel, 236, 365-372. https://doi.org/10.1016/j.fuel.2018.09.027

[8] Coskun, A. D., Kul, V. S., & Akansu, S. O. (2023). Experimental Investigation of the Effect of Acetone Additive to Diesel Fuel on Engine Performance and Exhaust Emissions at Partial Loads. Energy, Environment and Storage, 3(01), 12-18: https://doi.org/10.52924/WQJR9374

[9] D'Silva, R., Binu, K. G., & Bhat, T. (2015). Performance and emission characteristics of a CI engine fuelled with diesel and TiO2 nanoparticles as fuel additive. Materials Today: Proceedings, 2(4-5), 3728-3735. https://doi.org/10.1016/j.matpr.2015.07.162

[10] Kül, V. S., & Akansu, S. O. (2022). Experimental Investigation of the impact of boron nanoparticles and CNG on performance and emissions of Heavy-Duty diesel engines. Fuel, 324, 124470. https://doi.org/10.1016/j.fuel.2022.124470

[11] Patel, P. M., Rathod, G. P., & Patel, T. M. (2014). Effect of magnetic field on performance and emission of single cylinder four stroke diesel engine. IOSR Journal of Engineering, 4(5), 28-34. http://dx.doi.org/10.9790/3021-04552834

[12] Ghanati, S. G., Doğan, B., & Yeşilyurt, M. K. (2024). The effects of the usage of silicon dioxide (SiO2) and titanium dioxide (TiO2) as nano-sized fuel additives on the engine characteristics in diesel engines: a review. Biofuels, 15(2), 229-243. https://doi.org/10.1080/17597269.2023.2221882

[13] Sarma, C. J., Sharma, P., Bora, B. J., Bora, D. K., Senthilkumar, N., Balakrishnan, D., & Ayesh, A. I. (2023). Improving the combustion and emission performance of a diesel engine powered with mahua biodiesel and TiO2 nanoparticles additive. Alexandria Engineering Journal, 72, 387-398. https://doi.org/10.1016/j.aej.2023.03.070

[14] S. Gavhane, R., M. Kate, A., Pawar, A., Safaei, M. R., M. Soudagar, M. E., Mujtaba Abbas, M., ... & Shahapurkar, K. (2020). Effect of zinc oxide nano-additives and soybean biodiesel at varying loads and compression ratios on VCR diesel engine characteristics. Symmetry, 12(6), 1042. https://doi.org/10.3390/sym12061042

[15] Olt, J., Mikita, V., Roots, J., & Jasinskas, A. (2015). Cylinder pressure characteristics of turbocharged and naturally aspirated diesel engines. Procedia Engineering, 100, 350-359. https://doi.org/10.1016/j.proeng.2015.01.378

[16] Kül, V. S., & Akansu, S. O. (2024). The investigation of the performance and exhaust emissions of the compression-ignition engine with a mixture of diesel and aluminum particles. Process Safety and Environmental Protection, 189, 1161-1172. https://doi.org/10.1016/j.psep.2024.07.003

[17] Yuksel, T. (2024). Experimental investigation of the emission and performance of preheated and unheated garlic methyl ester fuels and diesel fuel in a diesel engine. Process Safety and Environmental Protection. https://doi.org/10.1016/j.psep.2024.03.012

[18] Kari, ., Vanthala, V. S. P., & Sagari, J. (2024). Performance and emission characteristics of a diesel engine fuelled with Mesua ferrea biodiesel with chromium oxide (Cr2O3) nanoparticles: Experimental Approach and Response Surface Methodology. International Journal of Thermofluids, 100637. https://doi.org/10.1016/j.ijft.2024.100637

[19] Bozkurt, A., & Çinar, G. (2024). Experimental Investigation of The Effects of Biodiesel/Methanol Mixtures on Diesel Fuel on Engine Performance and Emission Values in A Diesel Engine.*ENERGY, ENVIRONMENT AND STORAGE*, 58.https://doi.org/10.52924/KXEK8088

[20] Sinkala, H., Özarslan, S., & Benarous, A. (2024). Effect of Excess Air Ratio on Emissions, Performance and Efficiency of Gasoline Fueled Engines: A Review. ENERGY, ENVIRONMENT AND STORAGE, https://doi.org/10.52924/PUPX2065

Review Article

Energy, Environment and Storage (2024) 04-03:109-115

Energy, Environment and Storage

Journal Homepage: www.enenstrg.com

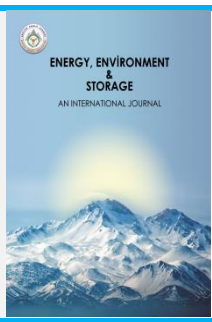

Research Progress of Battery Thermal Management Systems with Minichannels

Seyfi Sevinc[1,2*], Toygun Dagdevir [3]

[1]*Department of Mechanical Engineering, Faculty of Engineering Erciyes University, Kayseri, Türkiye ORCID: 0009-0009-2387-7992*

[2]*Department of Mechanical Engineering, Faculty of Engineering and Natural Sciences,*

[3]*Department of Mechanical Engineering, Faculty of Engineering Erciyes University, Kayseri, Türkiye ORCID: 0000-0001-7388-3391*

ABSTRACT. With the developing technology, energy storage systems, especially lithium-ion batteries (LiBs), play a critical role in electric vehicles and renewable energy applications. However, the performance and life of batteries are significantly affected by their operating temperatures. In this context, battery thermal management systems (BTMS) are of vital importance to ensure temperature control of batteries and to create a safe operating environment. BTMSs are divided into main two groups active and passive which require and does not require extra energy consumption, respectively. In this review, the basic principles, design criteria and application areas of battery thermal management systems are examined. First of all, the components of BTMS, passive and active cooling methods, heat dissipation and temperature monitoring techniques are detailed. In addition, the effects of different BTMS approaches on efficiency and performance are compared. The analysis of existing studies in the literature reveals the positive contributions of BTMS on battery life, charge-discharge efficiency and safety. In addition, future research areas and development opportunities are also highlighted. In conclusion, an effective thermal management system is a critical factor in the development of battery technology and has great potential in terms of sustainability of energy systems.

Keywords: Electric Vehicles, Li-ion Batteries, Battery Thermal Management Systems, Minichannels

Article History: Received: 28.09.2024; Accepted: 30.09.2024; Available Online: 30.09.2024

Doi: https://doi.org/10.52924/EUYV2071

1. INTRODUCTION

The world's population is increasing and people prefer city centers as their living space. It is predicted that the world population will be 9.1 billion in 2050 and 80% of the world's population will live in cities. Such large populations living together causes some problems and affects the quality of life. Some of these problems are noise and environmental pollution. Exhaust emissions from transportation vehicles are increasing and triggering environmental pollution. In the next stage, it becomes one of the causes of global warming and climate change. [1,2]

As a solution to the environmental problems caused by automobiles, internal combustion vehicle emissions had to be gradually reduced and reduced to zero. In order to combat climate change, the European Union (EU) made it mandatory for new cars and light commercial vehicles to be zero-emission after 2035. [3]

Electric vehicles (EVs) and hybrid electric vehicles (HEVs) are two methods we encounter to achieve zero-emission targets. Electric vehicles operate by transferring energy from the battery pack to the wheels via an electric motor. In this way, they do not emit emissions and operate without noise. However, long charging times and short ranges are the biggest obstacles to electric vehicles. For this reason, hybrid electric vehicles (HEVs) are offered as an intermediate product in the transition period to electric vehicles. The concept of hybrid refers to the use of 2 or more energy sources together. The most common HEVs are a combination of an electric motor and an internal combustion engine (ICE). The ICE powers the vehicle when needed, while the electric motor alone powers the vehicle when not needed. This makes them more economical and cleaner than internal combustion engine vehicles. HEVs are a good alternative to EVs because they do not require long charging times and do not have a range limitation. However, it should be noted that HEVs cannot provide zero-emission values. [4]

Li-ion batteries are used as a power source in electric vehicles. Compared to other energy storage systems, LiBs is superior to others due to its rechargeability, higher power and energy density, light weight and long life. [5] The batteries to be used in electric vehicles are required to cover

*Corresponding author: seyfisvnc@gmail.com

minimum space, lightweight and provide high performance while also being reliable. LiBs comes in 3 different forms: pouch, prismatic and cylindrical. While cylindrical and prismatic batteries are generally preferred in electric vehicles, pouch batteries are also used. They have superior aspects compared to each other. Cylindrical batteries are shaped by laying the anode, separator and cathode flat and then folding them like a carpet. Cylindrical batteries are easier to manufacture, have lower production costs, and are suitable for mass production. Due to their small size and high contact area, cylindrical cells have good thermal management. Prismatic cells are generally larger than cylindrical cells. They tend to have higher energy density compared to cylindrical batteries but less charge and discharge power. [6].

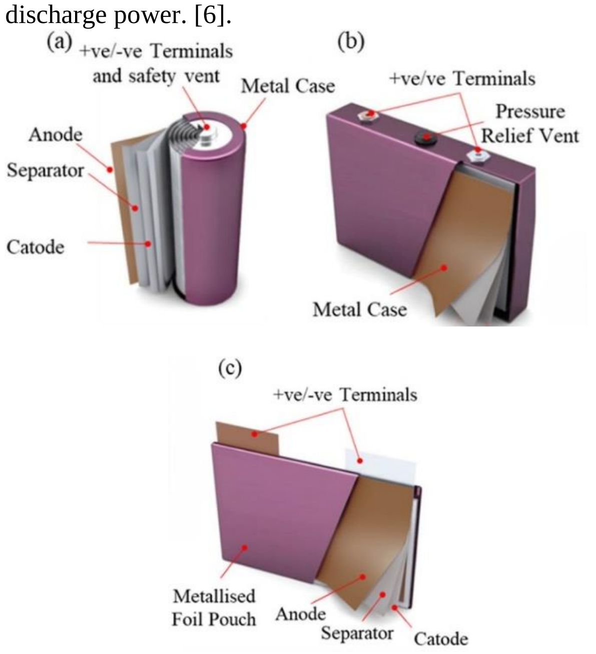

Fig. 1. Different type of batteries (a) Cylindrical (b)Prismatic (c)Pouch [7]

In LiBs, heat is generated due to internal electrochemical reactions during charging and discharging. Heat generation will increase the battery temperature. The increased temperature should be kept within certain levels (15℃ – 40℃) and the temperature difference across the LiB should not exceed 5℃. When these limits are exceeded, a phenomenon called thermal runaway occurs in the battery. Thermal runaway can cause the temperature to increase suddenly, the battery to burn or even explode. To prevent this, battery thermal management (BTMS) is essential. [8]

Cooling in batteries is done as active, passive and hybrid. In the active cooling method, which requires additional energy to operate, the coolant provides heat removal from the batteries with a pump or fan. Cooling with phase change material (PCM), heat pipe (HP) and thermoelectric cooler (TEC) is defined as passive cooling because it does not require an energy source. In hybrid cooling, active and passive cooling are combined. [9]

In this study, the latest developments related to BTMS using mini channels, which is one of the active cooling methods in thermal management of cylindrical and prismatic li-ion batteries used in electric vehicles, were examined. The results showed that the use of mini channels gave very good results in controlling the temperature.

In this study, the latest developments related to BTMS using mini channels, which is one of the active cooling methods in thermal management of cylindrical and prismatic li-ion batteries used in electric vehicles, were examined. The results showed that the use of mini channels gave very good results in controlling the temperature.

2. BATTERY HEAT GENERATION MECHANISM

LiBs store energy with electrons. When desired, the movement of these electrons allows the stored energy to be used in the desired place. The movement of electrons occurs due to the potential difference between the negative and positive regions. When examined in their internal structure, a LiB consists of 3 main parts: anode (negative electrode), cathode (positive electrode) and separator. In the resting state, lithium and electron remain together in the anode region. Electron and lithium movement begins during battery discharge. While electrons pass through a circuit from the negative current collector to the positive current collector and reach the anode region, lithium ions pass through the separator and reach the anode region. The separator does not allow electron passage, otherwise a short circuit occurs. However, lithium can pass through the separator. In addition, lithium is provided with a movement environment with the electrolyte material added to the battery. During charging, lithium in the cathode region passes through the separator and recombines with electrons in the anode region. If all of the lithium in the cathode region passes to the anode region, it means that the battery is fully charged. Thanks to this movement of lithium, LiBs gain rechargeable properties. During these processes, heat is generated within the battery, causing the battery temperature to increase. If the generated heat cannot be removed from the battery, a phenomenon called thermal runaway occurs due to uncontrolled lithium and electron movement. As a result of this event, the battery temperature suddenly increases 6-7 times, causing smoke and flame formation, and eventually the battery may explode. Therefore, battery thermal management is essential to prevent negative situations from occurring. [10, 11]

3. BATTERY THERMAL MANAGEMENT WITH MINICHANNELS

As mentioned above in chapter 2, thermal management of batteries is essential. For this reason, many active, passive and hybrid BTMS designs have been made by researchers. In this article, recent studies on the use of mini channels in cylindrical and prismatic battery thermal management has been reviewed.

3.1 Cylindrical Battery Thermal Managements

Heat transfer between the fluid and the solid surface is calculated from Newton's Law of Cooling, which is formulated as,

$$Q = h \times A \times dT \quad (1)$$

Wiriyasart et al. [12] numerically investigated the pressure drop and temperature distribution of a pack containing 444 cylindrical 18650 LiB under different cooling conditions. The cases where nanofluid was used and not used at three different mass flow rates and 3 different flow directions were investigated. It was assumed that there was a constant heat flux value of 3330 W/m^2 from the contact surface between the battery and the mini channel. The average battery temperature remained below 35°C in the case of underflow and overflow in different directions. The results showed that the battery surface temperature decreased as the coolant mass flow rate increased. However, there was a limit to this temperature drop and the pressure drop increased with the increasing mass flow rate. In the study, TiO2 nanoparticles were added at 0.25% and 0.5% by volume and it was observed that the battery temperature decreased. It was suggested that the battery surface temperature could be reduced by further increasing the nanoparticle ratio.

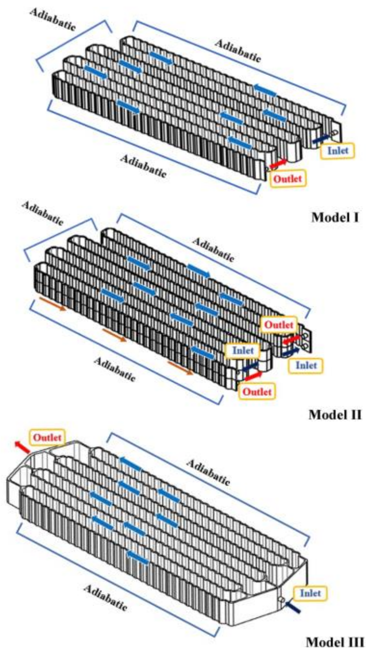

Fig. 2. Serpentine Mini Channel for 444 Cylindrical LiBs [12]

Xu et al. [13] conducted thermal analysis of 32 18650 LiB modules. Since the coolant temperature increases in the flow direction, the heat rejection rate of the package decreases. In order to prevent this, they aimed for a lightweight and uniform battery pack temperature with a wrench-shaped cold plate with a min-channel inside. The ambient temperature and fluid (water) inlet temperature were selected as 25°C. Analyses were performed for a discharge rate of 3C when water entered the channel at 0.1 m/s. As a result of the numerical analysis, it was seen that the wrench-shaped cold plate among 4 different designs provided the desired battery temperature values, with a maximum battery temperature of 30.32°C and a maximum temperature difference of 3.83°C. It was also noted that the weight was reduced by 19.68% in the wrench-shaped cold plate design. In addition, the pressure drop in this design was at the lowest level with 43.64 Pa compared to the others. The effect of the starting point of the bifurcation on the temperature for the wrench-shaped design was also examined. The results showed that starting the bifurcation after the 4th cell (8 cells in total) provided the most effective cooling. While starting the bifurcation early reduced the pressure drop, it will increase the weight.

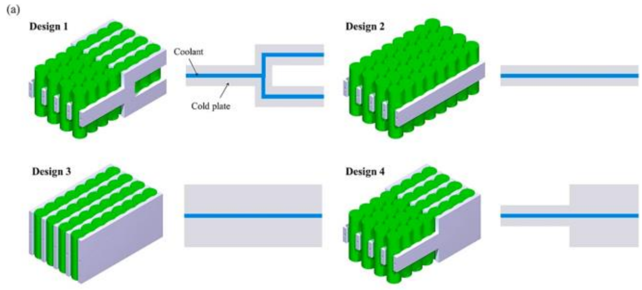

Fig. 3. Wrench Shaped Mini Channel Cold Plate [13]

Wang et al. [14] have conducted experimental and numerical studies. In the study that carried out with liquid cooled aluminium plate, they investigated the thermal behaviour of modular 18650 LiB system in mass flow and series and parallel cases. It was aimed to transfer the heat generated in the battery to the fluid through the aluminium in contact with the batteries. Water was used as coolant with laminar flow. When the mass flow rate was between 20-140 ml/min, it was observed that the maximum temperature and temperature difference decreased as the flow rate increased. However, when the flow rate was greater than 80 ml/min, the temperature drop rate decreased. In the analyses carried out with parallel cooling, the maximum temperature and temperature difference were 37.67°C and 5.76°C, while these values were 7.55°C and 6.74°C lower compared to series cooling. Therefore, parallel cooling is quite effective compared to series cooling. Finally, the effect of flow direction on parallel cooling was investigated and the maximum temperature was 37.74°C while the temperature difference was noted as 4.17°C. Considering that the ambient temperature and fluid temperature were 30°C throughout the experiment, the obtained data are quite satisfactory.

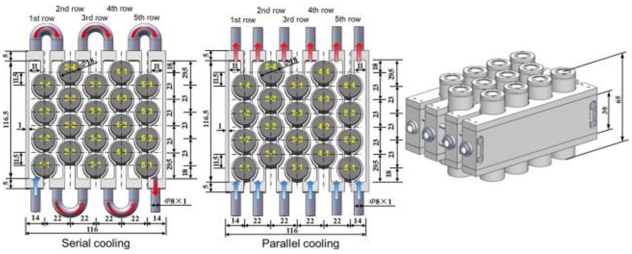

Fig. 4. Aluminium Cold Plate [14]

Wang et al. [11] investigated the combined use of PCM and mini channel with the design called hybrid wavy mini channel cold plate (HWMCP). They numerically investigated the temperature distribution of the battery at different discharge rates, PCM thickness, coolant mass flow rate, different flow directions and different array combinations. The analysis consisted of 33 18650 LiB as battery modules. Water and composite RT44HC/expanded graphite were selected as coolant and PCM. In order to compare the effect of the presence of PCM, analyses were performed on wavy mini channel cold plate (WMCP) and HWMCP with only water flow. When comparing HWMCP and WMCP, results were obtained for water mass flow rate of 0.001kg/s and battery discharge rates of 3C and 5C. Although the mass flow rate of water decreased with the replacement of water with PCM, the maximum temperature decreased by 0.8K and 1.3K with HWMCP, respectively. In addition, 90% of PCM melted at the end of 5C discharge rate, while 40% melted at 3C discharge rate. PCM did not melt until 400th second at 3C discharge rate. For this reason, maximum temperature increased. However, temperature HWMCP showed more effective results with the melting of PCM. The effect of flow direction and flow rate was also examined for PCM thickness of 4 mm and number of channels through which water passes as 6. In case of 3 flows at the top and 3 flows at the bottom in different directions, there was a 4.4K decrease in maximum temperature compared to flow in one direction. In addition, maximum temperature difference was 1.3K. Analyses were performed in cases where flow rate was 0.0010 kg/s, 0.0012 kg/s, 0.0014 kg/s, 0.0016 kg/s. When the flow rate was increased from 0.0010 kg/s to 0.0016 kg/s, the maximum temperature decreased from 328.2K to 323.3K. The reason for this high temperature is that PCM did not melt. Only 8% of PCM melted at 0.0016 kg/s. The effect of early melting was investigated with PCM having 3 different phase change temperatures. In the previous analysis, the phase change temperature was 314K-317K, while the maximum temperature decreased by more than 1K when the phase change temperature was 306K-309K. This showed the effect of PCM melting temperature on the maximum battery temperature. The results showed that HWMCP provided better thermal management than WMCP. However, it should be noted that the battery temperature above 50°C increases the possibility of thermal runaway.

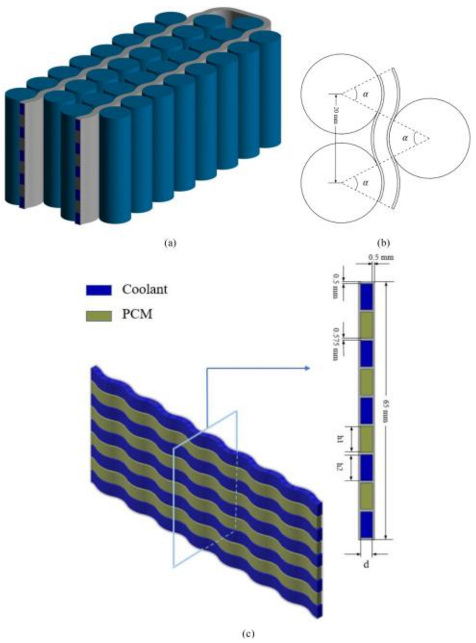

Fig. 5. PCM and Liquid Cooling with Serpentine Mini Channel [15]

Li et al. [16] performed thermal analysis of a battery pack containing 24 cylindrical 18650 LiB. They used a heat conducting block (HCB) through which coolant (water) passes for heat dissipation. The channel through which water passes is 6 pieces of 1 mm x 4 mm dimensions. Other boundary conditions are as follows: ambient temperature between 25°C and 45°C; water flow rate 0.4 m/s; water temperature 25°C; discharge rate 2C. In the analysis performed at 45°C ambient temperature, the battery temperature dropped below 30°C after 50 seconds. Since the heat dissipation from the batteries was too much, the discharge rate was insufficient to heat the battery. For this reason, the maximum battery temperature remained constant. The effect of water inlet temperatures was also investigated in the cases where the ambient temperature was 35°C and 45°C. In all cases, while the maximum temperature difference remained below 5°C, the possibility of thermal runaway increased when the water inlet temperature exceeded 35°C. As a result, due to the 135° contact angle between the HCB and the battery, the high heat transfer rate of the HCB and the high water inlet velocities, a very effective cooling was achieved and quite satisfactory temperature values were obtained despite the extreme conditions.

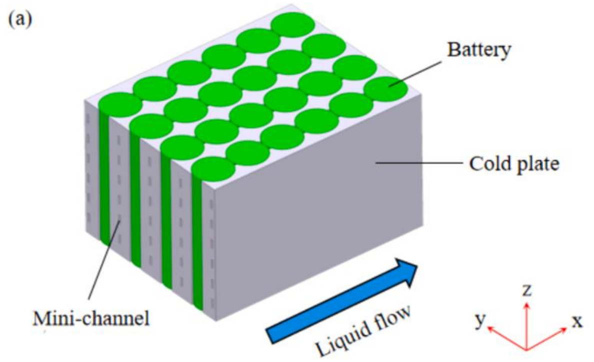

Fig. 6. Mini Channel Cold Plate Cooling with 24 LiB [16]

Xin et al. [17] numerically investigated the temperature, weight and power consumption effects of air and water cooled 32 pieces of 18650 LiBs with different flow rates and geometries at 3C discharge rate. A heat conducting block (HCB) with cooler passing through it was used as the heat transfer element. Analyses were performed under with 2, 3 and 4 HCBs; 4mm, 6mm, 8mm and 10mm fluid diameters and constant mass flow rate conditions. It was concluded that 6 mm pipe diameter was the most suitable for HCB. In the analyses with 2 and 3 HCBs, the effect of the pipe diameter on the temperature was minimal. Considering the maximum temperature, temperature difference and pressure drop, 3 HCBs were preferred.

Analyses were made for the case where there was no flow in the HCB and for the case where there was flow with 7 different flow rates. Since the temperature difference between the water and the battery was low at the beginning of the discharge process, the amount of heat transfer was low. For this reason, a rapid increase in the battery temperature was observed. Over time, the temperature gradient increased and as a result, the maximum temperature came to equilibrium. While the increase in the flow rate reduces the maximum temperature, the rate of decrease in the temperature decreases. This shows that it is unreasonable to increase the flow rate too much.

Although the water keeps the maximum battery temperature below 35°C, the battery temperature difference is over 5°C. In order to prevent this, the researchers have made an analysis for additional air cooling. In addition to the constant conditions of 6 mm pipe diameter, 0.002 kg/s mass flow rate and 3 HCBs, analyses were made for air at different velocities. For an air mass flow rate of 1 m/s, the maximum temperature was 30.67°C and the temperature difference was 0.58°C. Though these results are very successful in preventing thermal runaway, it should be taken into account that energy consumption increases.

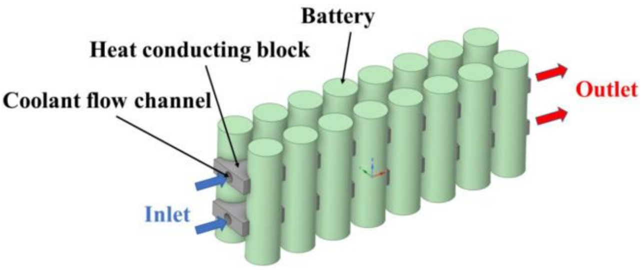

Fig. 7. Air and Liquid Cooling HCB [17]

3.2 Prismatic Battery Thermal Managements

Mini channel provides the desired cooling requirement while occupying a minimum volume in prismatic batteries. Efforts to increase heat transfer in prismatic batteries focus on the use of mini channels with different shapes and different attachments. In this section, recent studies on mini channels in prismatic batteries are compiled.

Dilbaz et al. [18] numerically performed the thermal analysis of 3 prismatic batteries with a capacity of 20Ah in their study with phase change material (PCM) and mini channel cooler. A rather extensive investigation was carried out in the cases of 3 different discharge rates (2C, 3C, 4C); water and Al2O3 nanoparticle added (0.5%, 1% and 2% by volume) nanofluid; 4 different geometry nanoparticles (Oblate spheroid, block, cylinder, and platelet); 4 different Reynolds numbers (250, 500, 750, 1000). The maximum temperature and maximum temperature difference were targeted to be below 50°C and 5°C in the study. In the analyses, when only RT-42 PCM was used at 4C discharge rate, maximum battery temperature and maximum temperature difference were 45.736°C and 1.96°C, while 100% of PCM melted at 260 seconds. Analyses were performed when PCM and serpentine mini channel (diameter 1.5 mm) were used together. At 3C discharge rate, when Re number was 500 and platelet-shaped 2% Al_2O_3 nanofluid added coolant was used, the maximum temperature was obtained as 47.85°C. It was determined that platelet-shaped nanofluid gave the best result among other nanofluids.

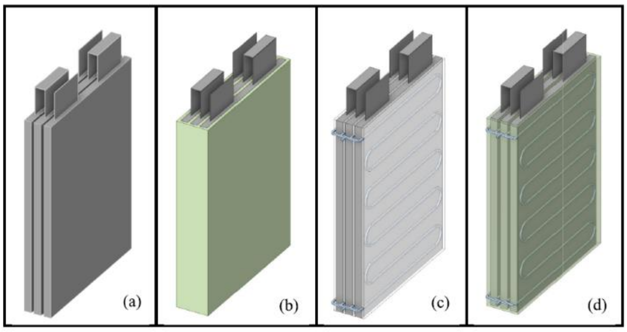

Fig. 8. PCM and Serpentine Mini Channel Cooling [18]

Jaffal et al. [19] performed experimental and numerical analysis of prismatic battery for 1C and 2C discharge range, 45°, 60°, 75° and 80° rib angles and semi-circular (SCR), trapezoidal (TRAP), and triangular (TRAN) rib shapes. The reason for using ribs is to disrupt the boundary layer and improve heat transfer. The flow Reynolds number is designed between 200 and 1000 and the cross-sectional length of the channel through which the fluid passes is 4 mm×5 mm. Heat transfer from battery to the channel is performed with constant heat flux.

CFD analyses were first performed on 4 different angles of semi-circular shaped ribs (SCR), at 800 Reynolds number and 1C discharge rate. The best result among them was obtained as 27.46°C for SCCP-SCR-45°. In the analyses where the Reynolds number was increased, better cooling was provided and temperature uniformity was provided. It was also determined that decreasing the rib angle improved heat transfer and ensured that the maximum temperature difference of the battery was at the desired levels. At 1000 Reynolds number and 45° rib angle, the Nusselt number increased by 58% compared to the empty channel. Knowing how much the pressure drop is while such large increases in heat transfer are provided will be important for the efficiency of the ribs. The friction factor decreased as the Reynolds number increased. However, decreasing the rib angle increased the friction factor. Compared to the flow without ribs, the 45° rib angle at 100 Reynolds number caused the friction factor to increase by 106%.

To investigate the effect of rib shapes on heat transfer, and pressure drop analyses were performed for the channel at 45° rib angle. The results showed that the SCCP-TRAN-45° design gave the best results. It was also noted that the Nusselt number increased by approximately 71%, while the overall hydrothermal performance increased by 30%.

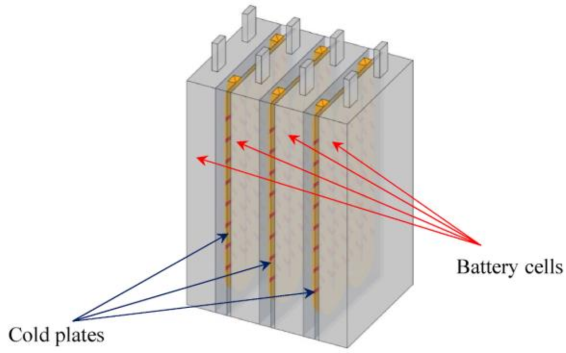

Fig. 9. Effect of Different Ange Ribs [19]

Zhao et al. [20] numerically analysed 10 LiFePO4 prismatic batteries with honeycomb liquid cooled cold plate (HLCP) design to determine the thermal behaviour. At the beginning of the analysis, the ambient temperature, coolant temperature and battery temperatures were input as 298.15K and the flow character was laminar. Three different honeycomb geometries of HLCP with 3mm channel height and 8mm channel width were designed. The analysis results at 5C discharge rate and 0.1m/s velocity inlet showed that the maximum battery temperature was lower than 304K with case 3, while the maximum battery temperature difference was 4.1K.

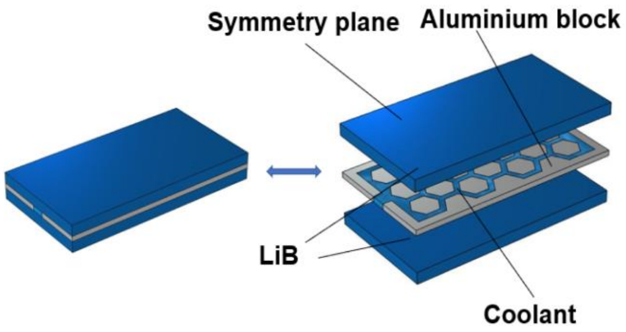

Fig. 10. Honeycomb Shaped Mini Channel Cold Plate [20]

Analyses were performed for 5 different cases where the coolant entered the channel from 1, 2 and 3 points. In the first 3 cases, the inlet velocity was reduced as the number of channels increased to maintain the total flow rate. The velocities in Case4 and Case5 were designed as 0.2m/s and 0.3m/s. The results showed that the maximum temperature did not depend on the increase in the number of inlet points. However, it was observed that the maximum temperature difference decreased if the number of inlet points increased. But, since this decrease was not significant, it was not taken into account in further analyses. The maximum temperature decreased to 300.6K by increasing the velocity to 0.3m/s. In order to better understand the effect of velocity, analyses were performed for 6 different inlet velocity values ranging from 0.01m/s to 0.5m/s. The results showed that increasing the inlet velocity more than 0.3m/s did not contribute significantly to the battery thermal management. In addition, the analysis performed on increasing the thickness of the HLCP showed that increasing the thickness without changing the flow rate did not contribute significantly to heat dissipation. Finally, it was observed that the flow direction had no effect on reducing the maximum temperature, but was successful in achieving a uniform temperature distribution. As a result, the importance and effectiveness of mini channel use in thermal management of prismatic LiBs was revealed.

Li et al. [21] numerically investigated the effect of a new type of pin-fin added mini channel cold plate on battery thermal management performance increase. Prismatic LiB with a capacity of 45Ah was selected as the battery, which will serve as heat generator in the battery package. A design was proposed in which the coolant enters the mini channel from 5 different points and flows in parallel. The mini channel section lengths were 3mm×8mm, while the cold plate thickness was analysed as 4mm. CFD analyses were performed for coolant inlet temperature, pin-fin heights (PFH) and different pin-fin arrangements. In the analyses, the maximum battery temperature increase, maximum battery temperature difference and pressure drop were examined and the pin-fin efficiency performance was investigated.

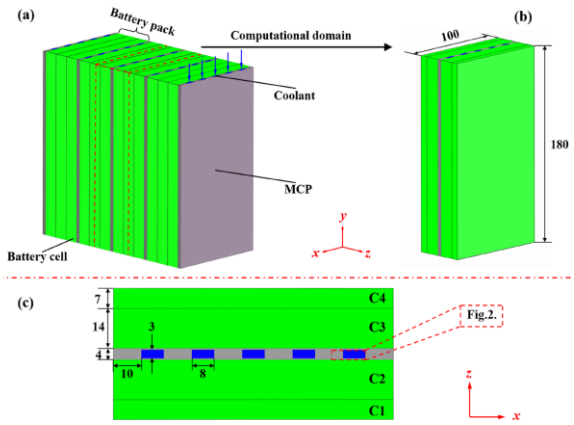

Fig. 11. Pin-fin Added Mini Channel Cold Plate [21]

Analyses were performed with the fluid at 3C discharge rate and 0.1m/s constant velocity in the mini channel without pin-fin (D1) and with pin-fin (D2, D3, D4, D5, D6). In the analysis, the ambient, battery and coolant channel inlet temperatures were selected as 298.15K. The results showed that the fluid velocity increased as the PFH increased, as expected, since the cross-section narrowed. In addition, the pin-fin increased the fluid contact surface area and improved the heat transfer. For more detailed examination, analyses were performed at 2C and 3C discharge rates with 0.1m/s and 0.4m/s fluid velocities. It was noted that the D2 design, which has the highest pin-fin height, reduced the maximum battery temperature by 4.822K at 0.4m/s and 3C discharge rate compared to D1. In the analysis performed at 2C discharge rate and 0.4m/s velocity, the maximum battery temperature difference remained below 5K in the all pin-fin arrangement analyses except D6. This value was 5.09K for D6 and 4.139K for D2.

The effect of Nusselt number and fanning-friction factor was also examined together to calculate the performance efficiency. In the analysis performed at 0.1 m/s inlet velocity, it was calculated that D2 design increased the Nusselt number by 83% compared to D1, but the fanning-friction factor increased by 238.9%. Therefore, heat transfer and friction coefficient should be evaluated together. The thermo-hydraulic performance of the best result D4 design was determined as 1.2935 and 1.4851 at 0.1 m/s and 0.4 m/s inlet velocities, respectively. With this result, the effectiveness of pin-fin usage in mini-channel battery thermal management was demonstrated.

3. CONCLUSIONS

This paper compiles the latest studies on the use of mini channels in thermal management of LiBs. The results obtained are as follows;

–Mini channels took up very little space while transferring heat from the battery. Therefore, it’s quite appropriate for battery packs.

–The efficiency coefficient increased by placing heat transfer enhancing elements (pin-fin, nanoparticle) inside the mini channel.

–Uniform battery temperature could be achieved by adjusting the fluid direction. However, its effect on the maximum temperature was minimal.

–As the fluid flow rate increased, the battery temperature approached a limit value and increasing the flow rate too much negatively affects power consumption.

–It has been shown that effective cooling is achieved by using high heat conduction blocks with mini channels which coolant passes through in it.

–Among the reviewed articles, Wang et al., PCM and Liquid Cooling with Serpentine Mini Channel, was considered to be the most original study.

Acknowledgments
I would like to thank my advisor who supported me in writing this article and the esteemed members of Energy, Environment and Storage Journal for providing us with this opportunity. A special thanks to my family for their support.

REFERENCES
[1] M. Jacyna, M. Wasiak, K. Lewczuk, and G. Karoń, “Noise and environmental pollution from transport: decisive problems in developing ecologically efficient transport systems,” Journal of Vibroengineering, Vol. 19, No. 7, pp. 5639–5655, Nov. 2017

[2] Judith Stephenson, Karen Newman, Susannah Mayhew, Population dynamics and climate change: what are the links?, Journal of Public Health, Volume 32, Issue 2, June 2010, Pages 150–156,

[3] EUROPEAN COMMISSION. The European green deal. COM (2019) 640 final. Brussels, 2019, 11.12: 2019.

[4] M. Ehsani, K. V. Singh, H. O. Bansal and R. T. Mehrjardi, "State of the Art and Trends in Electric and Hybrid Electric Vehicles," in Proceedings of the IEEE, vol. 109, no. 6, pp. 967-984, June 2021

[5] Maiorino, A., Cilenti, C., Petruzziello, F., & Aprea, C. (2023). A review on thermal management of battery packs for electric vehicles. Applied Thermal Engineering, 122035.

[6] Montanari, P. M., Hummes, D. N., Hunt, J. D., Hunt, B. B. D., & Schneider, P. S. (2022). A comparative study of different battery geometries used in electric vehicles. Available at SSRN 4084408.

[7] Rojas, O. E., & Khan, M. A. (2022). A review on electrical and mechanical performance parameters in lithium-ion battery packs. Journal of Cleaner Production, 378, 134381.

[8] Kalkan, O., Celen, A., & Bakirci, K. (2022). Multi-objective optimization of a mini channeled cold plate for using thermal management of a Li-Ion battery. Energy, 251, 123949.

[9] Kim, J., Oh, J., & Lee, H. (2019). Review on battery thermal management system for electric vehicles. Applied thermal engineering, 149, 192-212.

[10] AKULA, Rajesh; BALAJI, C. Thermal management of 18650 Li-ion battery using novel fins–PCM–EG composite heat sinks. Applied Energy, 2022, 316: 119048.

[11] DENG, Da. Li‐ ion batteries: basics, progress, and challenges. Energy Science & Engineering, 2015, 3.5: 385-418.

[12] Wiriyasart, S., Hommalee, C., Sirikasemsuk, S., Prurapark, R., & Naphon, P. (2020). Thermal management system with nanofluids for electric vehicle battery cooling modules. Case Studies in Thermal Engineering, 18, 100583.

[13] Xu, Q., Xie, Y., Huang, Y., Li, X., Huang, H., Bei, S., ... & Li, L. (2023). Enhancement of thermal management for cylindrical battery module based on a novel wrench-shaped design for the cold plate. Sustainable Energy Technologies and Assessments, 59, 103421.

[14] Wang, H., Tao, T., Xu, J., Mei, X., Liu, X., & Gou, P. (2020). Cooling capacity of a novel modular liquid-cooled battery thermal management system for cylindrical lithium ion batteries. Applied Thermal Engineering, 178, 115591.

[15] Wang, Y., Gao, T., Zhou, L., Gong, J., & Li, J. (2023). A parametric study of a hybrid battery thermal management system that couples PCM with wavy microchannel cold plate. Applied Thermal Engineering, 219, 119625.

[16] Li, L., Li, X., Xie, Y., Huang, H., Huang, Y., Wang, H., ... & Zheng, K. (2024). Adaptability enhancement of mini-channel cold plate for cylindrical battery module under various ambient temperatures. Applied Thermal Engineering, 123682.

[17] Xin, S., Wang, C., & Xi, H. (2023). Thermal management scheme and optimization of cylindrical lithium-ion battery pack based on air cooling and liquid cooling. Applied Thermal Engineering, 224, 120100.

[18] Dilbaz, F., Selimefendigil, F., & Öztop, H. F. (2024). Comparisons of different cooling systems for thermal management of lithium-ion battery packs: Phase change material, nano-enhanced channel cooling and hybrid method. Journal of Energy Storage, 90, 111865.

[19] Jaffal, H. M., Mahmoud, N. S., Imran, A. A., & Hasan, A. (2023). Performance enhancement of a novel serpentine channel cooled plate used for cooling of Li-ion battery module. International Journal of Thermal Sciences, 184, 107955.

[20] Zhao, D., Lei, Z., & An, C. (2023). Research on battery thermal management system based on liquid cooling plate with honeycomb-like flow channel. Applied Thermal Engineering, 218, 119324.

[21] Li, H., Chen, L., Zuo, H., Zhang, B., & Jia, G. (2024). Performance enhancement of a battery thermal management system using novel liquid cold plates with micro-channel featuring pin fins. Energy, 301, 131731.

Research Article

Energy, Environment and Storage (2024) 04-03:116-120

Energy, Environment and Storage

Journal Homepage: www.enenstrg.com

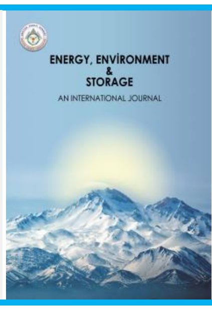

Investigation of The Effect of Adding Natural Gas to A Gasoline Engine On Engine Performance and Emissions

Talip Akbıyık[1], Nafiz Kahraman[2], Bilge Albayrak Çeper[3]

[1]Motor Vehicles andTransportation Technologies, Aksaray University, Aksaray, ORCID: 0000-0001-8580-8890

[2]Faculty of Aeronautıcs and Astronautıcs, Erciyes University, Kayseri, Türkiye, ORCID: 0000-0002-8698-8632

[3]Faculty of Aeronautıcs and Astronautıcs, Erciyes University, Kayseri, Türkiye, ORCID: 0000-0001-5556-5170

ABSTRACT Petroleum-based fuels are generally used in internal combustion engines. Petroleum-based fuels now have difficulty meeting Euro standards in terms of emissions. That's why different methods are used. One of these is that adding natural gas to fuels can be beneficial in reducing emissions and increasing engine performance. In the experimental study, the engine performance and emissions of adding natural gas at different rates (50, 100, 150 and 200 g/h) into the intake air of an engine using gasoline fuel at different torque values (5, 10, 15 and 20 Nm) at a constant 3000 rpm were examined. The engine used in the study is a Lombardini LGW 523 MPI gasoline two-cylinder engine. When the experimental results are examined, the addition of natural gas to gasoline fuel reduces fuel consumption. The lowest values in specific fuel consumption were obtained when natural gas was added. Emissions decreased with increasing torque. As the natural gas addition rate increased, the thermal efficiency increased.***Keywords:*** *Emission, power, gasoline, natural gas*

Article History: Received: 30.09.2024; Accepted: 30.09.2024; Available Online: 30.09.2024

Doi: https://doi.org/10.52924/MOOB3563

1. INTRODUCTION

Fuels constitute one of the most fundamental problems of automobile technology. Studies have been conducted on fuels that will be alternatives to traditional fuels or can be used together with them. These alternative fuels should be used with little or no modification to the engine. All liquid fuels and gaseous fuels except gasoline and diesel are considered alternative fuels. Gaseous fuels are used in internal combustion engines because they provide environmental and economic benefits as an alternative to existing fuels. Due to this feature, natural gas has become widespread in the transportation sector. The use of natural gas in spark ignition engines has become significantly widespread. For this reason, various studies have been carried out on the use of this gaseous fuel. Gonca et al. In their study, they examined the power change, effective pressure, thermal efficiency and exergy efficiency of adding liquefied hydrogen, methane, butane and propane to gasoline, iso-octane, benzene, toluene, hexane, ethanol and methanol fuels in a spark-ignition engine. The proportions of fuel additives vary between 10% and 50% by mass. As a result, they stated that the ratios of hydrogen, methane, butane and propane significantly affected the performance of the engine [1].

Akbıyık et al. In this study, they investigated the effect of boron additive addition to lubricating oil on engine performance and emissions when gasoline and natural gas were used as fuel in a spark-ignition engine. The test results showed that when gasoline and natural gas were used as fuel in the engine, the addition of boron in the lubricating oil caused an average reduction of 2.4-8% in specific fuel consumption. They found that the use of boron additive in lubricating oil caused a significant reduction in NOX emissions by 11.4-12.9% and there was no significant change in other emissions [2].

Chen et al. In this study, they compared the combustion characteristics and performance characteristics of a dual fuel engine running on natural gas/methanol and natural gas/gasoline. All experiments were carried out at an engine speed of 1600 rpm. As a result, the addition of both methanol and gasoline accelerated the combustion rate of natural gas, and the brake thermal efficiency (BTE) for the natural gas/methanol mixture increased from 27.3% to 28.1%. However, they stated that BTE for natural gas/gasoline mixture decreased from 27.3% to 25.5%. They stated that the total hydrocarbon and carbon monoxide emissions of natural gas engines decreased by adding methanol and increased with gasoline[3,4,5,6].

Örs et al. In this study, they investigated the effect of ethanol and methanol addition on engine performance, combustion and emissions in the SI engine. The experiments were carried out on a single-cylinder, four-stroke SI engine at different engine speeds at full engine load. They prepared test fuels by adding 10% ethanol and methanol to gasoline. According to the experimental results, they reported that the addition of methanol increased the Bsfc values by 10.3% compared to the addition of ethanol, while it caused a 6.12% decrease in the BTE values. They reported that although methanol addition reduced CO2, CO, HC and NOX emissions by 6.48%, 26.6%, 4.75% and 9.16%, respectively, compared to ethanol addition, it had 15.3% higher oxygen emission values because its oxygen content was higher than ethanol [7].

Tasev and Stoyanov reviewed various studies on the application of compressed natural gas (methane) as a gas fuel for the dual-fuel operating cycle of compression ignition engines. While some of the studies show that maximum cylinder pressure, heat release rate and maximum cylinder pressure rise rate decrease, others have observed this behavior only at low loads, medium and full loads, cylinder pressure, heat release rate and maximum cylinder pressure rise when used for CNG gas-diesel operating cycles. reported that it was associated with an increase in the rate of All analyzed studies did not explain that the ignition delay time increases depending on the amount of CNG supplied to the dual fuel mode engine [8].

Cahirul et al. [9] A comparative analysis of engine performance and exhaust emissions in a gasoline and compressed natural gas (CNG) fueled regenerated spark ignition automobile engine was performed. A new 1.6-litre 4-cylinder petrol engine with an electronically controlled solenoid-actuated valve was available. This system was converted to a dual-fuel system containing a computer powered by gasoline or CNG. Engine brake power, brake specific fuel consumption, brake thermal efficiency, exhaust gas temperature and exhaust emissions were measured at speed change at 50% and 80% throttle positions. Comparative analysis of the test results showed a reduction in brake power of 19.25% and 10.86% and brake specific fuel consumption (BSFC) of 15.96% and 14.68% at 50% and 80% throttle positions when filling the engine with CNG. A decrease like this occurred. The renewed engine produced an average of 40.84% higher NOx emissions, 1.6% higher brake thermal rates and 24.21% higher exhaust gas emissions in the 1500-5500 rpm speed range at 80% throttle. Other emission contents were measured to be significantly lower than gasoline emissions [9].

Yontar and Doğu [10] determined to experimentally and numerically examine the effects of CNG and gasoline fuels on engine performance and emissions in a double-row spark ignition engine. Yontar and Doğu [11] investigated the effects of gasoline and CNG fuels. Yontar and Doğu [12] investigated the effects of equivalence ratio and CNG addition on engine performance and emissions in a double-row ignition engine under low and high load conditions. Alrazenand Ahmad [13] obtained HCNG fueled spark ignition (SI) engine with its effects on performance and emissions. Bae et al. [14] studied the full load operating characteristics and thermal efficiency of a 1.4L turbo CNG SI engine.

Das et al. [15] presented a comparative evaluation of the performance characteristics of a spark-ignition engine using hydrogen and compressed natural gas as alternative fuels. Evansand Blaszczyk[16] designed a comparative study of the performance and exhaust emissions of a spark ignition engine running on natural gas and gasoline. Geok et al. [17] analyzed the experimental investigation of the performance and emissions of a compressed natural gas converted engine with sequential port injection.

Ariani et al. [18] This study conducts an experimental investigation on the impact of the use of mixer and non-mixer in the intake manifold on the performance and emissions of a diesel-CNG dual-fuel engine. The results show that adding mixer does not immediately improve combustion quality or reduce emissions. It is important to ensure that the homogeneous mixture is conditioned to the required air-fuel ratio before entering the combustion chamber. Proper mixer design, diameter size and placement of holes must be carefully considered.

2. MATERIAL AND METHOD

2.1. The experimental setup

In the experimental setup, engine load and speed are determined by a Net Brake electric dynamometer. Emission values: Alicat mass flow meter was used to adjust the amount of natural gas added from the manifold with the Federal combi exhaust emission device. The engine used in the experiments is Lombardini LGW 523 MPI.

The electric dynamometer used for measurement can measure up to a maximum of 8000 rpm and 83 Nm torque. CO, CO2, HC, O2, NO and lambda values were determined with the federal emission device. 50, 100, 150 and 200 grams of natural gas per hour were added from the intake manifold of the engine using an Alicat mass flow meter. The experimental engine is a Lombardini LGW 523 MPI 2-cylinder, water-cooled, injection and lambda-controlled engine. The experimental setup is given in Figure 1..

Figure 1. Schematic of the experimental setup

2.2. Test Method

In this study, natural gas was added to the intake air at different rates (50, 100, 150 and 200 g/s) at different torque values (5, 10, 15 and 20 Nm) in an engine using gasoline fuel. The effect on engine performance and emissions was examined by operating at a constant 3000 rpm. . Before the experiments, the test engine was run at idle until it reached the regime temperature. After the engine reached the regime temperature, it was gradually increased to the maximum load value with an electric dynamometer and tested at the determined torques. The amount of gasoline consumed in the experiments was determined by mass using the S loud cell. The amount of natural gas sent to the intake air to mix with the combustion air was determined with the Alicat gas mass flowmeter.

Experiments were carried out for 4 different fuel additions at constant engine speed and constant torques. In the experiments, the engine was kept constant at 3000 rpm. It was tested at 4 different torque values by adding 50, 100, 150 and 200 g/h natural gas to the combustion air. The engine was tested at 5, 10, 15 and 20 Nm of torque for each fuel. 90.8% of the natural gas used consists of methane..

3. RESULTS

The figures show the changes in different torque values of 5 different fuels at 3000 rpm. Specific fuel consumption indicates the amount of fuel consumed per unit power. Specific fuel consumption changes in studies conducted with gasoline and natural gas mixtures are given in Figure 2. Compared to gasoline, compressed natural gas fuels have higher calorific values and higher stoichiometric fuel-air ratios, resulting in less fuel being used for the same purpose [2]. This means that specific fuel consumption values are higher at all torque values in experiments conducted with gasoline fuel. As the natural gas addition rate increased, the specific fuel consumption value decreased. As the torque value increased, the specific fuel consumption value decreased. The lowest specific fuel consumption values were obtained at 20 Nm torque.

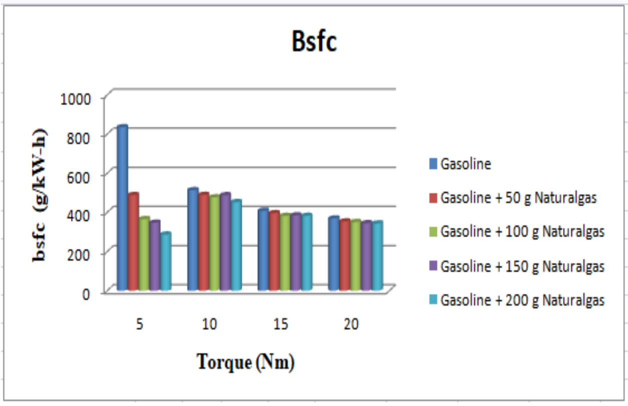

Figure 2. Specific fuel consumption depending on torque

In engines, power varies according to torque and speed. Since the speed and torque are constant in the experiments, the power values are the same, but there are small differences and this is due to the limits allowed in the experiments.

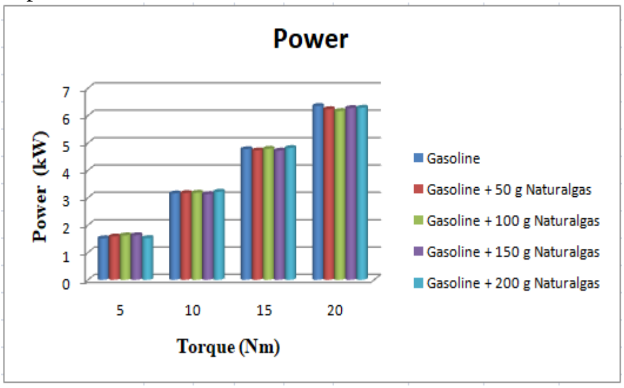

Figure 3. Power depending on torque

When Figure 4 is examined, it is seen that CO decreases as torque values increase. As the torque value increases and the air speed entering the cylinders increases, turbulence in the combustion chamber increases, resulting in a more homogeneous mixture [4]. Since this will improve fuel combustion, there will be a decrease in CO at high torque values. The addition of natural gas resulted in a reduction in CO emissions. At high torque values, combustion improves and CO emissions decrease with increasing pressure and temperature.

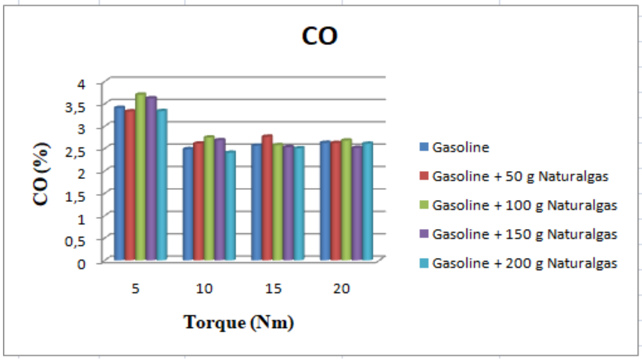

Figure 4. CO depending on torque

Hydrocarbon emissions result from fuel being expelled from the exhaust without being burned. When Figure 5 is examined, HC emissions also increase as torque increases. The highest HC emissions are in gasoline fuel. Low calorific value of natural gas and stoichiometric air since the fuel ratio is higher than gasoline, less fuel is sent to the cylinder to provide the equivalent amount of heat and stoichiometric mixture to gasoline and HC emissions are reduced [2]. Additionally, increasing torque values causes a slight increase in HC emissions.

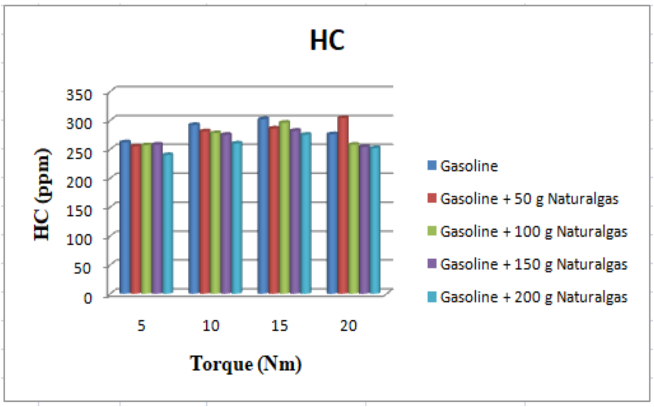

Figure 5. HC depending on torque

CO2 is a gas that causes global warming. In terms of CO2 emissions, fuels containing fewer or no carbon atoms are preferred. When the graph in Figure 6 is examined, CO2 emissions in natural gas mixtures either increase or remain constant. It is seen that as the torque value increases, CO2 emissions are higher than gasoline. The reason why CO2 emissions increase during the addition of natural gas is the increase in combustion efficiency.

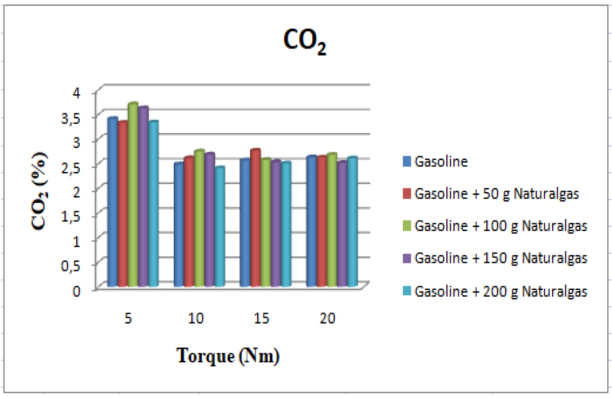

Figure 6. CO_2 depending on torque

When the figure is examined, it can be seen that NO emissions are lower in fuels with natural gas additives than in gasoline. NO emissions increase with increasing engine load in every fuel type. At maximum torque, the most filling is taken into the cylinder and temperatures increase. High temperatures cause NO emissions to increase [2]. The reason why NO emissions are low in studies carried out with natural gas fuels is that natural gas cools the mixture due to its high evaporation temperature and ultimately reduces the cycle temperature.

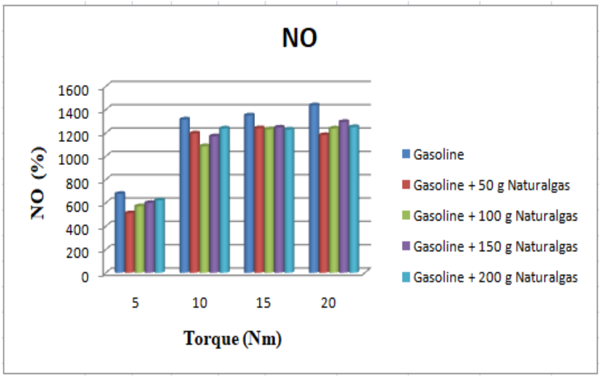

Figure 7. NO depending on torque

As the torque values increased, the thermal efficiency values also increased. As the proportion of natural gas in the fuel increased, the thermal efficiency value also increased. When examined in terms of thermal efficiency, the highest thermal efficiency values were obtained with Gasoline + 150 g natural gas fuel. Increasing the amount of added fuel prevents oxygen intake after a certain level, combustion worsens and the air fuel ratio changes. This deterioration causes an increase in HC and CO emissions [18].

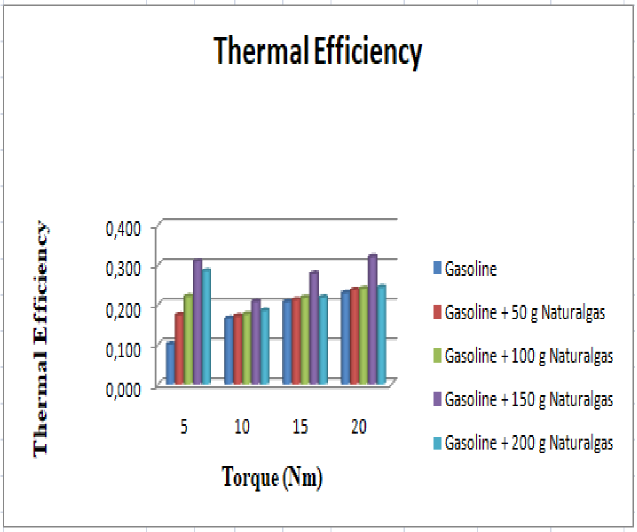

Figure 8. Thermal efficiency depending on torque

4. CONCLUSION

Specific fuel consumption decreased as the torque value increased. The highest specific fuel consumption value was obtained with the addition of 200 g of natural gas. The high calorific value of natural gas fuel caused less fuel consumption at constant torque value and the specific fuel consumption decreased.

Since the speed and torque are constant in the experiments, the power values are the same, but there are small differences and this is due to the limits allowed in the experiments.

When CO emissions were examined, the addition of natural gas had an impact on CO emissions. At high torque values, combustion improves and CO emissions decrease with increasing pressure and temperature.

Since the lower calorific value and stoichiometric air fuel ratio of natural gas is higher than gasoline, less fuel is sent to the cylinder to provide the equivalent heat amount and stoichiometric mixture to gasoline and HC emissions are reduced. In addition, increasing torque values cause a slight increase in HC emissions.

As the torque value increases, CO2 emissions are seen to be higher than gasoline. The reason for the increase in CO2 emissions when adding natural gas is due to the improvement in combustion efficiency.

NO emissions in each fuel type increase with increasing engine load. At maximum torque, the most filling is taken into the cylinder and temperatures increase. High temperatures cause NO emissions to increase. The reason why NO emissions are low in studies carried out with natural gas fuels is that natural gas cools the mixture due to its high evaporation temperature and ultimately reduces the cycle temperature.

REFERENCES

1. Gonca, G., Sahin, B., Hocaoglu, M. F., 2021, Influences of hydrogen and various gas fuel addition to differen liquid fuels on the performance characteristics of a spark ignition engine, International Journal Of Hydrogen Energy, 47 (2022) 12421-12431, https://doi.org/10.1016/j.ijhydene.2021.09.029

2. Akbiyik, T., Kahraman, N., Taner, T., 2022, Investigation Of TheEffect Of Boron Additive To Lubricating Oil On Engine Performance, Exhaust, AndEmissions, Fuel, Volume 312, 15 March 2022, 122931Https://Doi.Org/10.1016/J.Fuel.2021.122931

3. Chen, Z., Zhang, T., Wang, X., Chen, H., Geng, L., Zhang, T., 2021, A Comparative Study Of Combustion Performance And Emissions Of Dual-Fuel Engines Fueled With Natural Gas/Methanol And Natural Gas/Gasoline, Energy, Volume 237, 15 December 2021, 121586, https://doi.org/10.1016/j.energy.2021.121586

4. Chen, Z.,Wang, L., Zhang, Q., Zhang, X., Yang, B., Zeng K., 2019, Effect of Spark Timing and Methanol Addition on Combustion Characteristics and Emissions of Dual-Fuel Engine Fueled With Natural Gas and Methanol Under Lean Burn Condition, Energy Conversion and Management, Volume 181, 1 February 2019, Pages 519-527, https://doi.org/10.1016/j.enconman.2018.12.040

5. Chen, Z.,Wang, L., Zeng K., 2019, A Comparative Study on The Combustion And Emissions of Dual Fuel Engine Fueled with Natural Gas/Methanol, Natural Gas/Ethanol, and Natural Gas/n-Butanol, Energy Conversion and Manegement, Volume 192, 15 July 2019, Pages 11-19, https://doi.org/10.1016/j.enconman.2019.04.011

6. Wang, L.,Chen, Z.,Zhang, T.,Zeng K., 2019, Effect of Excess Air /Fuel Ratio And Methanol Addition on The Performance, Emissions, and combustion characteristics of A Natural Gas/Methanol Dual-Fuel Engine, Fuel, Volume 255, 1 November 2019, 115799, https://doi.org/10.1016/j.fuel.2019.115799

7. Örs, İ., Sayın, B., Ciniviz, M., 2020, A Comparative Study of Ethanol and Methanol Addition Effects on Engine Performance, Combustion and Emissions in the SI Engine, International Journal of Automotive Science And Teknology, Volume 4, Issue 2, 59 - 69, 30.06.2020, https://doi.org/10.30939/ijastech..713682

8. Tasev, A., Stoyanov, Y., 2024, Analysis of the CNG impact on some of the combustion parameters of dual-fuel compression ignition engines, AIP Conferece Proceedings, Volume 3078, Issue 1, https://doi.org/10.1063/5.0208335.

9. Jahirul, M. I., Masjuki, H. H., Saidur, R., Kalam, M. A., Jayed, M. H., Wazed, M. A.. 2010. Comparative engine performance and emission analysis of CNG and gasoline in a retrofitted car engine. Applied Thermal Engineering 30:2219–26. doi:10.1016/j.applthermaleng.2010.05.037.

10. Yontar A. A., Doğu Y. 2018. Experimentalandnumericalinvestigation of effects of CNG andgasolinefuels on engine performanceandemissions in a dualsequentialsparkignition engine. EnergySources, Part A: Recovery, UtilizationandEnvironmentalEffects 40 (18):2176–92. doi:10.1080/15567036.2018.1495783.

11. Yontar A. A., Doğu Y,. 2018b. Investigation of theeffects of gasolineand CNG fuels on a dualsequentialignition engine at lowandhighloadconditions. Fuel 232 (2018):114–23. doi:10.1016/j.fuel.2018.05.156.

12. Yontar A. A., Doğu Y,. 2019. Effects of equivalenceratioand CNG addition on engine performanceandemissions in a dualsequentialignition engine. International Journal of Engine Research. doi:10.1177/1468087419834190.

13. Alrazen H. A., Ahmad K. A.. 2018. HCNG fueled spark-ignition (SI) engine with its effects on performance and emissions. Renewable and Sustainable Energy Reviews 82 (1):324–42. doi:10.1016/j.rser.2017.09.035.

14. Bae J. W., Park C. W., Lee J. W., Kim Y. R., Kim C. G., Lee S. Y., Lee J. W.. 2018. A study on the full load operation characteristics and thermal efficiency of the 1.4L turbo CNG SI engine. Journal of the Korean Institute of Gas 22 (6):34–39.

15. Das L. M., Gulati R., Gupta P. K. 2000. A comparative evaluation of the performance characteristics of a spark ignition engine using hydrogen and compressed naturalgas as alternative fuels. International Journal of HydrogenEnergy 25 (8):783–93. doi:10.1016/S0360-3199(99)00103-2.

16. Evans R. L., Blaszczyk J. 1997. A comparative study of the performance and exhaust emissions of a spark ignition engine fuel led by naturalgas and gasoline. Proceedings of the Institution of Mechanical Engineers Part D Journal of Automobile Engineering 211 (1):39–47. doi:10.1243/0954407971526209.

17. Geok H. H., Mohamad T. I., Abdullah S., Ali Y., Shamsudeen A. 2009. Experimental investigation of performance and emissions of a sequential port injection compressed naturalgas converted engine. SAE paper 32-0026/20097026.

18. Arian, B., Felayati, F. M., Batutah, M. A., 2024, Experimental Analysis of the Influence of a Compressed Natural Gas (CNG) Air Mixer on Performance and Emissions in Partial Load CNG Diesel Dual Fuel Engines, Automotive Experiences, Vol. 7 No 2 (2024) pp 224-235 https://doi.org/10.31603/ae.11195